LASER DESORPTION-ATMOSPHERIC PRESSURE CHEMICAL IONIZATION
MASS SPECTROMETRY: A NEW IONIZATION METHOD BASED ON
EXISTING THEMES

By

JOSHUA J. COON

A DISSERTATION PRESENTED TO THE GRADUATE SCHOOL
OF THE UNIVERSITY OF FLORIDA IN PARTIAL FULFILLMENT
OF THE REQUIREMENTS FOR THE DEGREE OF
DOCTOR OF PHILOSOPHY

UNIVERSITY OF FLORIDA

2002

ACKNOWLEDGMENTS

A complete summary of all the people who have been pivotal in my development would be too lengthy for presentation here. Therefore, I will highlight those who were most influential during my time at the University of Florida and others who helped me to get here. My parents, Jacques and Sandra Coon, exposed me to a variety of activities and always supported my interests during my childhood. These experiences allowed me to develop a wide variety of skills, many of which I have employed here at UF. Their dedication to each other and me has been a source of inspiration as I set out to begin my own family.

Since we met in our undergraduate organic chemistry course, Heather Steele has been one of my biggest supporters. From the beginning she encouraged me to seek out the very best graduate experience possible. Now she has agreed to marry me and I only hope that over the years I will be able to reciprocate that support in equal proportions.

At UF I would like to start by thanking my advisor, Dr. Willard W. Harrison, who deserves tremendous thanks for taking a chance on me (a 3rd year student at the time). I greatly value both his guidance and wisdom, and over the past year I have attempted to stockpile as much of it as possible for future use. And together we have created a useful ionization method for mass spectrometry.

Andy Ottens and Dr. Kevin McHale are two colleagues that I have greatly benefited from knowing. Both of them have always been willing to assist with my

.

TABLE OF CONTENTS

Abstract of Dissertation Presented to the Graduate School
of the University of Florida in Partial Fulfillment of the
Requirements for the Degree of Doctor of Philosophy

LASER DESORPTION-ATMOSPHERIC PRESSURE CHEMICAL IONIZATION-
MASS SPECTROMETRY: A NEW IONIZATION METHOD BASED ON
EXISTING THEMES

By

Joshua J. Coon

December, 2002

Major Chair: Willard W. Harrison
Major Department: Chemistry

This dissertation considers the use of photons as energy inputs for the

desorption and or desorption/ionization of sample molecules for mass

spectrometric analysis. The first chapter can be considered a primer on the

subject, as it presents a variety of energy input methods, mass spectrometers,

and modes of coupling the two. The next two chapters discuss small molecule

detection experiments from biological tissue using a previously constructed laser

desorption/chemical ionization (LD/CI) mass spectrometer. Though results were

produced, the method presented several drawbacks limiting its potential for mass

spectrometric imaging. Namely, analysis within the confines of the mass

spectrometer vacuum system was most problematic.

To circumvent these problems, a novel laser desorption mass spectrometer interface was designed, constructed, and evaluated with the results presented in Chapter 4. The interface operates at atmospheric pressure (AP) and utilizes a laser pulse to desorb intact neutral molecules, followed by chemical ionization via reagent ions produced by a corona discharge (LD-APCI). This source employs a heated capillary AP inlet coupled to a quadrupole ion trap mass spectrometer and allows sampling under normal ambient air conditions. Chapter 5 focuses on fundamental aspects of the new method including temporal ion pulse width, laser fluence effects, and demonstrates quantitative potential.

Chapter 6 explores the ability of the LD-APCI method to desorb/ionize fragile biomolecules like peptides to determine the relative softness of the new ionization method. In comparison with atmospheric pressure-matrix-assisted laser-desorption/ionization (AP-MALDI) the method provided an ~ 1400 fold increase in analyte signal for certain analytes. Next, using the technique's ability to decouple the desorption and ionization processes, we present the first direct sampling of tryptic peptides from polyacryamide gels (PAGE) using the novel LD-APCI interface in Chapter 7. These results suggest the PAGE-LD-APCI-MS technique provides several advantages that could translate into a more convenient, robust methodology for the rapid identification and characterization of proteins. In the last chapter strategies regarding the further development of the method are considered.

CHAPTER 1
INTRODUCTION

Background

For several decades mass spectrometry, the art of measuring the mass of atoms and molecules, has experienced unusually rapid expansion. During the 1970s mass spectrometry was the method of choice for various applications including pharmaceutical, hydrocarbon, pesticide, and atomic analysis. However, the ability to perform mass spectrometry of large, fragile, and nonvolatile molecules, namely biomolecules, has been a more recent phenomenon whose success can be directly traced to the development of novel sample introduction and ionization methods.

For many years electron ionization (EI) was used as the primary ionization method for mass spectrometry. The method subjects gas-phase analyte molecules to energetic electrons (~ 70 eV) to cause an electronic transition resulting in the formation of a positive radical ion. Often the electron bombardment induces fragmentation of the intact gas-phase molecule, a benefit that can give structural information. Unfortunately the technique requires that analyte be introduced into the ion source as a gas-phase molecule – a detriment that for many years confined mass spectrometry to the analysis of small, volatile molecules.

Numerous methods to vaporize analyte molecules have been employed, some with more success than others. The first and most obvious method was

that of heating the sample to induce vaporization. This approach was not the answer, since most non-volatile and thermally-labile species tended to decompose upon exposure to heat. Other attempts called for the derivatization of the molecules' polar groups to generate derivatives of higher vapor pressure.[1-3] Though derivatization brought a limited set of new molecules within range, it did not significantly raise the mass limit for mass spectrometry.

Mass spectrometry would have to wait until 1974 for the inception of a novel desorption/ionization method, called plasma desorption (PD), to get its first sustained acquaintance with biomolecules.[4] Though the technique had a relatively short lifetime – like the half-life of the ^{252}Cf it utilized – its successors, operating on similar principles, remain in use today. By imparting high energy ions, fission fragments from ^{252}Cf, onto thin foils supporting an analyte, the approach induced desorption/ionization of the analyte directly from the condensed-phase into the gas-phase. The method delivered sizeable irradiances of up to 10^{13} W/cm^2, causing thermally labile species to be rapidly heated at a rate exceeding the rate of decomposition.[5] These pioneering experiments of Macfarlane and co-workers precipitated the development of a family of desorption/ionization techniques, coined energy-sudden methods. In order of appearance on the mass spectrometry scene they are secondary ion mass spectrometry (SIMS),[6,7] laser desorption/ionization (LDI),[8] fast-atom bombardment (FAB),[9,10] and matrix-assisted laser desorption/ionization (MALDI).[11,12] This continued evolution of desorption/ionization methodology over the past two decades has placed mass spectrometry at the forefront of

biological research.[13] The success of the evolved energy-sudden ionization method (MALDI) can be directly attributed to its ability to convert large molecules (MW > 1000 Da) from the condensed-phase into gas-phase ions for mass analysis.

Energy-Sudden Ionization

As outlined above, non-volatile species presented a significant problem, ultimately hindering the utility of mass spectrometry prior to the advent of the energy-sudden methods. The founding principle of these methods was first demonstrated and suggested by Beuhler and co-workers working on an alternative to compound derivatization called volatility enhancement.[14] In this study, the researchers used gas-phase reactions with NH_4^+ to ionize thermally-desorbed peptides from a metal surface. They observed that more rapid heating of the sample generated an increase in the intact gas-phase protonated molecule, while slower heating caused fragment species to dominate the resulting mass spectrum. Figure 1-1 presents a plot of the log of relative ion intensity vs. reciprocal absolute temperature for the protonated molecule ([PCA-His-Pro-NH_2 + H]$^+$, m/z 354) and the fragment (m/z 235) obtained by the researchers.

This study suggested that the volatility of thermally-labile species is competitive, a process involving both decomposition and evaporation. Unimolecular fragmentation, caused by thermal decomposition, occurs as a result of excitation to an unstable vibrational mode, where the rate of decomposition is determined by the time required for deposition of the excess
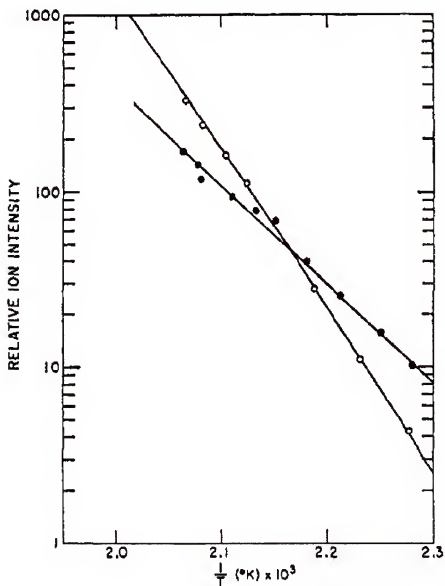
Figure 1-1. Relative intensity of the protonated molecule ([PCA-His-Pro-NH$_2$ + H]$^+$, m/z 354, open circles) and a fragment (m/z 235, closed circles) as a function of 1/T.[14]

energy into that mode.[5] The work of Buehler et al. demonstrates that as the rate of vaporization (rapid heating) is increased, it can surpass the rate of decomposition (intersection of two curves from Figure 1-1) causing the preferential desorption of intact molecules.

This principle governing the desorption/decomposition process can be exploited by use of ion, atom, and photon beams, which can deposit massive amounts of energy (~ 100s of joules) over extremely short periods of time (< 100 ns). Fundamental considerations of surface interactions to incident energy have been the subject of recent molecular dynamic (MD) simulations – experiments that have provided a reasonably good understanding of how the energy-sudden approaches work.[15-19] Figure 1-2 presents the results of a simulation with (a) displaying the temperature and defect density and (b) presenting the 2D pressure and displacement of an organic matrix layer following irradiation with a 15 ps laser pulse.[15] The authors note that a rapid energy transfer from vibrationally excited molecules explains the increase in temperature that can be observed in Figure 1-2A. A rapid rise in pressure can also be observed in Figure 1-2B, which is a result of a heating rate that is faster than the rate of mechanical relaxation. The authors propose that the increased pressure generates a compression shock wave into the cold part of the sample, which in turn creates forces normal to the surface. It is these forces that are ultimately responsible for the ablation/ejection of the surface material.[15] This ablation/ejection can be observed as a function of time in the displacement trace of Figure 1-2B. They
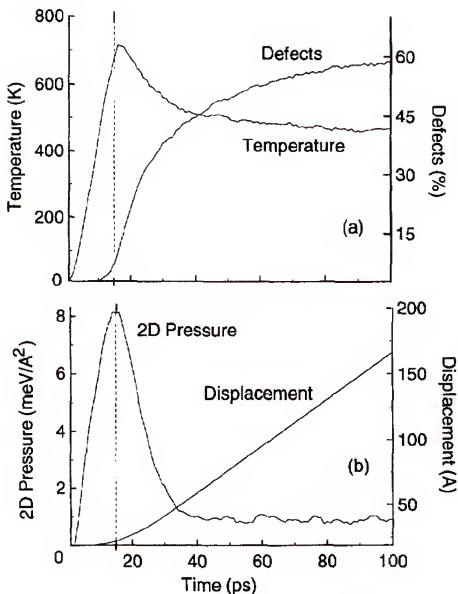
Figure 1-2. Simulated plots of surface material characteristics vs. time for molecules in the top 24 nm of the surface. (A) Shows the temperature and defect density with the dashed line denoting the end of the 15 ps laser pulse. (B) Plots the 2D pressure and the displacement of the surface.[15]

estimate that the ablated layer is accelerated in a short period of time (~ 15 ps) and then displaces at a fixed rate of ~ 200 m/s.

While these simulations have utilized photons for desorption, it is assumed that the process is similar when the sample is irradiated with atom or ion beams. Generally, atom, ion, or photon beams can simply be considered as vehicles for the rapid delivery of energy, with some bearing more practical benefits than others. Over the past three decades the energy-sudden approach has rapidly evolved and continues to play an invaluable role in the developing field of biological mass spectrometry.[13]

Ion Beams

Plasma-desorption

As previously mentioned, the first example of an energy-sudden ionization method for mass spectrometry can be found in the landmark work of Macfarlane and co-workers.[4,5] The PD-MS instrument, which consists of a ^{252}Cf source, sample foil, and time-of-flight (TOF) mass analyzer is presented in Figure 1-3.[5] ^{252}Cf has a 2.6 year half-life with 3% of the decay occurring by means of fission.[20] In PD-MS, a random fission event of ^{252}Cf produces two fragments traveling in opposite directions, one used for the time zero marker for the TOF measurement and the other to impart energy into the thin sample foil. Figure 1-4 displays the interaction of the fission fragments with the thin sample foil, where the fragment impinges on the backside and induces desorption/ionization.[5]

A PD-MS mass spectrum is displayed in Figure 1-5, where the sample was prepared by placing 2 μg of gramicidin (Figure 1-5A) and cyanocobalamin (Figure 1-5B) on the 1 μm thick Ni foil. Both the protonated and sodiated

molecule of gramicidin can be observed in Figure 1-5A. At the time the observation of the protonated molecule of such a large species was a considerable accomplishment, notwithstanding the fact that the low signal-to-noise spectra each represent the accumulation of 2 hours of data.

Though PD-MS clearly presented advantages for the analysis of biomolecules, it never ascended to a widespread level of success and application. Primary reasons for its lack of popularity included the use of radioactive ^{252}Cf, difficult sample preparation (a necessity for thin films), long acquisition times, and random ionization events. Regardless of its limited application, PD-MS represented a novel approach for extending the mass-range and applicability of mass spectrometry.

Secondary-ionization mass spectrometry

Shortly after the introduction of PD, primary ion beams, which ejected secondary ions for mass spectrometry (SIMS), were utilized to effect the desorption/ionization of organic molecules.[21-22] Prior to that, primary ion beams had been used for surface characterization of inorganic species via desorption/ionization of the more rugged atoms and molecules. It was a reduction of the ion flux that allowed for the desorption/ionization of the more fragile organic species. This new reduced flux method was coined static-SIMS, where the beam current density was lowered by approximately 5 orders of magnitude.[23]

Sample preparation for early SIMS experiments consisted of depositing sample material on top of a target, but the incident ion beam impinged on the
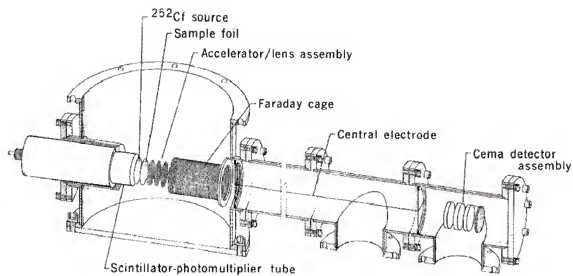
Figure 1-3. Schematic of a PD-TOF mass spectrometer.[5]
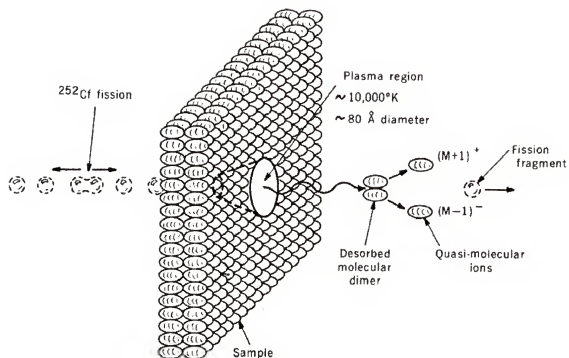
Figure 1-4. Proposed interaction of fission fragments with thin sample foil.[5]
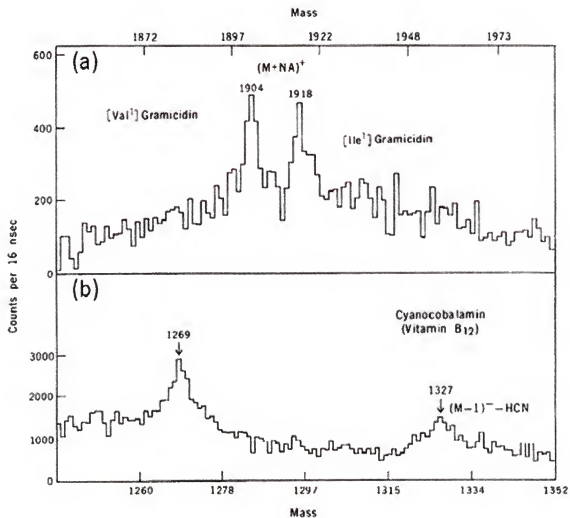
Figure 1-5. PD-MD mass spectra. (A) Positive ion mass spectrum of 2 μg gramicidin, and (B) the negative ion mass spectrum of 2 μg cyanocobalamin (vitamin B_{12}).[5]

front side of the target (sample side) rather than the backside of a target foil as in PD. A representative SIMS mass spectrum of vitamin B_{12} is presented in Figure 1-6.[24] For biological mass spectrometry, the SIMS method has generated relatively little impact. Certainly the method presented clear advantages over the PD technique; however, problems such as sample charging (due to irradiation with charged species) were persistent.

Atom Bombardment

To overcome the surface charging problem encountered in SIMS, Barber and co-workers utilized a fast beam of neutral atoms rather than ions for desorption/ionization.[9,10] To generate an atom beam, a cold cathode discharge ion source produced Ar^+ ions, which were then passed through a collision chamber (~ 1 mtorr) of Ar gas where neutralization occurred via charge exchange. This fast-atom beam was then directed to the sample-side of a target to effect desorption/ionization. A diagram of a FAB ion source is shown in Figure 1-7.[10]

Very rapidly after the introduction of FAB the practical working mass range of mass spectrometry was essentially doubled to ~ m/z 2,000 and later extended to ~ m/z 10,000. Besides the practicality and extended mass range capability of the FAB source, Barber and co-workers introduced another key concept, further elevating the desorption/ionization methods.[26] This distinctive addition was the incorporation of a matrix to contain the analyte of interest (most often glycerol). Though not fully-appreciated at the time, use of the matrix was pivotal to the success and evolution of the energy-sudden approach. A representative FAB mass spectrum of the large organic molecule vancomycin is presented in Figure

1-8.[24] FAB-MS, introduced in 1981, rapidly developed into the most widely
accepted desorption/ionization technique until the arrival of matrix-assisted laser-
desorption ionization (MALDI) in 1986.

Photon Beams

Laser desorption/ionization

Laser irradiation of organic surfaces for mass spectrometry was reported
as early as 1966 by Vastola et al., long before any of the above described
desorption/ionization methods were first discovered.[27] However, the scope of the
method at that time was limited to the analysis of organic salts, pre-charged
species of relatively low mass.[28-31] The first direct application of laser
desorption/ionization (LDI) for polar non-volatile biological molecules was
presented nearly a decade later by Posthumus and co-workers.[8] A CO_2 laser, at
10.6 μm, was used to desorb/ionize sample molecules placed neat on a stainless
steel target. The LDI-MS mass spectra of several molecules with MW < 1000
daltons were presented. Most often sodiated molecular ions were observed, with
a significant amount of fragmentation present in the mass spectra. Nonetheless,
this early work demonstrated that photons, like ion, and atom beams could be
used as a vehicle for rapid energy deposition.

2-step laser desorption/ionization

Shortly after this first LDI-MS application to biomolecules, Van Breeman et
al.[32] and Cotter[33] reported that a significant number of neutral molecules were
produced as a result of a laser desorption event and that these neutral molecules
had a longer lifetime in an ion source. Specifically, they demonstrated that laser
desorption ions were generated for a period of ~ 1 μs, while neutral molecules

were observed for 100s of μs (Figure 1-9). To exploit these desorbed neutral molecules, Cotter performed laser desorption in a chemical ionization source (LD/CI, P ~ 0.5 torr) where the desorbed neutral molecules were ionized with reagent ions from a chemical ionization gas.[33]

This concept of decoupling desorption from ionization marked a significant departure from the previous energy-sudden approaches where desorption/ionization was intimately entwined. In the following years, several different strategies were used to ionize a population of neutral molecules produced by a laser desorption event. These methods included electron ionization,[32] chemical ionization,[33-35] and resonant multiphoton ionization.[36-39] Even though the ionization method in each of these cases was different, the idea was the same: decoupling of the desorption and the ionization processes allows for the individual optimization of the two steps with increased efficiency and selectivity.

Matrix-assisted laser desorption/ionization

Despite the advantages that came from the decoupling of laser desorption from the ionization processes, these techniques were successful in desorbing only a few, relatively small peptides. The desorption event, which often induced fragmentation and decomposition, was the limiting factor for the production of gas-phase neutral biomolecules and peptides. The reason for the dissociation can be attributed to the fact that the resonant excitation of the analyte required for desorption is also directed into photo-dissociation pathways, generating practical mass limits of ~ 1000 Da for biopolymers.[40] This limitation was

overcome with the discovery that by using an absorbing, acidic matrix, biomolecules and peptides contained within that matrix could be desorbed/ionized (MALDI), producing intact molecular ions with little fragmentation.[11,12] Since that time MALDI has become one of the most important ionization methods for biomolecules. Figure 1-10 displays a MALDI-MS mass spectrum of porcine trypsin where a peak arising from the protonated molecule can be easily observed with no obvious fragmentation.[12] Today, mass analyzers coupled with the technique are able to provide markedly improved mass resolution and accuracy.

With the advent of MALDI and another important ionization method, electrospray (ESI),[41] the 1990s saw the inception of a new field, coined biological mass spectrometry, which has spurred an unprecedented interest in the technique. This mass spectrometric revolution can be directly correlated with the invention of these two novel and often complementary ionization methods. With these ionization sources, mass spectrometers are capable of analyzing peptides, proteins, sugars, nucleotides, and oligonucleotides with high sensitivity making mass spectrometry an invaluable tool in the burgeoning field of biotechnology.

A most unfortunate consequence of this rapid and widespread acceptance has been the neglect of fundamental research aimed to understand the ionization processes involved in MALDI, and to a somewhat lesser extent in ESI. Specifically for MALDI, there remains no agreement on a single mechanism that can explain why, or exactly how ionization occurs. In contrast to the desorption step, which is reasonably well characterized, the processes involved in ionization
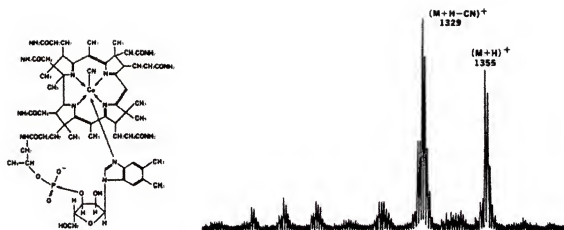
Figure 1-6. Structure of vitamin B$_{12}$ and its secondary ion mass spectrum.[24]
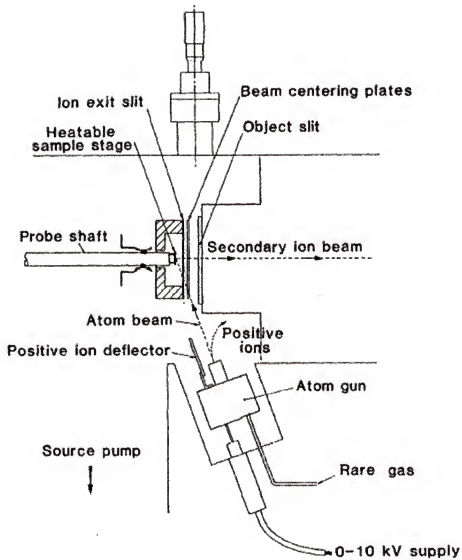
Figure 1-7. Schematic of a FAB ion source.[25]

Figure 1-8. Structure of vancomycin and its FAB-MS mass spectrum (MW = 1449).[24]

I DESORPTION FROM THE SURFACE

→|← 40 nS   Laser pulse

→ ← ~ 1μS   Ion desorbed

Neutral molecules desorbed

→   ← ~ 100μS
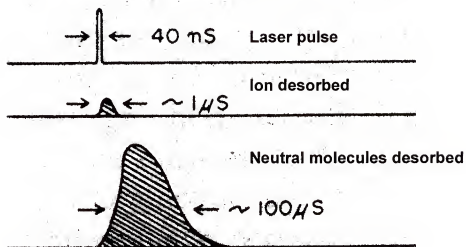
Figure 1-9. Temporal profiles of laser pulse, observed ions, and observed desorbed neutral molecules.[32]
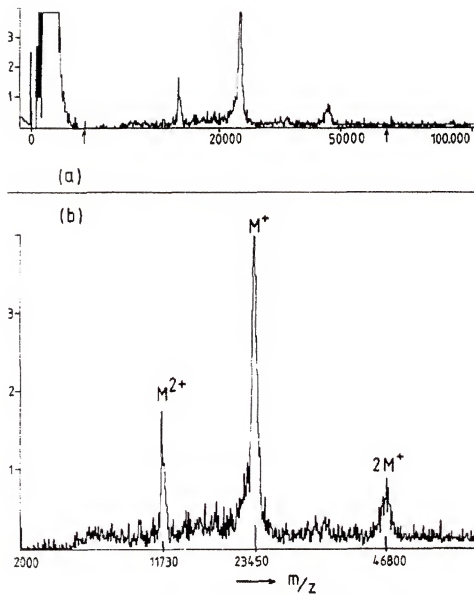
Figure 1-10. MALDI mass spectrum of porcine trypsin with (A) displaying the full-mass range (note the intense matrix background signal at m/z < 1000) and (B) presenting the molecular ion region.[12]

during MALDI continue to be debated.[42-49] One of the problems that has hindered the development of a unified model for MALDI is that for a variety of laser wavelengths (266 nm - 10.6 μm), laser pulse durations (120 fs – 100 ns), and matrix preparations, MALDI mass spectra are remarkably similar.[47] Zenobi and Knochenmuss presented a "standard model" for ionization in MALDI that will be briefly discussed below.[48]

For UV MALDI (where desorption occurs via delivery of UV photons) certain aromatic acid matrixes work with the most success, due to their high absorption in the UV. And because the matrix species is in a large excess, incident radiation will by probability almost always encounter matrix molecules (M) as it impinges the surface, effecting ionization as follows:

$$M + n(h\nu) \rightarrow M^{+} + e^{-+} \qquad\qquad 1.1$$

Equation 1.1 represents the most straightforward mechanism, that of multiphoton ionization of the ground-state matrix molecules. However, the multiple photon steps are argued to be unlikely because MALDI fluences are said to be too low.[45] And recent work by Papatanokis et al. using femtosecond laser pulse widths also raises questions regarding the validity of Equation 1.1, with the authors arguing that the multi-photon process could not occur on such short time-scales.[47] Equation 1.2 represents the resonant excitation of a ground-state

$$M + h\nu \rightarrow M^{*} \qquad\qquad 1.2$$

matrix molecule; a process that is statistically favored over Equation. 1.1. The excited matrix molecule could then participate in energy pooling (interaction of two excited matrix molecules) to form a more highly excited matrix molecule:

$$M^* + M^* \rightarrow M^{**} + M \qquad\qquad 1.3$$

The highly excited matrix molecule formed in Equation 1.3 can undergo direct ionization as shown in Equation 1.4, if its energy exceeds its ionization potential (IP), or if not, it could undergo collisional ionization, as shown in Equation 1.5:

$$M^{**} \rightarrow M^+ + e^- \qquad\qquad 1.4$$

$$M^{**} + M \rightarrow M^+ + M + e^- \qquad\qquad 1.5$$
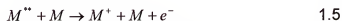
At this point, ionization of the analyte could occur via charge transfer, Equation 1.6, or proton transfer, Equation 1.7.

$$M^+ + A \rightarrow A^+ + M \qquad\qquad 1.6$$

$$MH^+ + A \rightarrow AH^+ + M \qquad\qquad 1.7$$

Note that these suggested pathways are only proposed mechanisms that continue to be the subject of considerable debate. Other recent work has suggested that ionization in MALDI is the result of desorption of highly charged clusters of matrix and analyte, where ionization of the analyte is effected by evaporation of the matrix.[48]

There is one aspect of the MALDI process that is clear – the matrix plays a crucial role in effecting both desorption and ionization. It is for this reason that only a few MALDI compatible matrixes have been identified over the past decade. Therefore, it can be said that MALDI, like its energy-sudden predecessors, involves a process in which desorption/ionization are intimately entwined. Today, end-users armed with a dozen or so common MALDI matrix compounds typically report special concoctions of matrix molecules, acid-

additives, and analytes to acquire MALDI-MS spectra, with optimal mixtures varying greatly from one molecule to the next.

Mass Analyzers for Energy-Sudden Ionization

Time-of-Flight Mass Spectrometry

Since the introduction of the energy-sudden ionization methods, virtually every type of mass analyzer available has been combined with them. Examples of such coupling include time-of-flight (TOF),[3,4,8,11,12] quadrupole,[34] Fourier transform,[35,50,51] orthogonal-acceleration-TOF (oa-TOF),[52,53] sector-TOF,[54] quadrupole ion trap-TOF,[55,56] and quadrupole ion trap (QIT)[68-111] mass analyzers. Of these, the mass analyzer that has received the most use with the pulsed energy-sudden methods is the TOF. Because the TOF mass analyzer has a theoretically unlimited mass range, it was the obvious method of choice during the early development of the energy-sudden methods, ionization methods whose aim was to desorb/ionize species of exceedingly high mass. Simplicity and its requirement of pulsed injection events also made it particularly well-suited for the new pulsed ion generation methods.

Notwithstanding these favorable attributes, there are some limitations of the TOF measurement that have generated interest in alternative types of mass analysis. In MALDI, ions are typically generated with a wide-spread of kinetic energy and spatial distribution within the source. These variations limit the achievable mass accuracy and resolution, since the TOF measurement assumes identical m/z's have identical kinetic energy and therefore time-of-flight. In MALDI-TOF mass spectrometers today, this problem has been somewhat relieved by a technique called delayed extraction, a method where the ion

extraction pulse is delayed to help reduce initial kinetic energy distributions.[58-60] But even with these improvements mass accuracy and resolution are still sensitive to sample thickness, position, and laser fluence.

A second detriment that has limited the potency of the TOF mass measurement is its inability to perform multiple stages of mass spectrometry. Often times, identification of a protein or peptide cannot be made based solely on mass, especially when sampling directly from complex mixtures where significant chemical noise can be problematic. To overcome these limitations several research groups have spent the last decade developing methods to couple the pulsed energy-sudden ionization methods with the QIT mass spectrometer.

Quadrupole Ion Trap-Mass Spectrometry

Quadrupole ion trap history

The QIT, along with the quadrupole mass filter, was invented in 1956 by Wolfgang Paul and Helmut Steinwedel, who shared the 1989 Nobel Prize for Physics for this significant contribution.[60,61] Figure 1-11 displays a cross-section of a QIT mass spectrometer. The QIT consists of three electrodes, a ring and two endcaps, where ions can be confined to the volume in-between. Unlike the quadrupole mass filter, which was rapidly developed and applied in the field of mass spectrometry, the QIT was for the most part restricted to the physics community until the mid-80's. Before that time the QIT was primarily operated in the "mass-selective stability" mode where the voltages applied to the electrodes were slowly increased to allow storage of a single increasing m/z, much like operation in a quadrupole mass filter.[62]
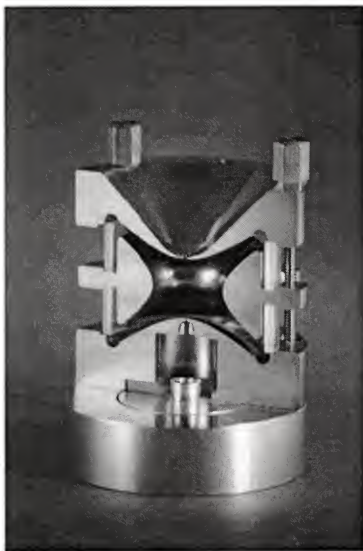
Figure 1-11. Cross-section of a quadrupole ion trap mass analyzer.

In 1983, Stafford et al. reported a new method of QIT operation called "mass-selective instability" where the full-range of m/z's were stored in the trap and then sequentially ejected to generate a complete mass spectrum.[63] Those researchers also discovered that by use of a He buffer gas l(~ 1 mtorr) inside the trap, mass resolution and sensitivity could be enhanced because the ions were collisionally focused to the center of the trap.[64,65] Shortly afterwards tandem MS capability was demonstrated on the QIT.[66] Tandem mass spectrometry was performed by trapping a wide range of m/z's, followed by isolation of the m/z window of interest, dissociation of the precursor ion, and finally mass analysis of the fragment ions. Unlike tandem-in-space mass spectrometers (e.g., triple quadrupole), the QIT is a tandem-in-time instrument that can perform multiple stages of mass spectrometry (MS[n]) within the confines of one device.

Basic quadrupole ion trap theory

In the QIT, an oscillating electric potential (RF) is used to generate a potential well inside the trapping volume that focuses ions into the center of the device. Once inside that potential well, an ion attempting to depart will experience a restoring force that increases linearly the further it travels from the center of the trap. Equation 1.8 can be used to calculate the potential at any given point inside the trap.

$$\Phi(r,z) = \frac{(U - V\cos\Omega t)}{2}\left[\frac{r^2 - 2z^2}{r^2_o}\right] + \frac{(U - V\cos\Omega t)}{2} \qquad 1.8$$

In this equation U is the amplitude of a DC offset applied to the endcaps, V is the amplitude of the RF applied to the ring, ω is the angular frequency of the

RF, and r_o is the distance between the center of the trap and the ring electrode. Equation 1.9 predicts the force on an ion in an electric field.

$$\vec{F}(r,z) = \vec{E}(r,z) = -e\vec{\nabla}\Phi(r,z) = m\vec{a}(r,z) \qquad 1.9$$

Equation 1.9 can be put into the form of a second-order linear differential equation named the Mathieu equation (Equation 1.13) by using the substitutions outlined in Equations 1.10 – 1.12.

$$a_z = -2a_r = \frac{-16eU}{m(r^2{}_o + 2z^2{}_o)\Omega^2} \qquad 1.10$$

$$q_z = -2q_r = \frac{-8eV}{m(r^2{}_o + 2z^2{}_o)\Omega^2} \qquad 1.11$$

$$\zeta = \frac{\Omega t}{2} \qquad 1.12$$

$$\frac{d^2u}{d\zeta^2} + (a_u - 2q_u\cos 2\zeta)u = 0 \qquad 1.13$$

The solutions to the Mathieu equation determine the ion trajectories; some of the ion trajectories can cause ions to be trapped and those regions are defined by the parameters a_z and q_z. Figure 1-12 shows one of those regions of stability and is referred to as a stability diagram. The cross-hatched region on the plot indicates overlapping areas where ions will be stable in both the axial dimension (z) and the radial dimension (r). In the mass-selective instability scan mode, the ion trap is operated along the $a_z = 0$ line, as shown in the figure. In that mode, masses become unstable and are ejected in the radial dimension when they reach the edge of the stability region ($q_{eject} = 0.908$). Recall that from Equation 1.11, for a given set of trapping conditions, the value of the q_z parameter will vary

as a function of mass. Therefore ions can be ejected from the trap sequentially in order of increasing mass by ramping the amplitude of the RF (V) to generate a mass spectrum. Equation 1.14 shows the relationship of m/z to V.

$$\frac{m}{z} \propto \frac{V}{q_z}$$ 1.14

In the late 80s a new method to increase mass resolution was developed called resonance ejection.[65,67] This method uses a supplementary AC waveform supplied to the endcap electrodes during the mass analysis RF ramp. When the ions become excited by the main RF, just prior to ejection, they come into resonance with the supplementary AC and are ejected in a more efficient manner causing an increase in mass resolution. Today QIT mass spectrometers, incorporating these fundamental operating principles, are capable of unit mass resolution and have typical working mass ranges of 15 – 2000 m/z.

Laser Desorption-Quadrupole Ion Trap-Mass Spectrometry

From the onset of the energy-sudden ionization methods the most obvious method of mass analysis, and therefore almost exclusively employed, was via a simple TOF measurement. However, after the invention of MALDI and the development of quadrupole ion trap (QIT) technology in the mid-80s, it became evident that the QIT presented numerous advantages, making it an attractive candidate for coupling to the pulsed laser desorption methods. At first glance it would seem that the QIT, a scanning type mass analyzer, would be a mismatch for a pulsed ionization method like MALDI; however, because the QIT functions as a storage device, an entire pulse of desorbed ions can be stored inside the
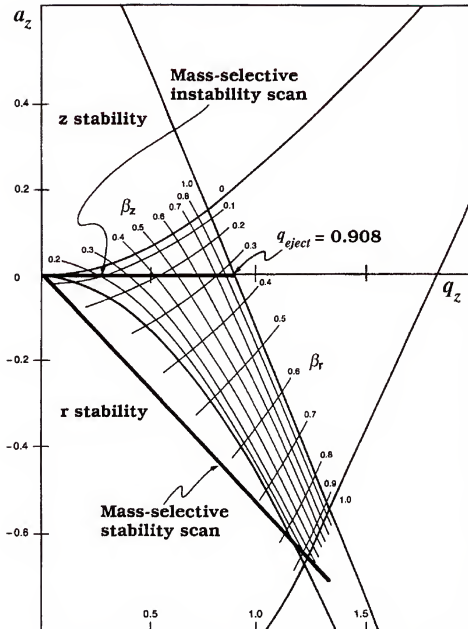
Figure 1-12. Stability diagram where the cross-hatched region indicates areas in which ions will be stable in both the axial dimension (z) and the radial dimension (r).[62]

trap, after which mass analysis can be performed. A second inherent strength possessed by the QIT is the capability for multiple stages of mass spectrometry (MS[n]).[64,66] The tandem mass spectrometry capabilities of the QIT make it an inviting choice for LD ionization because the large chemical noise background often created during LD can be conveniently removed.

The potential of the QIT as a mass analyzer for LD was first realized in 1989 by Heller and co-workers[68] and Louris et al.[69] In these first reports two different approaches for coupling LD-QIT-MS were outlined, the first method involving the LD inside the trap[68] and the second performing LD external to the trap with subsequent ion injection.[69] During the early 90s several research groups pursued development along both lines - today the latter approach has been demonstrated to be most advantageous.

Internal LD-QIT-MS

Development of internal LD-QIT-MS has mainly been the effort of three research groups: Cotter and co-workers,[68,70-74] Glish et al.,[75,76] and Hemberger and co-workers,[77-79] amongst a few others.[80-83] In each of these reports, with one exception,[81] delivery of photons was made possible by drilling a hole through the entire length of the QIT ring electrode (as shown in Figure 1-13).[77] A sample probe was then inserted in one side, placing the center of the sample on the apex of the ring electrode. Laser irradiation of the sample was achieved by focusing a photon beam through the opposite hole and onto the target. By rotation of the target, new sample could be exposed to the irradiation after the original spot was consumed.
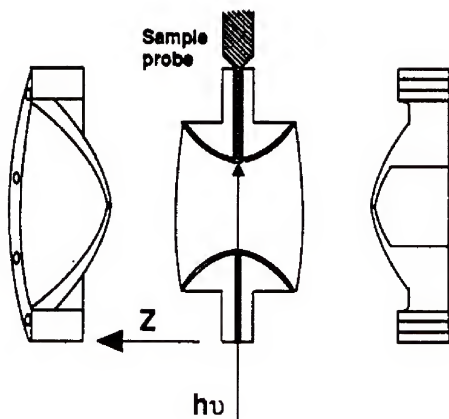
Figure 1-13. Schematic of an internal laser desorption-quadrupole ion trap mass analyzer where the target is located in a hole in the ring electrode.[77]

Using the internal ionization method, Cotter and co-workers reported the first direct coupling of MALDI to a QIT mass spectrometer.[70] However, in that report it was apparent that several aspects of the internal ionization experiment would require further development. Earlier experiments by Beavis and Chait (with different instrumentation) demonstrated that for MALDI, the kinetic energy of ions increased with increasing mass.[84] Because higher masses have larger kinetic energies, they were difficult to trap upon desorption/ionization within the confines of the QIT. Both Cotter et al. and Glish and co-workers reported the use of gas pulses to increase the pressure within the trap during desorption to help collisionally cool the ions.[74,76] Each demonstrated that elevating the QIT pressure did help increase the trapping efficiency, but pressure pulsing on such a rapid time scale was clearly an impractical solution. Cotter and Doroshenko also suggested the application of stored waveforms[71] and modifications of the ion injection RF voltages, which they dubbed controlled gating of the trapping field (CGTF),[72] to overcome the ion trapping problem; neither of the approaches has allowed the internal desorption method to become mainstream technique. Another significant problem presented by the internal desorption method is that of sample movement. Because the sample is confined to a small hole within the ring electrode, the only means for movement is target rotation.

External LD-QIT-MS

At the same time as the internal laser desorption experiments were being developed, numerous other research groups constructed and developed laser desorption sources that performed the desorption external to the ion trap.[69,85-101] These researchers correctly recognized that external ion generation would afford

greater opportunity for the collisional cooling of ions following the desorption event. Also of significance was that sample movement would not be the subject of restrictions, as in the case for the internal desorption experiment.

One of the first reported external laser desorption/QIT-MS interfaces can be seen in Figure 1-14.[85] Here the sample was inserted into the vacuum chamber using a probe interlock. On the end of the probe was a fiber optic for photon delivery and a flat target where the sample was placed. In that initial work no lens system was used for focusing of the desorbed ions into the QIT. Shortly after that, Schwartz and Bier presented a similar method, but added a set of focusing lenses to assist the transport of the desorbed ions into the mass analyzer.[86] Using that arrangement the authors presented MALDI-QIT-MS mass spectra of biomolecules and proteins as large as 40,000 daltons. Development of the external arrangement continued along these lines throughout the mid-90s, with several research groups reporting a variety of modest alterations.[87-96]

In the late-90s some noteworthy rearrangements of the original external desorption-QIT were reported.[97-101] In 1999, Troendle and co-workers at the University of Florida, reported the design and construction of a new LD-QIT-MS system, with a diagram of this instrument presented in Figure 1-15.[97] In this device, the sample was inserted through a vacuum interlock, on the end of a probe, and into a set of focusing lenses. A photon beam was brought into the vacuum chamber and deposited in an orthogonal fashion onto the target. The desorbed ion species were then extracted with the lens set, turned 90 degrees, and deposited into the QIT. While similar in that desorption was performed
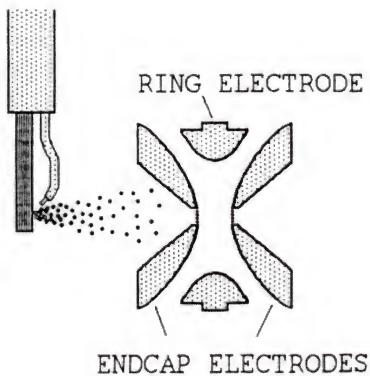
Figure 1-14. An early external laser desorption-quadrupole ion trap interface.[85]
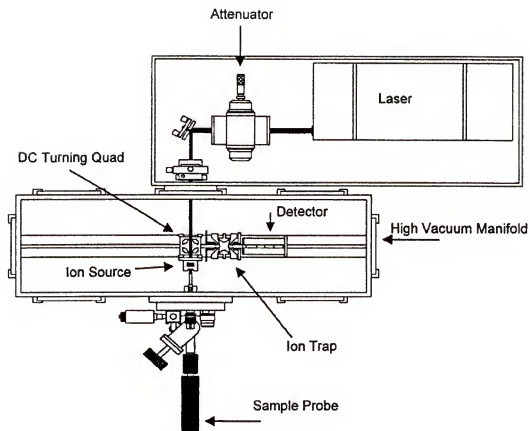
Figure 1-15. Another external laser desorption-quadrupole ion trap mass spectrometer design.[97]

external to the vacuum system, those researchers invested a significant effort to assure an orthogonal beam angle, which was of importance for possible mapping and imaging studies.

Other variations on the original external desorption QIT arrangement can be found in the work of Chait et al.[98,99] These researchers modified a Finnigan LCQ ion trap mass spectrometer, one that possesses an atmospheric pressure (AP) inlet to allow transport of AP generated ions, to accept a rotating compact disc (CD) which served as a MALDI target. This instrument can be viewed in Figure 1-16, where the rotating MALDI CD was placed in the region between the quadrupole and skimmer inlet of the mass spectrometer.[98] Because the pressure in the region where the desorption/ionization occurs was about an order of magnitude higher than in the QIT region, the MALDI generated ions were more efficiently cooled than in previous LD-QIT experiments. Though the instrument required extensive modification of the mass spectrometer, the authors reported that switching between the MALDI method and the standard API methods could be rapid and convenient.

The concept of a multi-purpose instrument that could accommodate both laser desorption experiments and other routine ionization methods was first realized and described by Lennon and Glish in 1997.[100] In that work, they presented a MALDI probe that could be inserted into an EI/CI source (Figure 1-17). A fiber optic was run down the length of the probe and was used to impinge photons on the backside of a target, where a MALDI matrix/analyte mixture was placed. The method has not been particularly useful because it requires
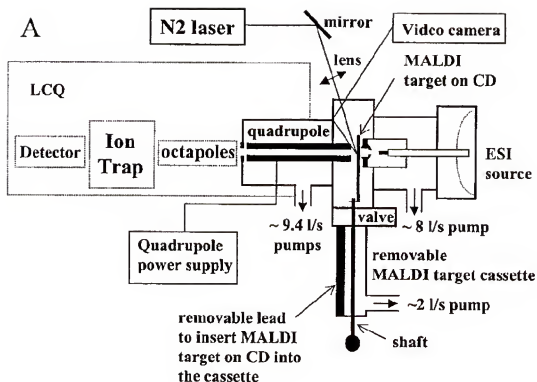
Figure 1-16. A modified AP-inlet ion trap instrument for performing MALDI-MS. Here the sample is placed on a CD that is inserted in-between the quadrupole and skimmer inlet.[98]
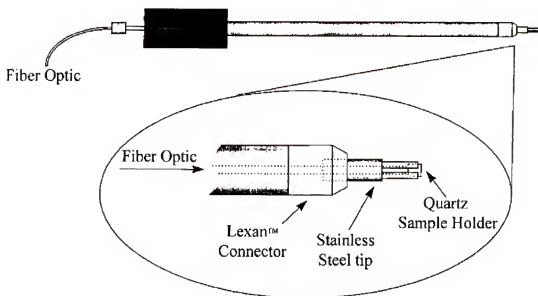
Figure 1-17. A MALDI probe that can be inserted into an EI/CI source of a quadrupole ion trap mass spectrometer.[100]

extremely thin layers of sample for successful desorption/ionization; however, their intimation of a versatile mass spectrometer with interchangeable ion sources has proven much more practical.

In 2000, researchers at the University of California, San Francisco introduced a novel concept in MALDI mass spectrometry.[102] This new idea was that MALDI could be performed at atmospheric pressure (AP-MALDI) where the desorbed ions could be sampled into a mass spectrometer using a standard AP inlet designed for ESI. AP-MALDI capitalizes on the multi-purpose instrument concept of Lennon and Glish, but does so with magnified practicality. ESI and MALDI are the two ionization methods currently employed for biological mass spectrometry, where one functions at AP and requires a mass spectrometer with an AP inlet (ESI), and the other operates in vacuum and requires a different type of mass spectrometer (MALDI). Now, with the ability to perform MALDI at AP, one mass spectrometer can be used for both methods, thus creating a single instrument capable of both important ionization modes.

That initial work was performed on an oa-TOF mass spectrometer; however, researchers quickly realized the ideal mass analyzer for the new AP-MALDI method was the QIT.[103-110] A schematic of an AP-MALDI interface for an QIT can be found in Figure 1-18, here the sample is affixed to a moveable target that is placed in front of the AP inlet on a QIT mass spectrometer.[103] In this fashion the laser can be pulsed onto the target causing the desorption/ionization of the sample. Because of the QIT's unique ability to store ions for an adjustable period of time before mass analysis, the QIT has been used almost exclusively
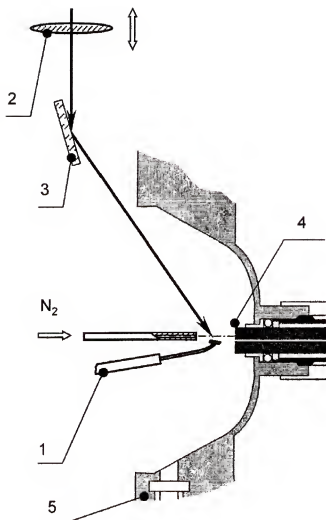
Figure 1-18. AP-MALDI source where after laser desorption/ionization, ions are transported into vacuum and deposited into a quadrupole ion trap for mass analysis: (1) target holder, (2) quartz lens, (3) mirror, (4) stainless steel capillary inlet, (5) inlet flange.[103]

for AP-MALDI. For example, with the laser firing at a 10 Hz repetition rate, the ion trap can be left open to ion accumulation for 1 second, which would allow the accumulation of ~ 10 laser pulses of desorbed ions prior to mass analysis. Multiple pulses per an ion accumulation period can enhance signal and thereby increase sensitivity.

The QIT also offers the ability to perform several stages of mass spectrometry, a method that can be invaluable for peptide sequencing and identification. This is a welcome improvement for MALDI-MS since MALDI-TOF instruments do not possess that capability. There are some limitations of the AP-MALDI-QIT-MS method, the most substantial being the limited mass range (< 2000 m/z) offered by commercial QIT's. This essentially limits AP-MALDI-QIT-MS to the analysis of lower molecular weight peptides, rather than intact proteins. Another area of concern for AP-MALDI-QIT-MS is sensitivity. Despite the ability to take multiple laser pulses per an ion accumulation period, sensitivity of the technique is still 2 -3 orders of magnitude lower than can be achieved with the tradition MALDI-TOF instrumentation.

Mass Spectrometric Imaging

A unique opportunity presented by the energy-sudden ionization methods is one of mass spectrometric imaging directly from a condensed phase substrate. Because the energy deposition vehicles (e.g., photon and ion beams) can be focused and deposited into specific target areas, the corresponding mass spectral assemblies of these discrete events can create specific ion images. The field of mass spectrometric imaging was first realized by use of laser microprobe mass spectrometry (LMMS), where the majority of application has

involved the imaging of small-rugged organic and inorganic species from biological tissue.[111-114] To analyze the more complicated and fragile organic and biological molecules, ion beams for SIMS imaging[115-122] and photon beams for MALDI-MS imaging[123-144] have been employed.

SIMS Imaging

In SIMS imaging, the incident static-ion beam is rastered across the sample with the sputtered secondary ions most often detected with a TOF mass spectrometer.[115,116] The incident ion beam can be focused to spot sizes as small as 10 nanometers, with sample penetration approximately 20 nanometers; however, typical working ranges are from 0.1 to 30 microns.[115] For all imaging experiments, there exists a tradeoff between spatial resolution (spot size) and sensitivity. This is always the case since sufficient ion current must be generated from the spot to produce a detectable signal.

Because ion beams are not able to desorb/ionize large biomolecules (m/z > 1000) SIMS imaging experiments are most often utilized for the analysis of smaller organic species. Another major drawback observed when using static ion beams, though not common in laser sampling, is the induction of chemical changes on the surface of the sample. As a result, depth profiling is not possible with static ion beams. Because of its inability to depth profile and produce a high yield of sputtered ions (due to limited beam penetration), the static ion beam has found limited use as a surface technique where the analyte is a major component.[117-122] Finally, because the method requires bombardment with high-energy incident ions, the imaging must be performed under high vacuum conditions.

MALDI-MS-Imaging

In contrast, laser beams are typically focused to ~ 25 μm, and can penetrate the sample surface by as little as 20 nm or to as much as several microns, depending on the sample surface, wavelength, and laser fluence used.[115] Therefore, applications involving the detection of trace level components require the somewhat relaxed spatial resolution provided by laser sampling on account of the increased sampling volume. And to allow the analysis of larger molecules, a MALDI matrix is typically deposited onto the surface to be imaged, with great care not to disrupt the spatial location of the analyte in the process. The MALDI-MS-imaging method has been applied for the imaging of biomolecules from tissue,[123-129] for coupling thin-layer chromatography (TLC) to MS,[130-134] and to profile polyacrylamide gel electrophoresis (PAGE) by MS.[135-144]

Imaging biological tissues

The premise of this method is to provide detailed spatial distribution information that has the potential to answer questions regarding site-specific transport, bioaccumulation, and biotransformation of biologically relevant compounds. Caprioli et al. have even reported that altered chemical/molecular distributions can be used to diagnose diseases such as stroke, cancer, and alcoholism.[123,126] But, because the technique requires a thin-slice of an organ or tissue, a more realistic application of the method is to identify the up- or down-regulated molecules from the diseased tissue as compared to the control.

Figure 1-19 displays a series of MALDI-MS ion density maps for four
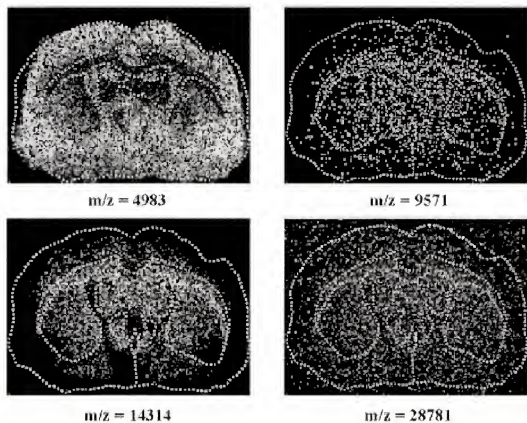
Figure 1-19. MALDI-MS ion density maps for four proteins imaged from a thin-section of rat brain.[115]

proteins imaged from a rat brain section.[115] A protein with m/z 4,983 is observed throughout the brain section while the protein at m/z 14,314 is confined to the interior regions. It should be noted that this section was imaged only once with each plot representing the signal of a selected m/z vs. position. Imaging entire tissue sections can generate an enormous amount of data, and consequently software and data processing limitations have been areas of continued development.[127]

Coupling with planar chromatography

The first reported application of MALDI-MS-imaging was in 1995 by Hercules and co-workers.[130] In that work, compounds were separated using thin-layer chromatography (TLC), after which the TLC plate was coated with a MALDI matrix and imaged. Plots of ion current vs. location provided the position of the analyte bands; however, molecular weight information could also be obtained by viewing the mass spectrum from the spot of interest. Since that first report several others have reported similar methods for directly imaging TLC plates.[131-134]

Polyacrylamide gel electrophoresis (PAGE) is another type of planar chromatography where proteins and peptides can be isolated and characterized. Most often the gel is stained following electrophoresis to visualize the individual protein bands, the bands are excised, the stain removed, the protein enzymatically digested, followed by the extraction of the digested protein for eventual mass spectrometric analysis. With the recent publication of the MALDI-MS-imaging work of Hercules et al., it became clear that PAGE should also be compatible for direct mass spectrometric imaging experiments. For MALDI-MS-

imaging of gels two main strategies have emerged: the first involves placing the matrix on the gel,[135-138] and the second transfers the proteins onto a membrane which is then coated with a matrix compound.[139-144]

Altogether MALDI-MS-imaging is conceptually inviting, but it has numerous practical issues that have limited its widespread application. A significant concern is how to apply the matrix without disrupting the analyte's spatial distribution, the very subject of the experiment. The matrix is typically deposited onto the surface as a solute in an organic solvent. The solvent must extract the analyte from the surface before it evaporates to achieve co-crystallization of the matrix/analyte. Too much solvent will cause elevated analyte signal, but at the same time can cause the analyte to migrate from its original location; too little solvent will not extract the analyte resulting in the absence of analyte signal, but spatial resolution will be preserved. Therefore, application of the matrix is critical with optimal methods varying widely upon the analyte and the substrate from which it is contained.

Another problem for MALDI-MS-imaging is that all experiments have been performed under vacuum MALDI conditions. Vacuum sampling presents numerous issues that further complicate the imaging experiment. For example, many samples, such as tissues, tend to shrink and distort upon exposure to vacuum, thereby blurring any subsequently obtained image information. Also, precise control of the sample can be difficult since all mechanical movement stages must be located within the vacuum. With the recent success of AP-MALDI, one might envision these problems could be easily eliminated.

CHAPTER 2
ELECTROSPRAY DEPOSITION OF A MALDI MATRIX FOR IMAGING MASS SPECTROMETRY

Background

Techniques capable of creating images of molecular compounds directly from complex biological samples, such as tissue, could provide important details of site-specific metabolism, compound compartmentalization, bioaccumulation, transport, and regional binding domains.[123-128] Recently, matrix-assisted laser desorption/ionization (MALDI) has been combined with mass spectrometry to map and image analytes such as drug compounds,[97,129,145-149] or proteins and peptides[123-128,150] directly from tissue. To perform imaging via MALDI-MS a variety of methods for matrix deposition have emerged including the dried droplet technique,[123-125] dried membrane blotting,[126,127] and direct electrospray matrix deposition.[123,145-148] For MALDI-MS imaging, the application of matrix would ideally combine the best extraction efficiency of the analyte from the substrate without perturbing the analyte's original spatial distribution. Therefore, matrix application methods, a process that can greatly affect extraction efficiency and the preservation of spatial distribution, are of paramount importance to the development of MALDI-MS imaging.

In the dried droplet approach, matrix dissolved in a solvent is simply deposited onto the surface to be imaged. After application, the solvent slowly evaporates, generating matrix crystals for MALDI-MS analysis. Often the dried-

droplet approach produces matrix crystals of varying sizes, an effect that can cause wide fluctuations in the resulting MALDI-MS signal. This has recently been demonstrated by Sweedler and co-workers who have utilized MS imaging to assess the heterogeneity within matrix crystals prepared via the dried-droplet approach.[124] A further problem that the dried droplet method presents for MALDI-MS imaging is that it can "blur" the analyte's spatial distribution, because the analyte, once extracted, can move freely within the matrix solution before solvent evaporation and incorporation into the matrix crystal structure.[145-146]

More recent MALDI-MS imaging experiments have employed either membrane blotting methods or direct electrospray matrix deposition to avoid the pitfalls of the dried droplet approach. Membrane blotting uses carbon-imbedded conductive polyethylene membranes to blot onto the tissue samples that are to be mapped, which can transfer the analyte to the membrane. Once blotted, the membranes are rinsed and then electrosprayed with a MALDI matrix.[126,127] Alternatively, the matrix can be directly deposited onto the substrate surface using the electrospray deposition method, altogether skipping the blotting step.[123,145-148]

This chapter investigates the characteristics of the matrix application process via electrospray deposition. Specifically, it aims to explore the electrospray matrix deposition factors affecting analyte extraction and spatial distribution preservation during the matrix deposition process.

Experimental

Instrumental

All experiments outlined in this chapter were performed on a laser microprobe quadrupole ion trap mass spectrometer designed and constructed at the University of Florida.[145-147,151] Details of this instrumentation have been outlined elsewhere, and will be briefly highlighted here.[145] The instrument (Figure 2-1) employs a modified Finnigan 4500 EI/CI ion source (San Jose, CA) coupled to a dc quadrupole deflector for turning ions 90° and transmitting them into a Finnigan ITS-40 ion trap for mass analysis. Laser irradiation was accomplished by using a Laser Science (Cambridge, MA) model VSL-337ND pulsed nitrogen laser operating at 337.1 nm. The photon beam was focused to a spot size of ~ 35 μm, using a fused silica plano convex lens (Melles Griot, Irvine, CA) with a focal length of 25.4 cm. For mapping, the instrument was outfitted with an x-y translational stage for micromanipulation of the target with respect to the laser beam.[145]

Data acquisition was achieved through the use of Gatorware, software written at the University of Florida for the ITS-40.[152] For tandem MS experiments, a stored waveform inverse Fourier transform (SWIFT) isolation was used for isolation of ions in the ion trap for the MS/MS experiments.[145] During SWIFT isolation, a model DS345 Stanford Research Systems (Sunnyvale, CA) synthesized function generator was used for waveform generation.
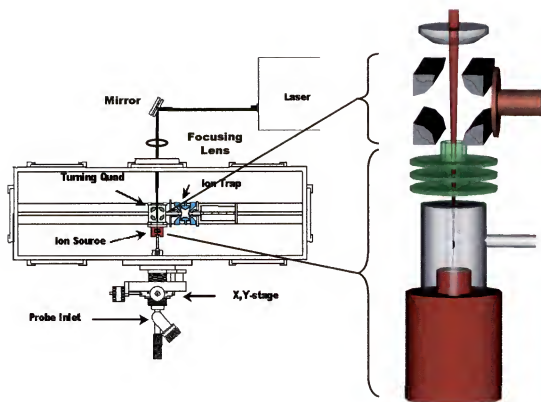
Figure 2-1. Schematic of laser microprobe ion trap mass spectrometer with an exploded view of the target and ion transport regions (drawing not to scale) on the right.

Sample Preparation

All solvents and chemicals used in these experiments were purchased

from Sigma Chemical (St. Louis, MO). Black inkjet refill ink was purchased (Nu-

kote, Franklin, TN) and spiked to a level of 5.27 mg spiperone/g ink. The ink was

subsequently added to an empty HP 51645G black inkjet cartridge (Hewlett

Packard, Palo Alto, CA) . Once filled, the cartridge was placed into a Hewlett

Packard 800 series inkjet printer that was used to print patterns directly onto

white inkjet business paper (Xerox, Rochester, NY).

Printed samples were prepared for analysis by first excising them from the

paper using a 1/8" hole punch. Once excised they were glued onto a stainless

steel target (4 mm diameter surface) with spray adhesive (3M, St. Paul, MN).

Next, the target was placed into an electrospray matrix deposition device.[145] In

this device, the target rested on a grounded turn-table which rotated at ~ 1

revolution per minute with the sample surface ~ 2 cm from the electrospray

needle. Matrix solution, consisting of 10 mg/mL 2,5-dihyroxybenzoic acid (DHB)

in a solvent of varied aqueous/methanol content with 1% acetic acid, was fed into

the electrospray needle via a fused silica capillary at a constant rate of 5 μL/min

with a syringe pump (Harvard Apparatus, South Natick, MA). The electrospray

power supply (Analytica, Branford, CT) was operated at +4.5 kV with

electrospray deposition times of 5 minutes, unless otherwise noted.

Results and Discussion

Detection Of Analyte From Paper Surface

To evaluate the electrospray deposition of MALDI matrix, it was necessary

to develop a model system where an analyte existed only in specific locations

with visible boundaries. For these experiments, a model system consisting of dosed ink applied to paper was chosen. The analyte, spiperone, an anti-psychotic pharmaceutical, was added to the ink reservoir of an inkjet printer. With this arrangement patterns could be drafted on word processing software for printing onto paper, resulting in the generation of user-designed patterns of analyte/ink on paper.

Preliminary studies were aimed towards the detection of spiperone directly from inked areas of the paper. Figure 2-2A shows the MALDI mass spectrum obtained after electrospray deposition of the MALDI matrix solution (70% aqueous methanol with 1% acetic acid) onto the surface of an ink-covered paper. The inset shows a relatively small peak occurring at m/z 396, possibly the protonated molecule of spiperone, making identification at this stage ambiguous. However, with the tandem MS capabilities of the ion trap, this ion was then isolated and fragmented to produce the product ion spectrum presented in Figure 2-2B. Here, product ions at m/z 165, 232, and 291 can be observed. When compared to a reference MS/MS mass spectrum of the spiperone [M+H]$^+$ (Figure 2-2C) identification of the suspect ion as spiperone can be confirmed. Figure 2-2D displays the structure of the spiperone molecule and presents its preferred dissociation pathways.

Analyte Migration During Printing Process

To assess analyte migration during the electrospray matrix deposition process, a simple line pattern was printed onto paper, as can be seen in Figure 2-3. Since there was a possibility that the spiperone migrated outwards on the
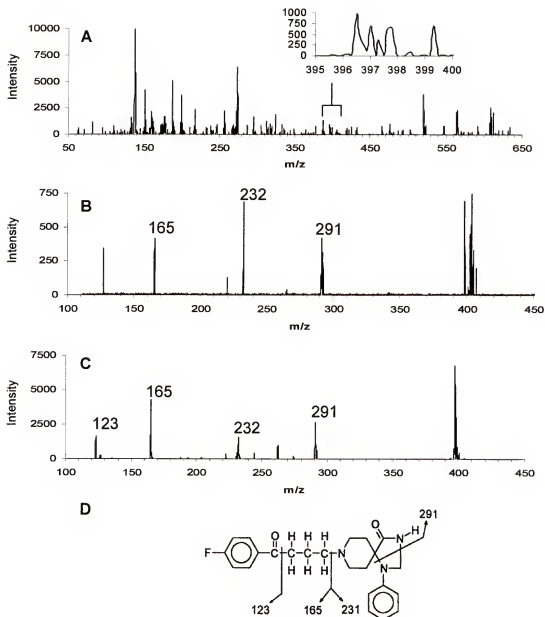
Figure 2-2. Detection of spiperone from inked paper. (A) displays MALDI-MS mass spectrum after desorption from inked paper. (B) shows the resulting product ion mass spectrum of m/z 396. (C) is the product ion spectrum of the m/z 396 ion of a spiperone standard. Diagram (D) shows the fragmentation pathways of the spiperone protonated molecule and was adapted from reference 97.
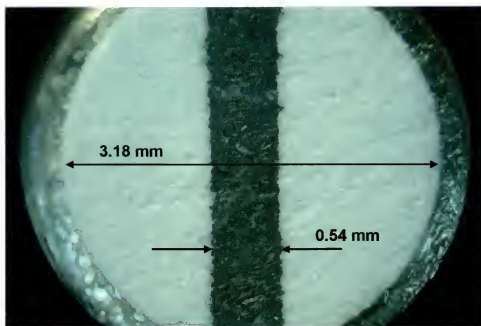
Figure 2-3. Photomicrograph of analyte/ink pattern on paper.

paper, away from the inked line during printing, it was necessary to verify if such migration occurred. To evaluate, two identical portions of paper, each containing a line of ink (~ 540 μm), were glued to two identical targets. After gluing, but prior to the electrospray deposition process, the black stripe shown in Figure 2-4A was excised, whilst the stripe shown in Figure 2-4B was not. Both samples were then electrosprayed with matrix for a period of 8 minutes under identical conditions with a matrix spray solution of 70% aqueous methanol with 1 % acetic acid. Figure 2-4C presents a plot of product ion intensities of the spiperone protonated molecule precursor ion for varying locations across the surface of both samples. Each data point represents the sum of the average of 40 single-shot MS/MS spectra. Analyte signal for the intact stripe analyses does increase at target positions located over the inked surface, while the removed stripe analyses shows no increase above the background at all locations across the surface. These data indicate that no detectable amount of spiperone had migrated prior to the electrospray matrix deposition process.

Electrospray Solution Composition

A close inspection of Figure 2-4C reveals that numerous sampling locations (> 10) produced detectable analyte signal while only 5 positions correspond to sampling over the inked portion (see Figure 2-4B). Therefore, spiperone must have migrated from its initial location, the ink band, during the matrix deposition process. Such a loss of spatial resolution is not desirable and ultimately degrades the utility of the MALDI-MS imaging technique.
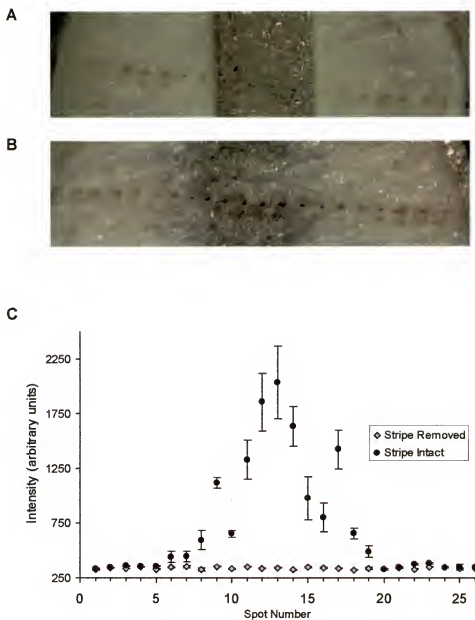
Figure 2-4. Photomicrographs of analyte/ink pattern on paper. (A) Presents analyte/ink stripe removed and (B) shows the analyte/ink strip left intact. (C) is a plot of product ion intensity vs. location for both samples (sampled spots can be observed in A,B with numbering from left to right).

Alternative MALDI matrix solution compositions were explored to decrease the extent of analyte migration and to preserve the analyte's original spatial distribution. We speculated that matrix solutions with more organic content would provide less time for the analyte to migrate due to faster solvent evaporation. Figure 2-5 displays the spatial profile of spiperone product ions across a surface following electrospray deposition of a 70% aqueous methanol matrix solution. Next, a 100% methanol matrix solution was deposited onto another surface, but analysis did not produce any detectable spiperone MS/MS product ions (Figure 2-6). In this case, the amount of spiperone extracted and incorporated into the MALDI matrix was below the detection limit of the instrument. This can be attributed to the much faster rate of evaporation for this matrix solution. As a compromise between the two extremes, a MALDI matrix solution composed of 85% aqueous methanol with 1 % acetic acid was prepared, with the resulting data are shown in Figure 2-7. In this case the spiperone was detected only in the region where ink had been initially applied to the paper.

These data show that with proper matrix solution composition, the electrospray matrix deposition method can preserve analyte spatial distribution for eventual MALDI-MS imaging experiments. However, it was also apparent that the relative intensity of the observed product ions with the 85% aqueous methanol matrix solution was about 5 times lower than those produced with the 70% aqueous methanol matrix solution. The trend observed in Figures 2-(5-7) is that the extraction efficiency of spiperone from ink/paper increases with
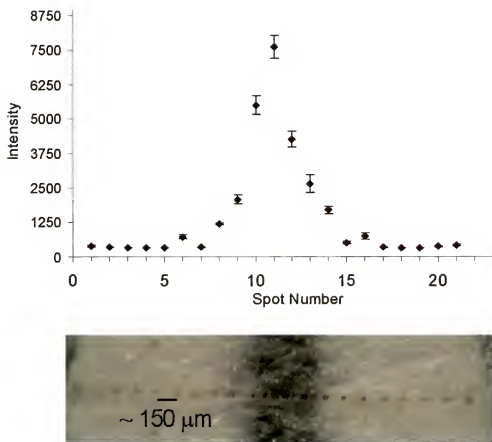
Figure 2-5. Spatial profile of spiperone product ions after electrospray deposition of 70% aqueous methanol solution of matrix. Note only three spots correlate with sampling from analyte/ink pattern area while spiperone product ions are detected at several locations.
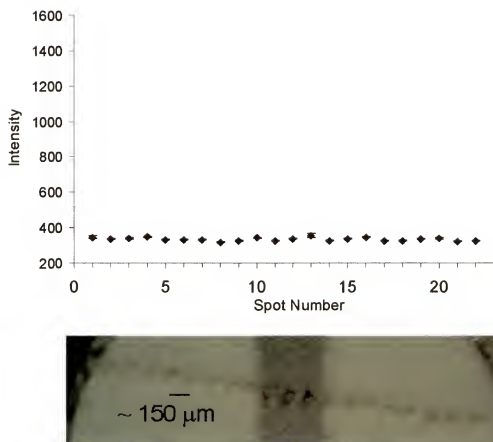
Figure 2-6. Spatial profile of spiperone product ions after electrospray deposition of methanol solution of matrix. Note no detectable spiperone product ions were detected.
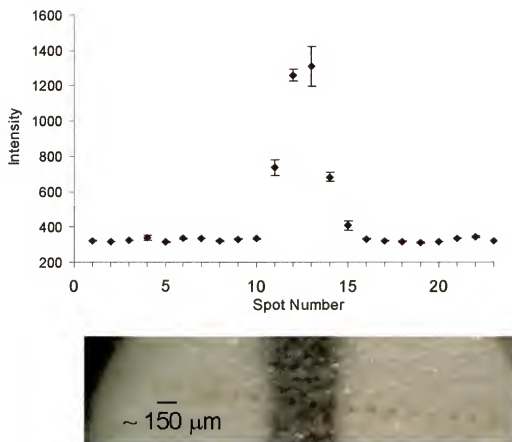
Figure 2-7. Spatial profile of spiperone product ions after electrospray deposition of 85% aqueous methanol solution of matrix. In this case, only the four spots sampled over the inked region show elevated signal.

increasing aqueous content of the MALDI matrix solution. Unfortunately, preservation of the analytes spatial distribution improves at the cost of sensitivity.

Electrospray Deposition Time

During the initial work it was observed that variations in electrospray deposition time caused noticeable fluctuations in product ion signal. Therefore, another series of experiments was performed to evaluate the effect of electrospray deposition time on analyte sensitivity. Paper samples that had their entire surface covered with spiperone dosed ink were glued to the target, then electrosprayed with the 85% aqueous methanol matrix solution for times varying from 0-6 minutes. After electrospray matrix deposition, tandem mass spectra were collected 30 scans deep into each sample. Each scan was composed of 30 single-shot mass spectra. Figure 2-8 shows the resulting signal after successive scans at the same location.

Initially, the greatest intensities were observed with an electrospray deposition time of one minute; however, this intensity falls off after ~ 5 scans. Electrospray deposition times of 2-3 minutes appear to give the most intense signals in the range of 5-10 scans, after which their intensities fall off. During longer electrospray deposition times (4-6 minutes), analyte signal remained present until nearly 25 scans, but the signals were much less intense.

These data suggest that electrospray deposition time, in addition to matrix solution composition, can also affect the preservation of spatial distribution. This conclusion is reflected in the data shown for the 5 and 6 minute electrospray deposition times. Since the analyte is continuously extracted out of the initially
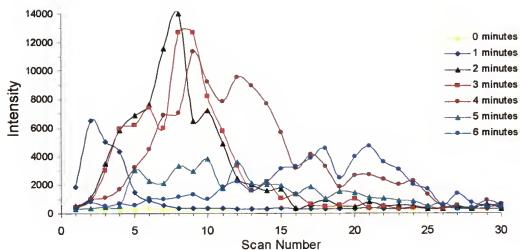
Figure 2-8. Plot of spiperone product ion intensity vs. successive scanning for varying electrospray matrix deposition times.

deposited layers and incorporated into the subsequent layers, one can conclude that spatial resolution should degrade proportionally with the length of electrospray deposition time. Therefore, to combine the best sensitivity and to maximize the preservation of analyte spatial distribution, shorter electrospray deposition times should be employed.

Conclusions

The experimental results presented here show that both matrix composition and electrospray deposition time are important factors contributing to sensitivity and preservation of spatial distribution. For these experiments the optimal MALDI matrix solution was determined to be 85% aqueous methanol with DHB at 10 mg/mL. Additionally, it was determined that matrix electrospray deposition times of 2-3 minutes were most favorable for preserving spatial distribution as well as maximizing sensitivity.

Aside from sensitivity and preservation of spatial distribution, MALDI-MS imaging and mapping experiments have not been able to provide quantitative information. Recently, several literature reports have discussed the use of internal standards for improving the quantitative ability of MALDI.[154-158] Unfortunately, quantitation in MALDI imaging experiments remains problematic. This is primarily a result of the inability to deliver internal standards homogenously into tissue without disrupting inherent analyte heterogeneity, the very subject of the investigation.

Although electrospray deposition of the MALDI matrix has been shown to be useful for preserving spatial distribution during mass spectrometric imaging, we propose it could be further exploited to circumvent the problems associated

with delivering internal standard into tissue or other complex matrices. For instance, a stable-isotope labeled version of the analyte could be incorporated into the matrix solution and subsequently electrospray deposited directly onto the tissue surface during the MALDI matrix application process. This approach would provide a simple method for homogenous internal standard distribution, thereby making quantitation in imaging experiments a more realistic goal.

Despite the possible benefits discussed above, optimal electrospray deposition conditions for the substrate and analyte utilized during these studies may differ greatly from those of other analytes and/or substrates. It is reasonable to expect that similar optimization experiments would need to be performed on other matrix/analyte systems before application of the technique. Unfortunately, for many natural analyte-containing matrices of interest (e.g.; tissue, gels, etc.) it is difficult to prepare samples with known analyte locations for study, such as the model used in this work. Consequently, MALDI-MS imaging will likely continue to be impaired by complications of the matrix application.

CHAPTER 3
THE DETECTION OF ENVIRONMENTAL TOXICANTS DIRECTLY FROM
BIOLOGICAL TISSUES

Background

Vast quantities of polychlorinated biphenyls (PCBs) were commercially produced and marketed during the twentieth century (an estimated 1.5 million metric tons) for a variety of industrial applications due to numerous favorable chemical properties including both chemical stability and miscibility with organic compounds.[159] Unfortunately, as a result of careless disposal, these same properties have made PCBs one of the most problematic environmental toxins of our time. Exposure to PCBs can cause a variety of health problems including liver lesions, hepatic carcinomas, reproductive, immune, and neurological disorders.[160] PCBs were marketed as mixtures of the 209 possible congeners of chlorinated biphenyls; however, only a handful of these congeners have shown toxicity.[161] The toxicity of certain congeners arises from the positions of the substituted chlorines, namely non-ortho substituted congeners exhibit planar geometries and consequently have a high affinity for binding to the enzyme aryl hydrocarbon hydroxylase (AHH).[160,161] 3,3',4,4'-tetrachloro-biphenyl (TCB) is one of these non-ortho substituted congeners and although it is contained in these PCB mixtures at a relatively low level, it makes a significant contribution to their toxicity.[162,163]

Trophic transfer (dietary intake) is a significant mechanism regarding the uptake of environmental contaminants such as TCB.[164-167] The toxicity of dietary xenobiotics, like TCB, is largely determined by the bioavailability of the toxic compound. Two important factors affecting the bioavailability of dietary toxins are: (1) the extent of intestinal biotransformation (metabolism)[168-171] and (2) the transport of the toxin and its metabolites to the bloodstream via intestinal transporter proteins such as P-glycoprotein (pgp).[172] Although it has been suggested that pgp plays an important role in the intestinal uptake of TCB, the protein has also been implicated in the efflux of numerous intravenously dosed drugs.[173-176] Of course, many pharmaceutical compounds require delivery to the site of action to be effective; in fact, efflux of chemotherapeutic drugs out of tumor cells has been proposed as a possible reason for tumor cell resistance.[176] Altogether, studies aimed at understanding the factors governing the systematic bioavailability of TCB could also provide gainful insight into enhancing the bioavailability of drugs to the specific site-of-action through pgp up- or down-regulation.

While systematic bioavailability can be determined on the macroscale with traditional analytical approaches (such as GC or LC/MS), these methods cannot provide the detailed spatial distribution information that could answer numerous questions regarding site-specific transport, bioaccumulation, and biotransformation of biologically relevant compounds. Probing techniques, such as focused laser beams, can provide a means of examining biological tissues with reasonably high fidelity. Furthermore, when combined with laser probing

techniques, tandem mass spectrometry can offer an extremely sensitive and selective means of detection. Therefore, we have examined the use of laser microprobe quadrupole ion trap mass spectrometry for mapping the spatial distribution of biologically important xenobiotics and their metabolites in the intestinal tissue of channel catfish. In summary, the high sensitivity and selectivity provided by laser microprobe quadrupole ion trap mass spectrometry presents a unique method to monitor the important environmental toxin TCB, and its biotransformation products at trace levels directly from tissue. This chapter will outline the development and optimization of laser microprobe quadrupole ion trap mass spectrometry for this application.

Experimental

Instrumental

The same laser microprobe ion trap mass spectrometer used and outlined in Chapter 2, with some important modifications, was also employed for these studies. For MALDI experiments a model VSL-337 ND pulsed nitrogen ultraviolet (UV) laser (Laser Science, Inc., Cambridge, MA) was used, while laser desorption-chemical ionization (LD/CI) was performed using an infrared (IR) laser, (μ-TEA, Laser Science, Inc., Cambridge, MA). The UV laser was focused to a spot size of ~ 35 microns with an irradiance of ~ 10^7 W/cm^2, while the IR laser was used with a spot size of ~ 100 microns corresponding to an irradiance of ~ 10^8 W/cm^2.

Because of the non-polar nature and high degree of chlorination, TCB was anticipated to preferentially form negative ions, perhaps rendering negative ion analysis of greater sensitivity. The home-built laser microprobe instrument

described in Chapter 2 had been used extensively in the positive ion detection mode, but modifications were necessary to perform analysis in the negative ion mode of detection.

This modification involved the gating of ions into the ion trap for mass analysis. The instrument was initially constructed to use one of the ion focusing lenses as a gate to allow ions into the mass analyzer region during a desired ion injection period as shown in Figure 3-1A ("gate open") and B ("gate closed"). Gating was accomplished by alternating the potential on the lens with respect to time as shown in Figure 3-2. In the positive mode, during times of ion injection, the gate is pulsed to a negative value to allow positive ions to pass, after which the lens is returned to a high positive voltage (~ +175V, "gate closed") so ions can no longer pass. Unfortunately, during construction of the instrument the gate circuitry was not designed to operate in the opposite polarity, which would be necessary for gating of negative ions. Therefore, a new circuit that would allow the gating of both positive and negative ions was designed and constructed.

Figure 3-3 is a schematic of the replacement circuit that can gate both positive and negative ions. The circuit is designed to use an external power supply for the distribution of the "gate open" voltage and utilizes $\pm$200V supplies directly from the existing mass spectrometer control electronics for "gate closed" operation. With the new circuit, positive or negative ion gating can be selected through the use of two double-pole double-throw switches.

After design, construction, and installation the new gate control circuit was tested, with the results presented in Figure 3-4. The plots in Figure 3-4 were
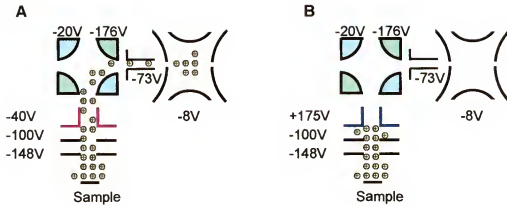
Figure 3-1. Diagram of lens assembly and typical voltages for positive ion mode operation. (A) corresponds to "gate open" and (B) to "gate closed".
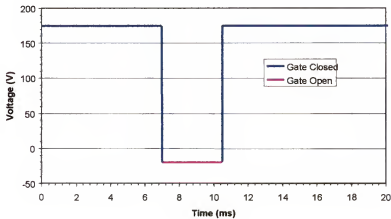
Figure 3-2. Temporal profile of gate lens voltage.
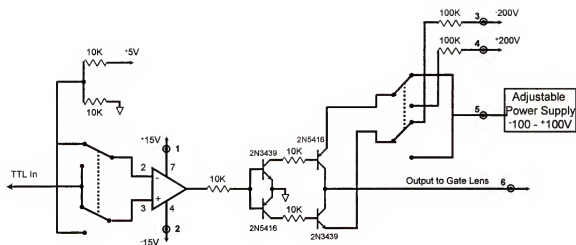
Figure 3-3. Schematic of replacement gate lens circuit.
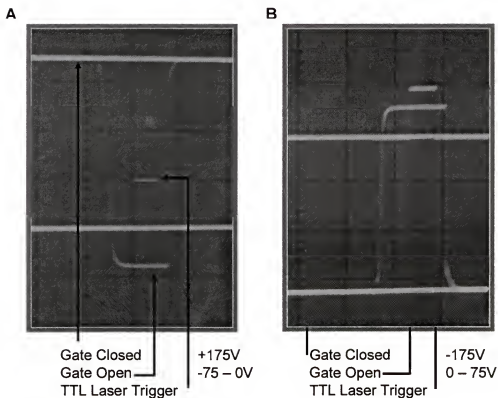
Figure 3-4. Output of constructed gate circuit. (A) shows operation in the positive mode with the "gate closed" voltage ~ +175V, then a brief pulse to -40V (gate open), while (B) shows the opposite for negative ion detection mode.

obtained by directing the output of the gate circuit to an oscilloscope. In the positive mode, the top trace shows the "gate closed" setting of +175V with a brief pulsing to -40V ("gate open"). In the negative mode, the opposite is observed where the potential applied to the lens will be −175V except during "gate open" periods where the gate is pulsed to +40V. Also shown is the TTL signal that triggers the laser to fire, hence initiating the desorption/ionization process. This signal was delayed to trigger ~ 1ms after the "gate open" signal so that the lens voltage was allowed to stabilize. An added benefit provided by the new circuitry was that the "gate open" voltage could be optimized to provide greater ion transmission by use of the external power supply.

Sample Preparation

All solvents and chemicals used in these experiments were purchased from Sigma Chemical (St. Louis, MO) unless otherwise noted. TCB was purchased from Ultra Scientific (Kingstown, RI). MALDI matrices were prepared at 10 mg/ml in a 70% aqueous methanol solution containing 1% acetic acid. Analytes were solvated in methanol and deposited directly onto the target, after solvent evaporation the matrix solution was applied for MALDI, or analyzed directly for LD/Cl.

For tissue dosing experiments, intestinal tissue was obtained by excising the entire small intestine from an adult male channel catfish immediately following sacrifice. Small sections (~ 8 mg) of the intestine were subsequently excised and the mucosa scraped off. A solution consisting of 100 ng/μl TCB in methanol was added to a 1% aqueous acetic acid solution to make a total

volume of 200 μL (enough to completely cover the tissue). The tissue was then allowed to incubate for a period of 1.5 hours; thereafter, the tissue was removed and rinsed with 2 – 10μL aliquots of 1% aqueous acetic acid, blotted dry, and placed on the target for analysis.

Results and Discussion

MALDI Optimization

For most analytes ionized during the MALDI process positive ion detection yields the best signal, but negative ions are also formed during MALDI.[49,177] In fact, some studies have shown that ion signals of certain compounds can be greater in the negative ion detection mode rather than in the positive mode.[178,179] Due to its high electron affinity, we suspected that TCB could prefer negative ion formation during MALDI. Therefore, preliminary MALDI studies with TCB utilized both positive and negative modes of ion detection to determine which was most suitable.

Both 2,5-dihydroxybenzoic acid (DHB) and 1,4-dihydroxynaphthalene (DHN) were evaluated as potential MALDI matrices for TCB and methoxychlor (another environmental contaminant of interest) analysis. While DHB is a relatively well established MALDI matrix, DHN has been used to a much lesser extent, but it has been reported to be an excellent matrix for promoting negative ion formation.[180] Each of the matrixes was assessed in both positive and negative ion modes of detection.

Figure 3-5 displays the positive ion MALDI mass spectra of DHB and DHB with the analyte methoxychlor. The DHB with methoxychlor sample was
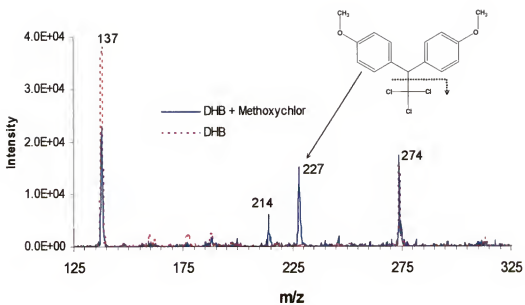
Figure 3-5. Positive ion MALDI mass spectra of DHB and DHB with
methoxychlor.
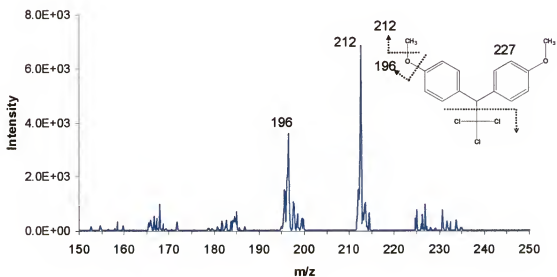
Figure 3-6. MS/MS mass spectrum of m/z 227 from methoxychlor.

prepared by pipetting 1 μl of a 0.20 μg/μL solution of methoxychlor in methanol directly onto the target surface. Afterwards, 2 μL of a saturated DHB in methanol solution was applied on top and allowed to crystallize. Prominent peaks at m/z 137 and 274, present in both mass spectra, are produced by DHB and correspond to the $[M-H_2O+H]^+$ and $2[M-H_2O+H]^+$ respectively of DHB. However, m/z 227 is produced only when methoxychlor is present and corresponds to the $[M-CCl_3]^+$ of methoxychlor. Figure 3-6 displays the MS/MS mass spectrum of m/z 227, which produces products at m/z 212 and 196. These fragments correspond to the loss of methyl and methoxy groups as shown in the inset.

Neither of the matrixes used were able to generate ions of TCB in either the positive or negative ionization modes. DHB, in the positive ion mode, was the only matrix found suitable for ionization of the contaminant compound methoxychlor.

Laser Desorption-Chemical Ionization

Instead of using an acidic-absorbing matrix to promote desorption/ionization, as in MALDI, a laser beam can also be used to desorb neutral molecules into the gas-phase that can subsequently be ionized by ion molecule-reactions with a reagent gas (LD/CI).[33-35] However, because tissue exhibits a poor absorption at 337 nm and the maximum energy output of the UV laser used for the MALDI experiments was relatively low, a different laser was used for LD/CI experiments. For direct tissue analysis the desorption wavelength should overlap with absorption bands naturally occurring in the tissue, since no

exogenous matrix is added. Therefore, laser desorption was accomplished by irradiation in the IR at a wavelength of 10.6 μm, a laser that had previously been used for LD/CI experiments from tissue.[97]

Negative chemical ionization

Negative chemical ionization (NCI) has been used extensively for the mass spectrometric detection of numerous environmental toxins, including polychlorinated biphenyls.[161,181-187] NCI employs thermal electrons, produced in the ion source by collisions of an electron beam with a reagent gas at pressures of ~0.5 torr, producing thermal electrons:

$$e^- \xrightarrow{\quad reagent-gas \quad} e_{th}^- \qquad\qquad 3.1$$

that can ionize gas-phase analyte molecules by thermal electron attachment. Ideally, the thermal electrons will attach to the analyte via the resonance electron capture mechanism outlined in Equation 3-2. However, often times the thermal electrons interact with the analyte dissociatively, causing the analytically useless process shown in Equation 3-3:

$$M + e_{th}^- \rightarrow [M^-]^* \rightarrow M^- \qquad\qquad 3.2$$

$$M + e_{th}^- \rightarrow [M^-]^* \rightarrow [M - Cl] + Cl^- \qquad\qquad 3.3$$
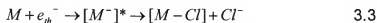
The fragmentation can be lessened by increasing the reagent gas pressure in the ion source, hence making thermal electrons of lower energy and increasing analyte molecular ion-reagent gas collisions that can help dissipate the excess internal energy.

Notwithstanding the high sensitivity for the detection of electrophilic compounds, NCI-MS irreproducibility is widely known.[184,188-191] For instance, a

study of methane electron capture NCI performed by five independent laboratories, with operating conditions as standardized as possible, on 2,2',3,3'-TCB revealed that only three of the five laboratories observed the formation of the [M]$^-$ molecular ion.[184] Of these, one laboratory obtained an 83% relative abundance of the molecular ion while the other two laboratories were only able to observe the molecular ion at 3% relative abundance.

Positive chemical ionization

Because of NCI's lack of reproducibility, positive chemical ionization (PCI) was also investigated for the contaminants of interest; in fact, the use of PCI to ionize TCB is not without precedence.[162,163] March and co-workers have reported GC-MS methodology to separate and quantify mixtures of PCBs.[191] They noticed that a pentachlorobiphenyl isomer co-eluted with TCB, and under NCI conditions a small portion of the pentachloro-isomer dissociated with a neutral loss of chlorine causing interferences with the TCB molecular ion. In that work, the problem was alleviated by use of methane PCI.

For the PCI experiments described here, methane was also employed as the reagent gas. Under PCI conditions, methane (P ~ 0.5 torr) is bombarded with electrons causing ionization of the reagent gas as illustrated:

$$CH_4 + e^- \rightarrow CH_4^{+\cdot}, CH_3^+, CH_2^{+\cdot} \qquad 3.4$$

These ions can then interact with methane molecules to generate the useful reagent ions CH_5^+, $C_2H_5^+$, and $C_3H_5^+$ by: [190,191]

$$CH_4^{+\cdot} + CH_4 \rightarrow CH_5^+ + CH_3^\cdot \qquad 3.5$$

$$CH_3^+ + CH_4 \rightarrow C_2H_5^+ + H_2 \qquad 3.6$$

$$CH_2^+ + CH_4 \rightarrow C_2H_4^{+\cdot} + H_2 \rightarrow C_2H_3^+ + H_2 + H^\cdot \qquad 3.7$$

$$C_2H_3^+ + CH_4 \rightarrow C_3H_5^+ + H_2 \qquad 3.8$$
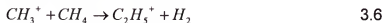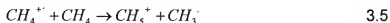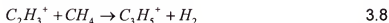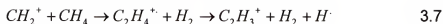
These reagent ions interact with analyte gas-phase molecules (M) mainly as Brønsted Acids causing proton transfer:

$$M + CH_5^+ \rightarrow [M+H]^+ + CH_4 \qquad 3.9$$

providing the gas-phase proton affinity of the analyte is greater than that of the reagent ion.

Tuning for chemical ionization

Tuning for both positive and negative CI was performed by introducing gas-phase perfluorotributylamine (PFTBA) into the source via a leak valve. The structure of PFTBA is presented in Figure 3-7 along with its electron impact (EI) mass spectrum (Figure 3-8, acquired on the laser microprobe instrument). EI ionization induces significant fragmentation of the molecule as evidenced by the mass spectrum. The positive and negative CI mass spectra are presented in Figure 3-9 and 3-10, respectively. Here no significant fragment ions are observed below m/z 400, indicating CI as the more gentle ionization process. Note the intensity scales differ for the positive and negative CI data, an artifact that is due to data collection on differing days rather than one of method sensitivity. Since the PFTBA was introduced through a leak valve, the amount introduced varied greatly from one day to the next. Therefore, these data present a qualitative representation of the two ionization methods.
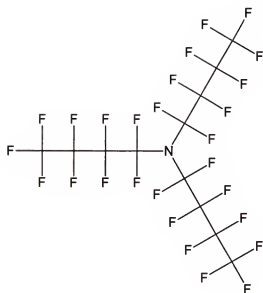
Figure 3-7. Structure of PFTBA.
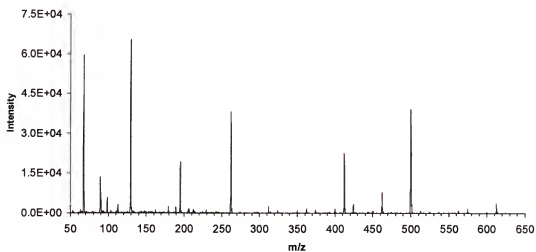
Figure 3-8. Electron impact (EI) mass spectrum of PFTBA (acquired on the laser microprobe mass spectrometer).
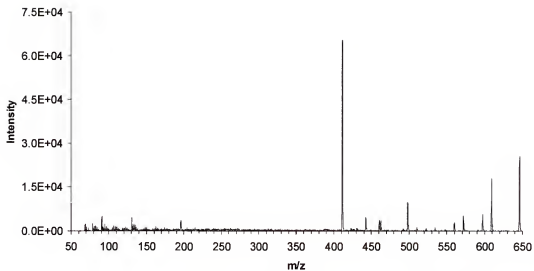
Figure 3-9. Positive chemical ionization (PCI) mass spectrum of PFTBA.
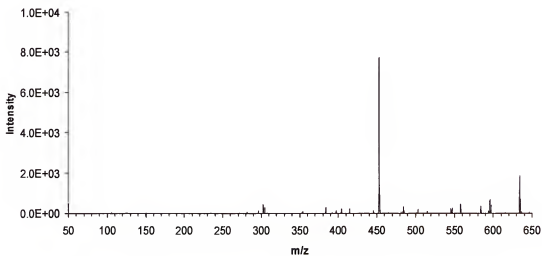
Figure 3-10. Negative chemical ionization (NCI) mass spectrum of PFTBA.

LD/CI optimization

For LD/CI optimization studies, the analytes were dissolved in methanol and deposited directly onto the target surface for analysis. Figure 3-11 presents the positive LD/CI mass spectrum (single-shot mass spectrum) of methoxychlor after deposition of 200 ng sample onto the target. The protonated molecule of methoxychlor was observed with consecutive neutral losses of chlorine. When methoxychlor was sampled under NCI conditions, no detectable analyte ions were observed.

Figure 3-12 displays the positive ion LD/CI mass spectrum of TCB (single-shot mass spectrum, 200 ng loaded) that includes both $[M]^{+\cdot}$ and $[M+H]^+$ ions. The molecular radical cations are likely formed by charge exchange processes and have been previously observed for this compound under methane PCI conditions.[163] A closer view of the molecular ion region is presented in Figure 3-13, with a simulated isotopic distribution presented in Figure 3-14. Though the resolution is somewhat lower in Figure 3-13, the simulated isotopic distribution correlates well with the obtained data. The MS/MS mass spectrum (Figure 3-15), of the five dalton wide molecular ion window, also displays overlapping isotopic distributions due to loss of $Cl^{\cdot}$ and HCl. This distribution (Figure 3-16) correlates well with the theoretical isotopic distribution (Figure 3-17), with a ratio of $[M-Cl]^{+\cdot}$ to $[M-Cl+H]^+$ ions of ~ 1:1.

Laser Desorption/Chemical Ionization of TCB from Tissue

A series of tissue dosing experiments was employed to evaluate the LD/CI-MS methodology for its ability to detect environmental contaminants
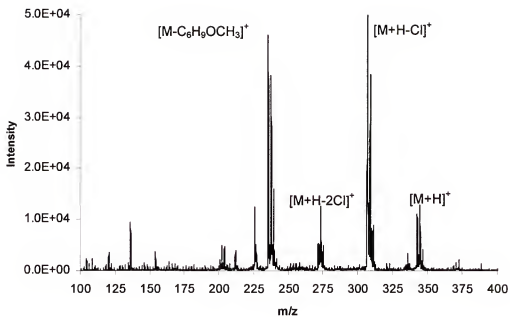
Figure 3-11. LD/CI positive ion mass spectrum methoxychlor (200 ng loaded, single-shot spectrum).
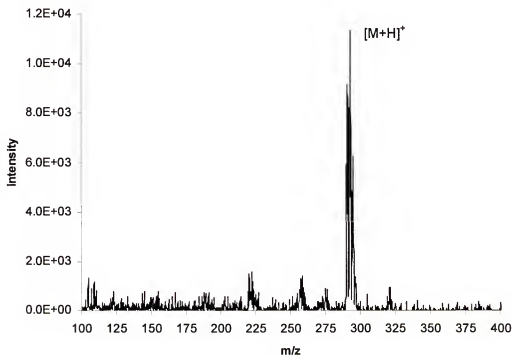
Figure 3-12. LD/CI positive ion mass spectrum of TCB (200 ng loaded, single-shot spectrum).
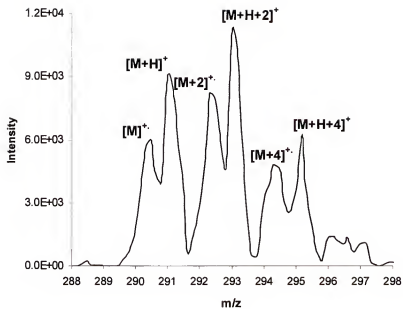
Figure 3-13. Molecular ion region of LD/CI-MS mass spectrum of TCB.
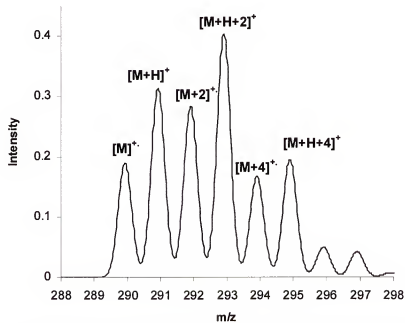
Figure 3-14. Simulated theoretical isotopic distribution for TCB molecular ion.
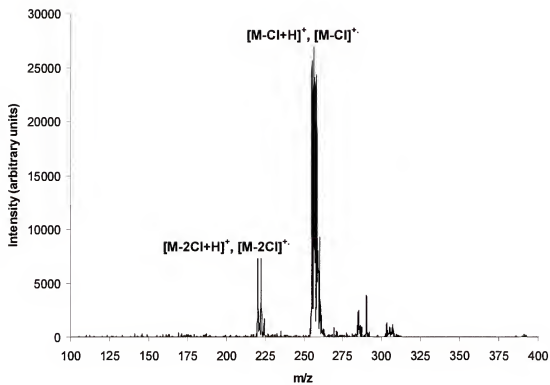
Figure 3-15. Positive LD/CI-MS/MS mass spectrum of TCB molecular ion window.
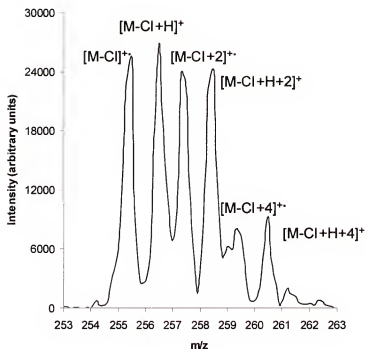
Figure 3-16. Inset of base peak from TCB MS/MS mass spectrum corresponding to the loss of Cl.
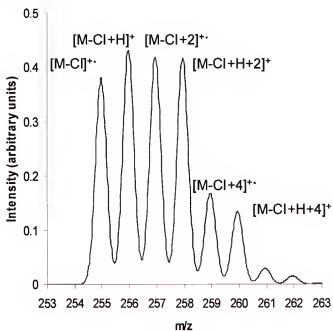
Figure 3-17. Simulated isotopic distribution of [M-Cl] product ion region.

directly from tissue. Intestinal tissue was dosed at 0, 50, 100, and 300 ng TCB/mg tissue using the method described above (see Sample Preparation). Note these figures represent the total amount of TCB present in the incubation solution and assumes the tissue absorbed all TCB present.

After dosing and rinsing, the tissue was placed onto the target and inserted into vacuum for LD/CI-MS analysis. When full-scan mass spectra were acquired from these samples, there was a peak at nearly every mass making identification of TCB impossible (Figure 3-18). However, when the TCB molecular ion was isolated, followed by collision-induced dissociation the resulting MS/MS spectra (Figure 3-19) did indicate the presence of the TCB. Figure 3-20 presents a plot of TCB product ion intensity vs. the incubation dosage utilized. These data demonstrate the ability of the laser microprobe mass spectrometer to detect trace levels of analyte directly from complex matrixes such as tissue.

However, certain problems did arise generating concern about practical use of the method for potential imaging experiments. Several of the concerns arose because the sampling process was carried out inside the vacuum chamber. The first problem was that of tissue shrinkage and deformation after insertion into the high vacuum region for analysis. Another problem was the degradation of signal after successive laser desorption events. Since the IR laser has a significant penetration depth, a large amount of material was removed from the tissue with each pulse, with the majority of that material being deposited on the stainless steel volume containing the sample and the
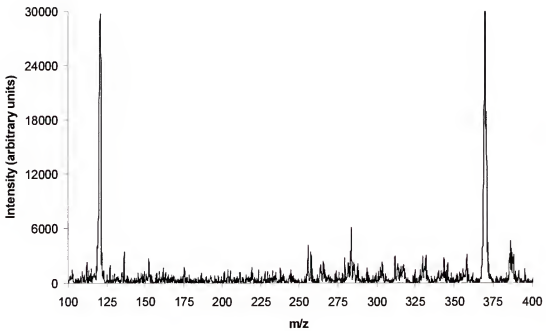
Figure 3-18. Positive LD/CI-MS mass spectrum of TCB dosed tissue. Notice identification of TCB impossible due to high background produced from direct analysis of tissue.
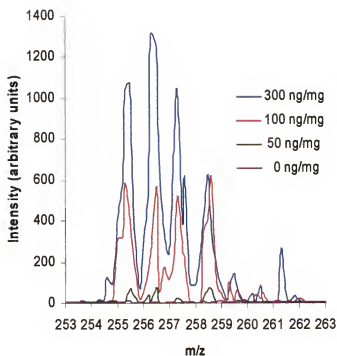
Figure 3-19. MS/MS mass spectrum of TCB dosed tissue for varying TCB
dosage levels. Here a distinct isotopic pattern for the TCB product
ion [M-Cl]$^+$ can be observed allowing for the identification of TCB.
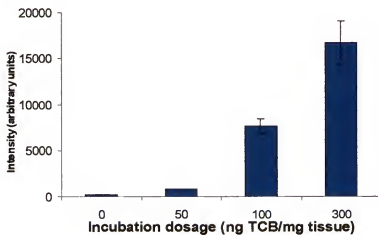
Figure 3-20. Plot of TCB product ion intensity for varying tissue dosage levels.

subsequent extraction lenses. After a few pulses, ions were no longer effectively extracted due to the coating of material on the extraction lens. Next, precise sample movement for imaging and laser focusing options were also severely restricted by the confines of the vacuum system. Therefore, even though these data demonstrate the instrument capable of detecting compounds directly from tissue, the practical application of mapping or imaging is not straightforward.

Conclusions

Contaminant molecules, such as TCB, represent a biologically important class of compounds whose persistence continues to threaten our natural environment. Diet represents the most likely scenario for exposure to humans; hence, knowledge of uptake and transfer of these compounds into the bloodstream via the small intestine is of high importance to help reduce or limit exposure. Imaging mass spectrometry presents a unique opportunity through which to monitor intestinal uptake and metabolism of these biologically important xenobiotics.

The success of imaging mass spectrometry first relies on the ability to desorb/ionize the analyte of interest. Results presented herein demonstrate that none of the MALDI matrixes studied in either mode of ionization was capable of ionizing TCB. DHB was found to ionize the contaminant methoxychlor in the positive mode. However, an alternative to MALDI, LD/CI, was found to ionize both TCB and methoxychlor in the positive mode with good success.

Because most environmental contaminants are relatively non-polar, location of suitable ionization methods will always be challenging. Due to their high electron affinities, especially TCB, it was expected NCI chemical ionization

would produce superior results; however, no detectable analyte ions were generated for either compound during NCI-MS analysis. This result is somewhat troubling, yet not surprising, considering numerous reports of irreproducibility for the technique.[184,188-191] However, the laser microprobe ion trap instrument, with LD/PCI, was used to detect TCB directly from intestinal tissue at environmentally relevant levels (low ppm). Finally, despite the ability to detect TCB directly from tissue, incorporation of this methodology for imaging-MS, in its present form, appears to be questionable at best.

LASER DESORPTION-ATMOSPHERIC PRESSURE CHEMICAL IONIZATION:
A NEW IONIZATION METHOD BASED ON EXISTING THEMES

Background

Laser desorption/ionization techniques for mass spectrometry have rapidly developed over the past 20 years. In particular, matrix-assisted laser desorption/ionization (MALDI) has since its inception[11,12] produced a dramatic effect on biological mass spectrometry. While MALDI has proven a robust and often preferred method for desorption/ionization of numerous analytes, certain low mass organic compounds are more efficiently desorbed/ionized via laser desorption/chemical ionization (LD/CI).[97,146,149] This technique takes advantage of the relatively large number of desorbed neutral molecules produced during laser desorption by ionizing them with reagent ions of a CI gas at source pressures ~ 0.5 torr.[33,34] In many respects MALDI and LD/CI are complementary techniques; MALDI is typically used for the desorption/ionization of larger biomolecules, while LD/CI is advantageous for smaller organic analytes and avoids MALDI matrix background ions.

Recently, Laiko et al. have demonstrated the utility of atmospheric pressure (AP) MALDI (AP-MALDI) for mass analysis.[102,103] Although these studies have indicated that AP-MALDI and vacuum MALDI have similar ionization processes, there are a few notable differences. AP-MALDI can be considered a softer ionization technique when compared to vacuum MALDI,

because AP generated ions are more efficiently thermalized.[102] And recent research has demonstrated that MALDI generated ions produced at elevated source pressures (~ 7.5 Torr) show less fragmentation than those produced under normal MALDI vacuum conditions (~ < 10^{-3} Torr).[193-195]

In addition to the effective collisional cooling of ions formed at AP, several other benefits can be realized. First, sample manipulation is much simpler at AP than under vacuum. Second, restrictions of laser focusing optics imposed by the vacuum system are removed, allowing for the use of near-field optical probes that can reduce laser spot size.[196] Third, AP sampling can eliminate adverse vacuum effects on sensitive samples such as biological tissue. Finally, instruments with AP sampling inlets are potentially compatible with several ionization techniques (i.e., electrospray (ESI), atmospheric pressure chemical ionization (APCI), AP-MALDI, laser desorption-atmospheric pressure chemical ionization (LD-APCI)).

Although the ionization steps involved with AP-MALDI are not completely understood at this time, the process is similar to conventional vacuum MALDI.[102] Thus, LD-APCI-MS should produce results analogous to LD/CI-MS. Kolaitis and Lubman were able to ionize laser desorbed neutral molecules at AP using a ^{63}Ni atmospheric pressure ion source.[197] The ions were generated in an ion mobility drift tube and then injected through an orifice into vacuum for mass analysis. Their work was the first study to demonstrate laser desorption of neutral molecules followed by chemical ionization at AP. The work presented here

builds on that study by use of a more efficient ionization method for the desorbed neutral molecules.

Atmospheric Pressure Chemical Ionization
Corona discharges and mass spectrometry

Under high pressure conditions (> 200 torr), two electrodes whose geometry create a non-uniform electric field can be used to generate a corona discharge.[198] An example of two such electrodes can be seen in Figure 4-1 where an asymmetric field is created between the tip of a sharpened electrode and a neighboring plane (the sampling orifice in this case).[199] Corona discharges are characterized by relatively low discharge currents and hence incomplete breakdown of the gas in the discharge gap region.[198] And because they can be formed under ambient conditions, the corona discharge has found extensive use as an ion generator in a variety of devices.

For mass spectrometric purposes the corona discharge can be used as a robust and simple electron emitter for primary ion formation. The first use of the corona discharge as an ionization source for mass spectrometry was reported in 1966 by Shahin.[200] In that work a variety of ionic species from ambient air were produced and measured by a quadrupole mass analyzer. In the early 1970s Horning and co-workers introduced a novel ionization method they called atmospheric pressure ionization (API) that effected ionization of gas chromatography (GC) and liquid chromatography (LC) effluents.[201-205] However, that source used a Ni[63] β-particle emitter to effect the ionization of gas-phase analyte neutral molecules. In later iterations of the API source, the Ni[63] β-particle

emitter was replaced by the corona discharge, a more convenient source of ionizing electrons.[205-212]

Ionization in API (hereafter referred to as APCI) occurs initially in the region closest to the corona discharge needle by electron ionization as follows:

$$N_2 + e^- \rightarrow N_2^+ + 2e^- \qquad \text{Eqn. 4.1}$$

Under ambient conditions, nitrogen ions will form the primary ion species due to nitrogen's high abundance. After formation the N_2^+ reacts very rapidly through the following series of equations:[205]

$$N_2^+ + 2N_2 \rightarrow N_4^+ + N_2 \qquad \text{Eqn. 4.2}$$

$$N_4^+ + H_2O \rightarrow H_2O^+ + 2N_2 \qquad \text{Eqn. 4.3}$$

$$H_2O^+ + H_2O \rightarrow H_3O^+ + OH \qquad \text{Eqn. 4.4}$$

$$H_3O^+ + H_2O + N_2 \rightarrow H^+(H_2O)_2 + N_2 \qquad \text{Eqn. 4.5}$$

$$H^+(H_2O)_{n-1} + H_2O + N_2 \rightarrow H^+(H_2O)n + N_2 \qquad \text{Eqn. 4.6}$$
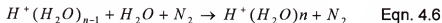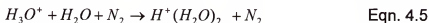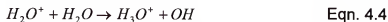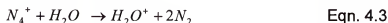
The most stable species formed from the ambient corona discharge are protonated water and protonated water clusters. Ionization of a gas-phase analyte molecule (M) can occur by proton transfer,

$$H_3O^+ + M \rightarrow (M+H)^+ + H_2O \qquad \text{Eqn 4.7}$$
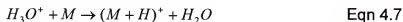
providing the gas-phase proton affinity of the analyte is higher than that of protonated water.

The APCI source

APCI sources were one of the first interfaces that allowed the coupling of liquid chromatography (LC) to mass spectrometry. Figure 4-1 displays a
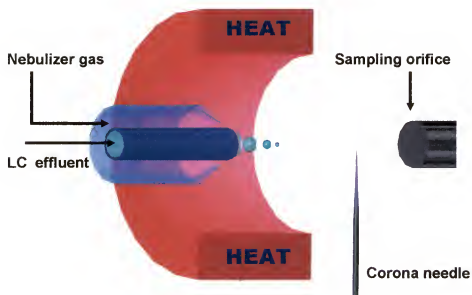
Figure 4-1. Diagram of an APCI source where solvent is evaporated and ionization occurs by passing gas-phase analyte molecules over a corona discharge.

representation of an APCI interface where the LC effluent is nebulized with pneumatic assistance. Next, solvent is evaporated from the droplets by heating to generate gas-phase analyte molecules that are then passed over the corona discharge where ionization can occur. Finally, after ionization, the ions are sampled through a small orifice and passed to the mass analyzer.

The APCI source represented a significant advance in mass spectrometry; however, the technique is limited to the analysis of small, rugged organic molecules. The limitation can be attributed to the heating step that induces decomposition of thermally-labile compounds like biomolecules, a problem that could be eliminated by use of an energy-sudden approach to accomplish desorption.

Laser Desorption-Atmospheric Pressure Chemical Ionization

We have designed and constructed an LD-APCI source that uses a laser pulse to desorb intact neutral molecules, followed by chemical ionization via reagent ions produced by a corona discharge.[213] As described above, corona discharges are widely used as electron emitters for primary ion formation in atmospheric pressure chemical ionization (APCI) sources, but these neutral molecules are delivered into the corona discharge region as gas or liquid chromatograph effluents.[190]

In our approach, however, the neutral molecules are produced by means of laser desorption from a target near the discharge. Laiko et al. reported using a corona discharge during preliminary AP-MALDI studies, but noted only an increase in matrix signal and showed no benefit for analyte ionization.[102] Our experiments are aimed to limit MALDI generated ions, emphasizing the laser

desorption of neutral molecules, followed by subsequent ionization with the corona discharge. Decoupling of the desorption and ionization processes will allow individual optimization of these two steps with increased efficiency and selectivity. This chapter reports initial results with the LD-APCI source that indicate the feasibility and advantages of the technique and evidence of its promise for further development.

<div align="center">Experimental</div>

Mass Spectrometer

A Finnigan GCQ quadrupole ion trap mass spectrometer (ThermoFinnigan, Austin, TX, USA) that was previously adapted to accept a two-stage differentially-pumped vacuum manifold was used for these studies.[214] This instrument had also been outfitted with an Analytica AP inlet (Branford, MA, USA) that was mounted before the first differentially pumped region of the vacuum manifold (Figure 4-2). The blue shaded region in that diagram represented areas held at AP, with the gray region depicting the first differentially pumped region held at ~ 1 torr.

In that AP inlet design, the heated capillary was recessed into the AP inlet manifold several centimeters (~ 10) making access to the heated capillary difficult. Therefore the original AP inlet was modified to create a more accessible environment for the LD-APCI source, accomplished by shortening the length of the AP inlet manifold so that it was terminated just before the heated capillary entrance (Figure 4-3). No other alterations to the AP inlet system were made. The intermediate pressure region between the heated capillary exit and the
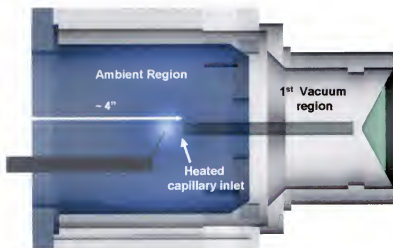
Figure 4-2. Original Analytica AP interface with heated capillary recessed ~ 4".
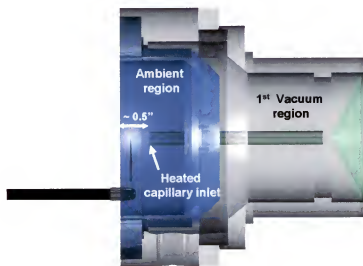
Figure 4-3. Modified AP interface with heated capillary recessed ~ 0.5".

skimmer entrance was backed by two 360 L/min Pfeiffer-Balzers mechanical pumps (Nashua, NH, USA). Ions sampled through the skimmer cone were transported by an octopole through the second differentially pumped region of the vacuum chamber to the quadrupole ion trap during the ion injection step of the scan function. Mass analysis was effected by resonantly ejecting the ions from the quadrupole ion trap to an off-axis conversion dynode held at −15 kV (for positive ion analysis), whereby the secondary ions were detected by an electron multiplier set at -1600 V.

LD-APCI Source Design, Construction, and Operation

The first step in constructing the LD-APCI source was the design of an anchoring and scaffold system that could be used to support or rapidly remove the source. A base-plate was affixed to the modified AP inlet manifold (Figure 4-4) that was designed to serve as a rail for simple position adjustment or for source removal. The LD-APCI source foundation was constructed from a block of aluminum that had one side machined to interface with the base-plate rail, while the other side was milled flat to function as an open breadboard for supporting the individual source components. An XYZ translation stage (model M-460A, Newport, RI, USA) was mounted onto the source foundation to provide a mechanism for target movement (Figure 4-5).

A polymeric insulator (delrin) was designed and mounted to the translation stage (Figure 4-5). Next a metal target rail was affixed to the insulator so that an offset voltage could be applied to the target. A target-holding device was constructed so that its position could be roughly manipulated by sliding along the target rail to a desired location. The targets, produced from stainless steel, were

designed to be rapidly interchangeable. They were secured by a set screw in the target holding device.

A hole was bored through the length of the source foundation so that a long insulator tube could pass through (Figure 4-6). The tube contained a high voltage line that was used to deliver the offset potential to the corona needle. A metal cap was fitted over the insulator tube and allowed to make electrical contact. An additional hole was bored vertically through the cap so that a corona needle holder could be mounted with its position vertically adjustable by use of a set screw.

A mirror system was designed to deliver the photon beam to the target in an orthogonal fashion. The mirrors can be observed in Figure 4-5, again each mirror mounted such that its position could be easily modified. Laser focusing was accomplished through the use of an adjustable focusing lens device (Figure 4-5). This device was designed such that a lens holding sleeve could be moved, a process that altered the focal length and ultimately the laser spot size.

For the experiments outlined in this chapter the corona needle was positioned approximately 1.5 cm (on-axis) from the heated capillary inlet (Figures 4-(6,7)) and operated at potentials (V_1) of +5.3 and +8.1 kV, from a standard ESI power supply (Analytica, Branford, MA, USA). Samples were applied to a 4 mm diameter stainless steel target. The target was approximately centered between the heated capillary inlet and the corona needle and was slightly offset (ca. 2mm) from center. To improve ion transport at AP, an offset potential (V_2) of +2 kV was applied to the target by a power supply (Model 205A, Bertan Associates Inc.,
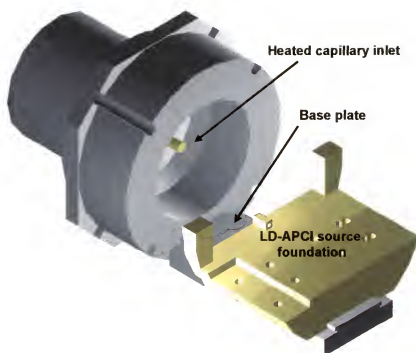
Figure 4-4. Modified AP interface with added base-plate rail system and LD-APCI source foundation.
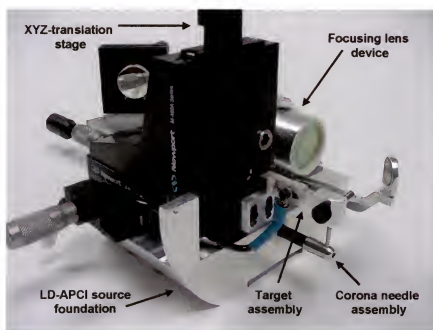
Figure 4-5. Photograph of completed LD-APCI source
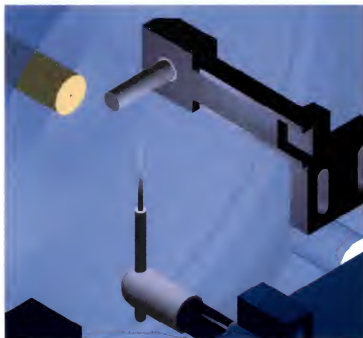
Figure 4-6. Close-up of LD-APCI source displaying the target and corona needle assemblies.
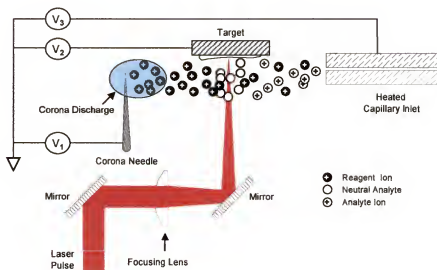
Figure 4-7. Overview of LD-APCI source.

Hicksville, NY, USA). Desorption of neutral molecules was accomplished by irradiation of the target with a 10.6-μm pulsed CO_2 laser (μ-TEA, Laser Science Inc., Franklin, MA, USA). A 10 cm focal length zinc selenide lens (Laser Research Optics, Providence, RI, USA) focused the beam to a spot size of either 1.35 mm (~ 5 x 10^6 W/cm^2) or 0.20 mm (~ 2 x 10^8 W/cm^2). Laser triggering was synchronized to coincide with the prescan period of the scan function, which was 3 ms before the ion injection period of each microscan.

Sample Preparation

Standard solutions of spiperone and reserpine (Sigma, St. Louis, MO, USA) were prepared at various concentrations in a solvent of 50% aqueous methanol with 0.10% formic acid. For the LD-APCI analysis, an aliquot of standard solution was deposited onto the stainless steel probe, dried, and topped with 4 μL of glycerol (Fisher Scientific, Fair Lawn, NJ, USA). After this sample solution was mixed *in situ* with a small glass rod, the target was placed on the LD-APCI device. The sample did not require x-y manipulation during analysis, as the glycerol matrix allowed continual analyte refreshment on the target surface.

Results and Discussion

An understanding of the desorption/ionization processes for LD-APCI requires careful exploration of several important steps. Initial studies focused on blank signals observed. With no sample applied to the target and only the corona discharge on, the most abundant ions were m/z 55 and 73, corresponding to $[H_3O(H_2O)_2]^+$ and $[H_3O(H_2O)_3]^+$, respectively, which is consistent with reagent ions observed under ambient air APCI conditions.[215-217] Next, a series of

experiments utilizing glycerol as a target substrate was performed to evaluate the LD-APCI source. When neat glycerol was applied to the target, again only the corona discharge on, the resulting spectrum was unchanged from that taken without glycerol on the target. Subjecting the glycerol to laser desorption (with the corona discharge on), the $[M+H]^+$ of glycerol was observed, in addition to the $[2M+H-H_2O]^+$, and $[2M+H]^+$ cluster ions of glycerol. When the corona discharge was turned off, these ions were not observed.

For analytical evaluation of the LD-APCI source, the antipsychotic drug spiperone was chosen as a target compound.[218] The sample consisted of 3 µg of spiperone delivered to the target tip, allowed to dry, and followed by 4 µL of glycerol. The laser irradiance was initially adjusted to ~ 2 x 10^8 W/cm^2 by manipulation of the focusing lens. As indicated in Figure 4-8A, by turning the discharge on and off while maintaining laser desorption, the resulting ion chromatogram for the $[M+H]^+$ of spiperone (m/z 396) shows the effect of the corona discharge. Figure 4-8B and C portray mass spectra obtained with and without the corona discharge. Each spectrum represents a single analytical scan, the average of 2 microscans, each consisting of 1 laser pulse followed by mass analysis. With the discharge off (Figure 4-8B), a weak signal for the m/z 396 was observed, indicating the presence of AP-IR-MALDI ions. With the corona discharge on (Figure 4-8C), the m/z 396 signal increased approximately 150 fold, showing that the corona discharge has a significant effect on the production of the spiperone molecular ion.
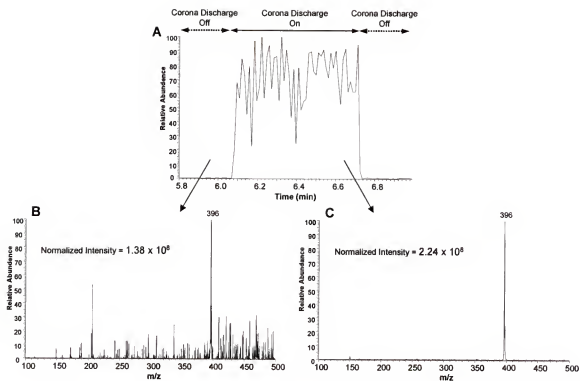
Figure 4-8. LD-APCI of 3 µg spiperone in 4 µL glycerol (A) Ion chromatogram for [M+H]+ of spiperone (m/z 396) during constant scanning with corona discharge toggled off and on. (B) Mass spectrum with corona discharge off. (C) Mass spectrum with corona discharge on.

For the LD-APCI technique described here, the intended role of the laser is that of gas-phase analyte molecule production. Thus, the laser irradiance was lowered to ~ 5 x 10^6 W/cm^2, with the aim of desorbing analyte molecules without concomitant ion formation. At this reduced power, no spiperone ions at m/z 396 were observed without simultaneous use of the corona discharge. With the discharge on, a strong spiperone signal resulted. However, since no glycerol related ions were seen, the corona voltage was raised to +8.1 kV to increase the discharge current and enhance the reagent ion population from the ambient water vapor. The resulting increase in analyte signal required the ion trapping time to be lowered from 100 ms to 7 ms. In general, extending the duration of the ion trapping period can increase sensitivity. However, because of the substantial number of ions being generated via LD-APCI (under the higher corona needle voltage, +8.1 kV), ion trapping times longer than 7 ms induced space charge effects, causing mass shifts.

With the increased sensitivity, subsequent experiments were conducted using a 150-fold reduction of spiperone to 20 ng, still contained in 4 μL of glycerol. The LD-APCI mass spectrum in Figure 4-9 shows the resulting ion signal, again the average of two single shot spectra (normalized intensity = 5.15 x 10^7). The [M+H]$^+$ for spiperone is observed as the base peak, while glycerol related ions [2M+H-H$_2$O]$^+$, and [2M+H]$^+$ at m/z 167 and 185 were also produced. We have tentatively identified the 241 m/z as the [M+H$_2$O+H]$^+$ ion of the contaminant diethyl phthalate.
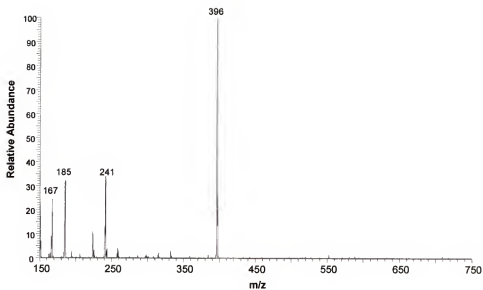
Figure 4-9. LD-APCI mass spectrum of 20 ng spiperone, [M+H]$^+$ = 396, in 4 μL of glycerol.
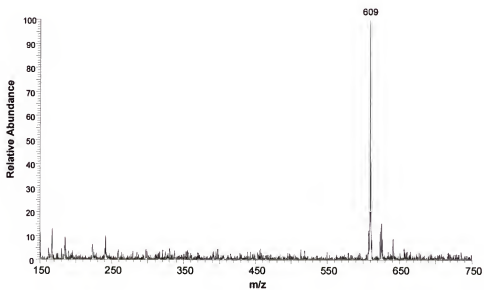
Figure 4-10. LD-APCI mass spectrum of 20 ng reserpine, [M+H]+ = 609, in 4 μL of glycerol.

To evaluate the technique with another sample type, 20 ng samples of reserpine were next analyzed. Figure 4-10 displays a mass spectrum of reserpine using the same LD-APCI conditions that were employed Figure 4-9. As in the case of spiperone, the $[M+H]^+$ of reserpine was produced as the base peak. An oxidation product of reserpine was observed at 16 u higher than the $[M+H]^+$, and was verified by tandem mass spectrometery.

Despite the 150-fold reduction in spiperone mass used to generate the signal in Figure 4-9, the ion signal only dropped to 1/4 of that shown in Figure 4-8. More spiperone was present under Figure 4-8 conditions, and more neutral spiperone molecules were presumably desorbed, but the lower corona discharge voltage resulted in a reduced ionization efficiency.

Under the 5×10^6 W/cm^2 laser irradiance and +8.1 kV corona needle voltage conditions, the sample produced a stable analyte signal for approximately 20 minutes with continuous laser desorption, at which time the glycerol/analyte mixture was consumed. When the irradiance was reduced 5 fold to 10^6 W/cm^2, the analyte signal intensity remained at the previous level (data not shown). Moreover, the sample yielded this ion signal for a period of 45 minutes with no noticeable depletion of the glycerol/analyte mixture. Since the 10^6 W/cm^2 irradiance produced a similar analyte signal with less material desorbed per shot, it is likely that the main factor currently limiting ionization efficiency is the magnitude of the reagent ion population.

In addition to the corona needle voltage, potentials supplied to the target and the heated (V_3) capillary strongly influenced analyte signal. For example, the

heated capillary offset was set to +40 V for the spectrum collected for spiperone in Figure 4-9, which shows a strong [M+H]$^+$ signal. However, when reserpine was sampled under these conditions, very little [M+H]$^+$ was observed. Raising the heated capillary offset to +120 V resulted in the spectrum in Figure 4-10, showing an intense [M+H]$^+$ peak. This may be evidence that reserpine tends to form clusters under the present LD-APCI conditions. Declustering may be enhanced by increasing the heated capillary offset potential, which in turn accelerates the ions in the region between the heated capillary and the skimmer cone,[215] a conclusion also supported by the reduction of glycerol related clusters, comparing Figures 4-9 and 4-10.

These data suggest the LD-APCI methodology presented here – a single laser pulse with chemical ionization, followed by a 7 ms ion accumulation period – produces a stronger ion current than was observed under AP-MALDI conditions.[103] In that study, multiple laser pulses (4-8) were used during ion accumulation, for which ion trapping times of 200 – 400 ms were employed. The contrast in ion signals is in keeping with a previous report that a significantly larger amount of material is desorbed during IR irradiation compared to UV.[45,46] Moreover, for desorption with a CO_2 laser, it has been demonstrated that a larger population of neutral molecules compared to ions is produced.[32] That report is also in agreement with the results reported here (Figure 4-8) as indicated by the large increase in analyte signal with the corona discharge on.

Conclusions

Further development of LD-APCI will require systematic studies of the various potentials supplied to the heated capillary, target, and corona needle.

Another important consideration is the source geometry (e.g., corona needle positioning), which likely plays a substantial role in analyte ion production. Laser irradiance and wavelength are key parameters that must be measured. The investigation of pneumatic assistance or counter current gas flows, combined with changes in the reagent gas makeup (presently ambient air), could provide increased ionization efficiency and or selectivity. Laser triggering and ion gating experiments will further promote the understanding of the steps involved in AP-LD/CI. Pulsing of the corona discharge, time-delayed appropriately after each laser pulse, could add advantageous temporal resolution[219] and preferential discrimination among ion signals.

Although the source parameters have not yet been optimized, we have demonstrated LD-APCI to be a viable and potentially useful technique. While we are in the initial stages of development, the sensitivity observed thus far is encouraging. By future use of the MS/MS mode of the ion trap to reduce chemical noise, combined with optimization of the source, we expect substantial increases in sensitivity.

LASER DESORPTION AT ATMOSPHERIC PRESSURE: FUNDAMENTAL
STUDIES AND THEIR MASS SPECTROMETRIC IMPLICATIONS

Background

Since the initial reports of atmospheric pressure-matrix-assisted laser desorption/ionization (AP-MALDI) two years ago,[102,103] several laboratories have been pursuing the development of AP-MALDI,[104-109] atmospheric pressure laser desorption/ionization from porous silicon (AP-DIOS),[110] and laser desorption-atmospheric pressure chemical ionization (LD-APCI).[220-222] Though each of the techniques may possess certain advantages with respect to the others, they also share some important similarities. First, quadrupole ion trap mass spectrometers (QIT-MS) have been used almost exclusively for AP-laser desorption studies; second, each of the methods employs an absorbing analyte-containing matrix to effect either the desorption/ionization of gas-phase analyte ions (AP-MALDI, AP-DIOS) or the desorption of gas-phase analyte molecules (LD-APCI). Therefore, studies aimed to understand the basic processes in AP-laser desorption (AP-LD) could play a significant role in their continued development.

Unlike vacuum MALDI-TOF-MS instruments, AP-LD-QIT-MS allows the accumulation of ions generated from multiple laser pulses into a single mass analysis event. Indeed, the majority of the reported AP-LD experiments have taken advantage of this opportunity by asynchronously coupling laser pulses (~ 10 Hz) with fixed ion trapping periods of (~200-500 ms).[103-110] In an AP-MALDI

experiment, Laiko et al. report that this approach generates a quasi-continuous ion beam;[109] however, it seems unlikely that MALDI-generated ions would be continuously produced during the entire 100 ms intermission of the nanosecond laser pulses. Moreover, the temporal width of each ion pulse relative to the injection period may have important implications regarding efficient ion injection across the entire mass range. This is because most QIT-MS systems are designed to use several levels of radiofrequency (RF) amplitude during a fixed ion injection period to optimally inject ions across the mass range. Consequently, a fundamental understanding of the ion pulse temporal profile following AP-LD will be essential for its for optimal coupling to QIT-MS.

As with all laser desorption/ionization methods used in mass spectrometry, laser fluence is another important factor that can affect the ion signal generated during AP-LD experiments. The effect of laser fluence on conventional vacuum MALDI-MS has been an active area of research over the past decade.[223-226] In those studies the analyte signal generated over a variety of laser fluences indicates that a certain desorption/ionization threshold exists and that this threshold varies with the desorption wavelength and matrix. In other words, the threshold represents a certain magnitude of laser fluence below which no ions can be detected. Dreisewerd and co-workers utilized a second laser to perform photoionization of laser desorbed matrix molecules to understand both the desorption and the desorption/ionization processes.[227] They determined that photoionized molecules could be observed at lower fluences than direct laser ionized molecules. Though it was expected that neutral molecules would be

desorbed at laser fluences below the desorption/ionization threshold, this two-step approach was able to provide direct evidence.

Other researchers have used molecular dynamic (MD) simulations to gain knowledge of the desorption process.[15-19] Simulation does pose a means to observe the desorption process of both analyte and matrix molecules, above and below the desorption/ionization threshold. However, an experimental method like LD-APCI that could observe both desorbed matrix and analyte neutral molecules could corroborate the simulations.

Another area where AP-LD distinguishes itself from its vacuum counterparts is its compatibility with a broader range of sample matrixes. For example, recent AP-LD studies have directly analyzed aqueous-based solutions for peptides in the liquid form.[109,221] Aside from convenience, the ability to directly sample liquid matrices, including aqueous solutions, holds a great deal of quantitative potential. Several researchers have reported quantitation with MALDI-MS, but cite matrix crystal inheterogeneity as a major limitation to reproducibility.[228-239] Solutions, on the other hand, are homogenous and their surfaces are renewable, properties that should provide notable enhancements in shot-to-shot ion-yield precision.

This chapter explores several fundamental parameters affecting the AP-LD process. Factors such as laser pulse timing, temporal ion yield, and the threshold desorption/ionization fluences are considered. And through the use of liquid analyte-containing matrixes, we present evidence of quantitative potential for the AP-LD technique LD-APCI.

Experimental

AP-Laser Desorption-Mass Spectrometry

The interface and mass spectrometer used in these experiments have been described in detail in Chapter 4. Briefly, the source utilizes a heated capillary, AP inlet (ThermoFinnigan, San Jose, CA, USA) to transport the AP generated ions into vacuum for mass analysis. Laser desorption was achieved by irradiation of the target with a pulsed CO_2 laser operating at 10.6 μm (μ-TEA, Laser Science Inc., Franklin, MA, USA). Laser fluence was adjusted by manipulation of a 10 cm focal length zinc selenide lens (Laser Research Optics, Providence, RI, USA) to vary the magnitude of the irradiated area. The laser pulsing was synchronized to coincide with the start of the ion injection period of each microscan.

Samples were applied directly to a 4 mm diameter stainless steel removable target located ~ 3 mm axially from the heated capillary inlet and ~ 2 mm offset from center. The target was held at an offset potential of +2 kV (model 205A, Bertan Associates, Hicksville, NY, USA). For LD-APCI studies a corona needle was positioned ~ 3 cm from the inlet of the heated capillary with the tip axially aligned. A potential of +8.1 kV (V_1), from a standard ESI power supply (Analytica, Branford, MA, USA) was used to generate the corona discharge. For AP-IR-MALDI the corona needle was left in place, but no voltage was applied.

The mass spectrometer, a modified quadrupole ion trap system (Finnigan GCQ, ThermoFinnigan, Austin, TX, USA), was adapted to accept a two-stage differentially pumped vacuum chamber and fitted with an Analytica ESI source manifold (Branford, MA, USA).[214] This manifold was further modified to accept a

metal heated capillary AP inlet. To prevent solvation of the ions, the heated capillary was maintained at 200 °C for the work presented here; an offset potential of +70 V was applied to assist de-clustering.

Sample Preparation

Chemicals were purchased from Sigma (St. Louis, MO, USA) and were used without further purification. The analyte was dissolved at various concentrations in methanol. Next, a small portion of the analyte solution (1-10 μLs) was mixed with glycerol (~ 1 mL) (Fisher Scientific, Fair Lawn, NJ, USA) and vortexed to ensure homogeneity. For the quantitative study, these solutions were prepared at a variety of concentrations. A 2 μL volume of the solution was then deposited onto the surface of the target for sampling. By using liquid matrixes, such as aqueous glycerol, the target stage did not require x-y manipulation.

A polyacrylamide gel was purchased from BioRad (15% Tris-HCl Ready Gels, Hercules, CA, USA) and was loaded with 1000 pmol of the protein horse cytochrome c followed by electrophoresis and staining. The protein containing spots were excised, brought to dryness, and rehydrated in a trypsin (Promega, Madison, Wisconsin, USA) containing solution. After rehydration the gel slices were incubated at 37 °C for 20 hours, after which the slices were placed on the LD-APCI target and directly analyzed. A fuller account on the details of direct gel analysis with LD-APCI-MS can be found elsewhere.[222]

Results and Discussion

Temporal Pulse Width

The temporal width of ion pulses generated following a laser desorption event at AP is of notable significance for the optimal coupling of all AP-LD methods to QIT-MS. To date, no study has been published detailing temporal pulse profiles for any of the AP-LD approaches (AP-MALDI, AP-DIOS, LD-APCI). In this chapter we closely examine the temporal ion pulse profiles generated during AP-LD and discuss their important consequences.

Two different solutions of spiperone, an anti-psychotic pharmaceutical, in a matrix of glycerol were prepared. The first, at 8 ppm, was used for LD-APCI analysis; the second, at a level of 100 ppm with 0.1% trifluoroacetic acid, was employed under AP-MALDI conditions. A CO_2 laser emitting photons at 10.6 μm, having a fluence of ~ 5500 J/m^2 for AP-MALDI and ~ 2500 J/m^2 for LD-APCI, was used for desorption and was triggered to fire at the beginning of the ion trapping period. During LD-APCI, desorbed neutral analyte molecules were then ionized in the gas-phase by reagent ions produced by a corona discharge.[220-222] For AP-MALDI, the corona discharge was not used, but all other conditions, except laser fluence, were held constant. Under continuous scanning, the ion trapping period was varied from 0 to 100 ms in small increments. Afterwards, 10 scans, each composed of 10 single-shot mass spectra, were averaged from each ion trapping period segment and the absolute signal intensity of the spiperone protonated molecule was plotted vs. the magnitude of the ion trapping period (Figure 5-1). Note the AP-MALDI generated signal was multiplied by a factor of 90. In both cases, ions were first detected at a trapping period of ~ 6 ms with the

signal increasing as the trapping period was lengthened. Extending the trapping period past 30 ms did not show significant increases in ion signal.

Polynomial curves were fit to each data series and are also shown in Figure 5-1. Using the equation from each curve, ion intensities were calculated for ion trapping periods from 0 -30 ms in 1 ms increments. The magnitude of change between each trapping time was calculated and plotted in Figure 5-2. This plot represents the temporal ion flux during LD-APCI and AP-MALDI and demonstrates that the majority of the ion flux occurs during a 10 ms period for both methods. In each case the earliest ion trapping period that ions were observed was between 5 and 6 ms, which is also the period that carries the greatest ion flux. The 5 ms delay can be attributed to transport time, i.e., for any given set of AP-LD parameters there exists a fixed time required for ion transport from AP into the ion trap. Following that period, the largest flux of ions arrives at the ion trap during the following millisecond, after which ions continue to be formed over the course of the next 20-25 ms, but the signal continuously decays.

For AP-MALDI, a process that accomplishes desorption and ionization in a single-step rather than two as in LD-APCI, it is surprising that the temporal ion flux occurs on about the same time-scale. But since the chemical ionization is occurring at AP, where protonation reactions will occur on a rapid time-scale, ion transport is evidently the lengthiest step. In either case, the bulk of the ion signal arrives over a relatively short 10 ms period. Therefore, ion pulses on the order of 10 ms, spaced 100 ms apart (10 Hz laser repetition rate) during asynchronous AP-LD experiments, can hardly be considered a continuous source of ions as
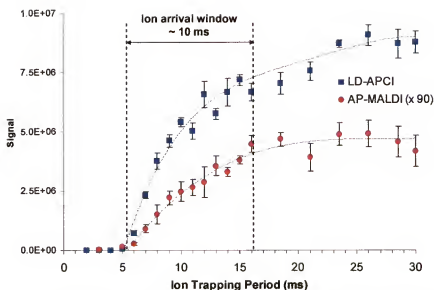
Figure 5-1. Ion signals for LD-APCI and AP-MALDI (signal x 90) as a function of ion trapping period.
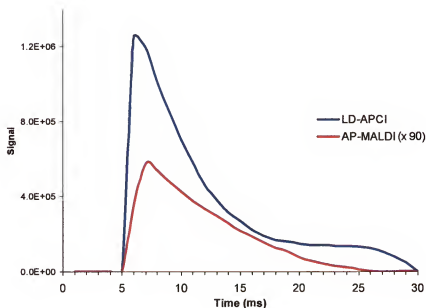
Figure 5-2. Plot of temporal ion flux for LD-APCI and AP-MALDI (signal x 90). The ions initially arrive at the ion trap ~ 5 ms after the laser pulse (t = 0). In both methods, the bulk of the ions arrive within a 10 ms window.

previously suggested.[109] Generation of a continuous ion beam would require sampling at repetition rates of 100 Hz (1 pulse every 10 ms). However, sampling this rapidly is simply not compatible without synchronization because of rapid sample consumption.

With this data in mind, consider the following typical AP-LD scenario: a 200 ms ion trapping period for which AP-LD is to be performed asynchronously with a laser operating at 10 Hz on a QIT-MS. Let us assume that all steps comprising the scan function, aside from ion injection and mass analysis, (e.g., pre-injection, post-injection, multiplier rise time, post-scan time, etc.) consume ~ 35 ms. We shall also assume that we wish to analyze across a mass range of 500 – 2000 m/z, a typical mass range for applications such as tryptic peptide analysis. With the normal scan-rate of 0.18 ms/amu, scanning would consume ~ 270 ms. The entire scan would persist 505 ms, with ion injection accounting for only 200 of those; thus, the correlating duty cycle would be approximately 40% at best, putting only 1 or 2 of the 5 laser pulses to analytical use. Moreover, as described above, the majority of the ions are generated for only 10 ms following the laser pulse and assuming 2 laser pulses occurred during ion injection, the resultant duty cycle would be ~ 4%. This number is in sharp contrast to the "close to 100% duty cycles" reported by Laiko, Moyer, and Cotter for similar AP-MALDI experiments on an ion trap.[103] Those authors must have rounded up. Further, to perform MS/MS, one of the most distinct advantages of the AP-LD-QIT-MS experiment, the duty cycle will drop even lower since additional time will be added to the scan function for ion isolation and fragmentation.

Besides the significant waste of sample in asynchronous AP-LD, ion injection is also a concern. Contemporary ion trap instruments with AP inlets typically utilize multiple levels of RF during ion injection so that all masses throughout the scan range will be successfully injected and stored. For the 200 ms ion injection period discussed above, Figure 5-3A displays the four ion injection RF levels, with each lasting for ~ 50 ms. Also shown as dashed lines are two laser pulses separated by 100 ms (10 Hz operation) with the ion generation period shaded. Note that the pulses will always be separated by 100 ms, but without synchronization they will randomly shift from one scan to the next within the 200 ms window. An unfortunate artifact of this random shifting is that the ion pulses will be randomly injected into different RF environments from one scan to the next; hence, a large number of averaged scans will be needed to generate suitable spectra.

This problem is not unique to the asynchronous mode of operation, but rather is universal to all AP-LD experiments. For example, Figure 5-4 presents the LD-APCI-MS analysis of tryptic peptides of the protein cytochrome C directly from a polyacrylamide gel. In this work one laser pulse, triggered to fire at the onset of ion injection, was used to initiate the generation of an ion pulse that was collected at a single level of injection RF. The tryptic peptides should theoretically be produced at equal amounts, but the injection RF level is optimal for m/z's ~ 700, causing them to appear with the highest intensities, while those of lower or higher masses detected at lower abundances. Using multiple injection levels for a single laser pulse is also problematic because the majority of
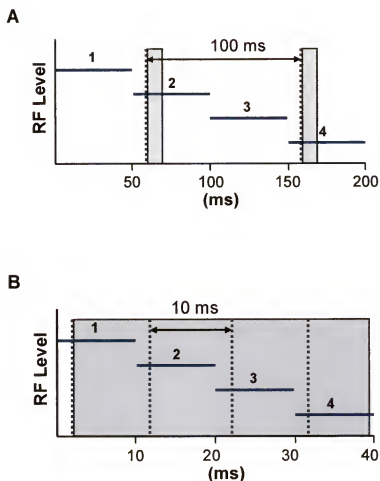
Figure 5-3. Plots of RF level vs. time for a QIT-MS scan function. (A) Diagram depicting a typical AP-LD-QIT-MS experiment with a 200 ms ion injection period having four levels of injection RF, each persisting ~ 50 ms. Dashed lines represent laser pulses separated by 100 ms (10 Hz) with the shaded area displaying the resulting 10 ms ion pulse. (B) Diagram depicting an optimized AP-LD-QIT-MS experiment. Ion trapping period reduced to 40 ms with laser pulses separated by 10 ms (100 Hz) triggered to fire with the onset of each injection RF level.
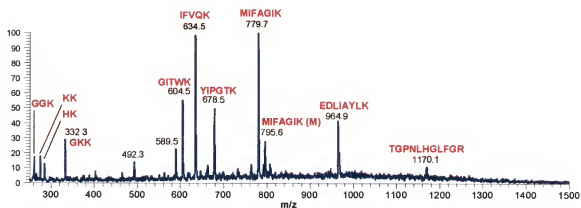
Figure 5-4. LD-APCI-MS mass spectrum of a polyacrylamide gel containing an enzymatically (trypsin) digested protein (cytochrome c) with the detected tryptic peptides labeled. The mass spectrum was obtained using a fixed injection RF that was optimized for m/z's 779 and 634. Note peptides of lower and higher mass detected at lower abundances as a result of injection at non-optimal RF level.

the ion signal arrives unevenly through the course of a 5-10 ms span.

Furthermore, single laser pulses do not take advantage of the QIT's unique

ability to store multiple laser pulses per mass analysis.

The ideal AP-LD-QIT-MS interface would have lasers that operate with

high repetition rates (~ 100 Hz), and the ion pulses they generate should be

triggered to correspond with changes in injection RF levels so that the entire

mass range could be consistently injected into the ion trap scan after scan.

Figure 5-3B shows a more optimized AP-LD experiment employing a 100 Hz

laser that is synchronized to the ion injection RF levels. With this approach the

duty cycle would be enhanced, sample would not be wasted, and the resultant

analysis could be performed with higher precision across the entire mass range.

Laser Fluence

Laser fluence is an important factor that affects the ion signal generated in

both AP-MALDI and LD-APCI. To study these effects, a 15 ppm solution of

spiperone in glycerol was employed. Note that laser fluence was varied by

adjustment of the beam diameter and that the laser profile was near-Gaussian

rather than flat-topped and homogenous. Nonetheless, the fluences were

calculated using the diameter of the beam and assumes a homogenous photon

distribution.

Figure 5-5 presents a log/log plot of the spiperone protonated molecule

signal vs. laser fluence (J/m^2) for AP -MALDI and LD-APCI. Under AP -MALDI

conditions, the molecular ion of spiperone was observed – with a signal-to-

background > 3 – at a fluence of ~ 5500 J/m^2. In contrast, LD-APCI produced a
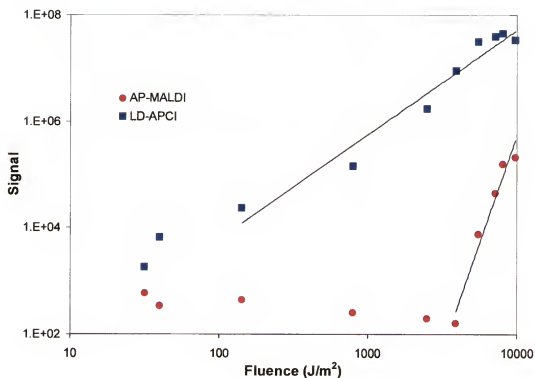
Figure 5-5. Ion signals for LD-APCI and AP-IR-MALDI as a function of laser fluence. Power functions were fitted to the data with the powers m = 2.0 for LD-APCI and m = 8.1 for AP-IR-MALDI.

similar signal at the much lower fluence of ~ 150 J/m^2. The solid lines through each series represent best fits of the data to power functions. The slope of the power function (m) is 2.0 for LD-APCI and 8.1 for AP -MALDI.

LD-APCI provides a means to ionize laser-desorbed analyte molecules and, these data suggest that for the analyte/matrix used here, the desorption threshold fluence was ~ 150 J/m^2. Without the benefit of the corona discharge (AP -MALDI) the analyte must be directly desorbed as an ion, translating to a desorption/ionization threshold fluence that is significantly higher, ~ 5500 J/m^2. Dreiseword et al. reported that the threshold for desorption of photoionized neutral matrix molecules was significantly lower than that for ion desorption.[239] Furthermore, they reported that signal dependence on fluence is steeper for ion desorption than for molecule desorption (slope of power function), an observation that is further substantiated in our results; however, note that their study resorted to observation of the bulk matrix molecules, while ours allowed for the analysis of those of the minority analyte.

These results also bear information about the AP-LD process. Specifically, for this analyte and others previously studied,[220-222] the use of a supplementary ionization method, like the corona discharge, can enhance the ionization efficiency of the MALDI process. Moreover, in cases where sample is limited, LD-APCI can allow the employment of lower fluences and hence offer reduced rates of sample consumption.

Quantitative Possibilities

Because AP-LD offers the unique ability to sample a wide variety of solutions in the liquid-phase, regardless of volatility, we have explored the

potential for quantitation from solutions using LD-APCI-MS. For this study we once again utilized solutions of the analyte spiperone in glycerol. Figure 5-6 presents a LD-APCI-MS calibration curve for spiperone with four series of laser fluences plotted. At concentrations above 25 ppm the curve deviates from linearity. Initially we presumed the deviation was caused by a desorbed population of spiperone molecules that exceeded the available reagent ion species at the elevated spiperone concentrations. But a closer inspection reveals that for the lowest laser fluence used, 2500 J/m^2, the signal at 25 ppm was approximately equal to that attained at 15 ppm; however, for the highest fluence used , 7200 J/m^2, the signal produced at 25 ppm is significantly larger than that at 15 ppm, so it nearly maintains linearity. Thus if the reagent population was the limiting factor, the lowest laser fluence – a fluence that would desorb the least amount of analyte molecules – would maintain linearity for a longer period than would the highest laser fluence.

We believe these data may indicate that glycerol, the solvating matrix, plays a more significant role in the ionization process than initially expected. Because the corona discharge was operated in an ambient environment we expect the major reagent ion species to be protonated water molecules.[200-210] And ionization of the analyte molecules would occur either by direct proton-transfer reactions from the protonated water molecules or through interaction with protonated glycerol molecules. Since the gas-phase proton affinity of glycerol (209 kcal/mol) is higher than that of water (165 kcal/mol),[240] protonation of glycerol should occur to a large extent. Regardless, the amine containing
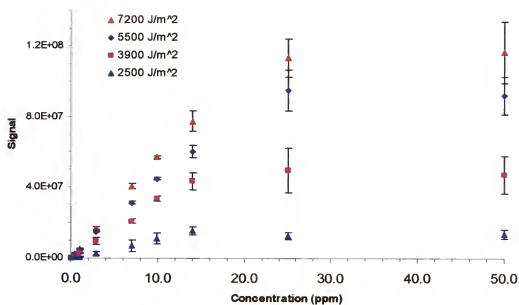
Figure 5-6. LD-APCI-MS calibration curve for spiperone contained in a glycerol solution for a series of laser fluences.
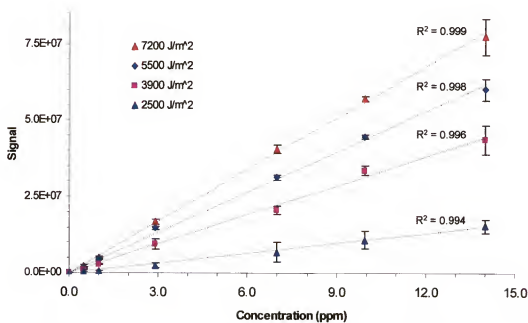
Figure 5-7. Linear region of LD-APCI-MS calibration curve for spiperone under several laser fluences.

spiperone molecule has a gas-phase proton affinity that exceeds both water and glycerol (exact measurements have not been published for this molecule). Therefore, we initially presumed that even if glycerol did serve as an intermediary host to the ionizing protons, its presence should not be critical since direct ionization of the spiperone from protonated water should be more strongly favored. These results suggest that glycerol may not only be involved, but more important to the gas-phase ionization process than expected.

The linear portion of the calibration curve is presented in Figure 5-7. A linear function was fit to the data for each laser fluence series and the resulting correlation coefficient is shown in the figure. Notice that the slope of the curve increases with increasing laser fluence, a trend that demonstrates the population of desorbed neutral molecules is a function of laser fluence. Concentration limits of detection were determined to be ~ 5 ppb. More importantly, this work provides evidence that by sampling directly from the surface of solutions, quantitative results can be attained with relative ease. And unlike their vacuum counterparts, the AP-LD methods are particularly well-suited for direct solution analysis.

Conclusions

AP-LD methods for ion trap mass spectrometers have developed rapidly over the past two years. Interest in AP-MALDI alone has stimulated the three principal QIT-MS manufacturers to develop and make available commercial interfaces within the past year. Despite this interest, surprisingly little effort has been reported on the fundamental processes common to all AP-LD experiments. And though the AP-LD methods are seemingly straightforward, knowledge of such processes will almost certainly be a prerequisite for their optimal

employment in mass spectrometry. Therefore, it was the modest goal of this research to explore some of the most basic of these processes – e.g., temporal ion flux – and to discuss their mass spectrometric implications.

In this chapter we have determined the ion pulse produced during LD-APCI and AP-MALDI to be relatively short, ~ 10 ms. With such short ion pulses, asynchronous modes of coupling AP-LD to QIT-MS will typically result in duty cycles on the order of ~ 4%. Furthermore, random laser pulses within a fixed ion injection period will produce highly erratic mass spectra when scanning across a wide mass range due to the injection of ions into varying levels of RF amplitude. We have proposed a simple resolution – rapid laser pulses that are synchronized to changes in the injection RF levels – that would reduce sample consumption, improve duty cycle, and provide enhanced scan-to-scan reproducibility.

Laser fluence, another fundamental parameter of importance, was studied for both AP-MALDI and LD-APCI. First, the threshold fluence for molecular desorption was determined to be ~ 150 J/m^2 (LD-APCI), while the threshold fluence for desorption/ionization was ~ 5500 J/m^2 (AP-IR-MALDI). LD-APCI provided a novel means to observe the desorbed neutral analyte molecules and has potential to provide corroboration with molecular dynamic (MD) simulations. Second, this work demonstrates that a secondary means of ionization following laser desorption, such as a corona discharge, can significantly enhance ion signal and allow for the employment of reduced fluences that could reduce sample consumption.

Finally, quantitative analysis, a promising potential application of the AP-LD methods was presented. Based on these results herein, quantitation can become an important application of AP-LD.

LASER DESORPTION-ATMOSPHERIC PRESSURE CHEMICAL IONIZATION
MASS SPECTROMETRY FOR THE ANALYSIS OF PEPTIDES FROM
AQUEOUS SOLUTIONS

Background

Of late a new method for performing matrix-assisted laser

desorption/ionization (MALDI) at atmospheric pressure (AP) has been introduced

as AP-MALDI.[102] For this technique, the heated capillary inlet of a Finnigan LCQ

ion trap mass spectrometer was utilized to transport AP-MALDI generated ions

into vacuum for mass analysis.[103-108] More recently, an infrared (IR) laser at 3.0

μm was used to perform AP-IR-MALDI of peptides directly from aqueous

solutions.[109]

Taking a different approach, we have used an IR laser at 10.6 μm to effect

the desorption of neutral molecules at AP, followed by ionization in the gas-

phase with a corona discharge (LD-APCI).[220-222] By separating the desorption

and ionization processes, the signal of the AP-IR-MALDI generated spectra was

enhanced 150-fold.[220] Kolaitis and Lubman, recognizing these advantages,

reported the first chemical ionization of laser-desorbed neutral molecules at AP

using a [63]Ni atmospheric pressure ion source in 1986.[197] Our work builds on that

study through the use of a corona discharge, a more efficient ionization method,

and via laser desorption in the IR as opposed to the ultraviolet (UV) used in that

work. This technique, draws on the fact that a substantially larger number of

gas-phase neutral molecules, as opposed to ions, is produced during a

desorption event.[32] Moreover, the corona discharge is known to provide efficient ionization and because it operates at AP, the process is quite gentle.

There are several advantages driving the development of AP laser desorption/ionization. First, AP-generated ions are more efficiently thermalized than those produced under vacuum conditions, producing spectra showing less fragmentation.[102] Second, AP sampling allows for the examination of vacuum-sensitive samples such as tissue, without adverse effects, and permits the exploration of new matrices like liquid water. Third, restrictions of laser focusing optics, imposed by the vacuum system, are removed at AP, thereby allowing use of near-field optical probes that can greatly reduce laser spot size.[196] Finally, instruments possessing atmospheric pressure inlets would be compatible with a variety of ionization sources (electrospray (ESI), atmospheric pressure chemical ionization (APCI), AP-MALDI, LD-APCI).

The notion of decoupling desorption from ionization is not without precedence. For instance, Cotter and co-workers reported that a significant number of neutral molecules were produced as a result of a laser desorption event and that these neutral molecules had a longer lifetime in an ion source.[32,33] Specifically, they demonstrated that laser desorbed ions were generated for a period of ~ 1 µs, while neutral molecules were observed for 100s of µs. To exploit these desorbed neutral molecules, Cotter performed laser desorption in a chemical ionization source (LD/CI, P ~ 0.5 torr) where the desorbed neutral molecules were ionized with reagent ions from a chemical ionization gas.[33]

In the following years, several different approaches were used to ionize the population of neutral molecules produced after a laser desorption event. These methods included electron impact ionization,[32] chemical ionization,[33-35] and resonant multiphoton ionization.[36-39] Even though the ionization method in each of these cases was different, the idea was the same: decoupling of the desorption and the ionization processes allows for the individual optimization of the two steps with increased efficiency and selectivity.

Despite the advantages that came from the decoupling of laser desorption from the ionization processes, these techniques were successful in desorbing only a few, relatively small peptides. The desorption event, that often induced fragmentation and decomposition, was the limiting factor for the production of gas-phase neutral biomolecules and peptides. This limitation was overcome with the discovery that by using an absorbing, acidic matrix, biomolecules and peptides contained within that matrix could be desorbed/ionized (MALDI), producing intact molecular ions with little fragmentation.[40,48] Since that time MALDI has become one of the most important ionization methods for biomolecules.

As a consequence of this success, the concept of decoupling desorption from ionization has received little attention over the past decade. Even so, Speir and Amster utilized a common MALDI matrix as a substrate for the peptide gramicidin S to demonstrate the functionality of LD/CI.[241] In more recent work, Belov et al. enhanced the MALDI signal of gramicidin S by reacting the produced gas-phase neutral peptide molecules with Na^+ ions.[242]

We describe here the use of an IR laser pulse to desorb gas-phase neutral peptide molecules at AP followed by ionization in the gas phase using a corona discharge. In this orientation, the corona discharge can assume a variety of roles. In this chapter two of these roles are examined: (1) to provide a means for the gas-phase ionization of laser-desorbed peptide molecules and (2) to probe the AP-IR-MALDI process, exploring the efficiency of common MALDI modifiers, such as trifluoroacetic acid (TFA).

Other significant advantages could be gained from decoupling desorption from ionization. In MALDI, matrixes must not only assist with the transport of the analyte into the gas-phase, but must also provide a means for ionization. However, in LD-APCI the matrix containing the analyte need not assist with the ionization, thereby opening the door to many new possible analyte containing matrixes, including biological solutions, tissues,[97,141,146] polyacrylamide gels,[222,243] and thin-layer chromatography plates.

Experimental

Laser Desorption Interface and Mass Spectrometer

A more detailed account of the LD-APCI source interface and mass spectrometer used in this chapter can be found in Chapter 4. Briefly, this design utilizes a heated capillary, AP inlet (ThermoFinnigan, San Jose, CA, USA) to transport the AP generated ions into vacuum for mass analysis. Samples were applied directly to a 4 mm diameter stainless steel removable target that was located ~ 3 mm axially from the heated capillary inlet and ~ 2 mm offset from center. The target was held at an offset potential of +2 kV (model 205A, Bertan Associates, Hicksville, NY, USA). The corona needle was positioned ~ 3 cm

from the inlet of the heated capillary with the tip axially aligned. A potential of +8.1 kV, from a standard ESI power supply (Analytica, Branford, MA, USA) was used to generate the corona discharge.

Laser desorption was achieved by irradiation of the target with a pulsed CO_2 laser, operating at 10.6 μm (μ-TEA, Laser Science Inc., Franklin, MA, USA). The beam was focused to a spot diameter of ~ 1.5 mm (~ 1400 J/m^2, assuming homogenous beam distribution) using a 10 cm focal length zinc selenide lens (Laser Research Optics, Providence, RI, USA). The laser pulsing was synchronized to coincide with the prescan period of the scan function, which was 1 ms before the ion injection period of each microscan.

The mass spectrometer used in these studies, a modified quadrupole ion trap system (Finnigan GCQ, ThermoFinnigan, Austin, TX, USA), was adapted to accept a two-stage differentially pumped vacuum chamber and fitted with an Analytica ESI source manifold (Branford, MA, USA).[214] This manifold was further modified to accept a metal heated capillary AP inlet. To prevent solvation of the ions, the heated capillary was maintained at 200 °C for the work presented here; an offset potential of +130 V was applied to assist de-clustering.

Sample Preparation

The peptides leu-enkephalin, neurotensin 8-13, des-Pro^2 bradykinin, bradykinin, vasopressin, and angiotensin I (Sigma, St. Louis, MO, USA) were dissolved in water (HPLC grade, Fisher Scientific, Fair Lawn, NJ, USA) at a concentration of 1 mg/ml. For sample preparation, an aliquot of each solution was mixed with an equal amount of glycerol (Fisher Scientific, Fair Lawn, NJ,

USA) and vortexed to ensure homogeneity. A small amount of the mixture was deposited onto the surface of the target for sampling (typically $0.15 - 0.25$ μl). In some cases the peptide containing aqueous glycerol solution was dosed with 0.1% TFA. In spectra which portray 10 pmol loaded on target, the initial aqueous solution was diluted 10-fold, then mixed with glycerol in equal proportions as described above. By using liquid matrices, such as aqueous glycerol, the target stage did not require x-y manipulation and despite the small volumes applied to the target, analyte signal could typically be generated for a continuous 10 minute period.

Results and Discussion

In the past few years, several research groups have reported the use of aqueous glycerol solutions for IR-MALDI experiments, some using laser emitting at wavelengths ~ 3 μm,[244,245] and others at 10.6 μm.[246] In those studies, the water was evaporated or frozen before introduction into the vacuum system of the mass spectrometer. More recently, aqueous glycerol solutions, used without freezing or evaporation, have been successfully employed for AP-IR-MALDI of peptides with a laser emitting at 3 μm.[109] Based on the success of these collective works, we elected to utilize aqueous glycerol solutions of peptides to study the LD-APCI process for peptides and to provide a direct comparison to AP-IR-MALDI.

A Comparison of AP-IR-MALDI and LD-APCI

Our initial studies were to determine any benefit gained through the use of the corona discharge, and for this evaluation, the pentapeptide leu-enkephalin

was chosen. The effect of the corona discharge can be observed in Figure 6-1A, which displays the ion chromatogram of the $[M+H]^+$ ion of leu-enkephalin at m/z 556, with the corona discharge turned off and on during continuous scanning. Figures 6-1B and C exhibit mass spectra that were obtained without and with the corona discharge, respectively. The spectrum presented in Figure 6-1B represents the average of 100 single-shot mass spectra (required to generate a quality spectrum), while Figure 6-1C represents the average of only 5 single-shot mass spectra.

Some significant differences can be observed comparing Figure 6-1B and C. Perhaps most distinguishing is the pronounced $[M+Na]^+$ peak observed under AP-IR-MALDI conditions (corona discharge off), whilst the $[M+H]^+$ dominates the LD-APCI spectrum (corona discharge on) with an enhancement by a factor of ~ 1400. This demonstrates that under the AP-IR-MALDI conditions, cationization is the dominating ionization process. In contrast, the initiation of the corona discharge establishes an alternative means of ionization, namely gas-phase proton transfer explaining the substantial enhancement of the protonated molecule that is observed.

Another noteworthy observation is that the absolute intensity of the sodiated molecular ion increases by an order of magnitude with the use of the corona discharge. One plausible explanation is that as a consequence of laser irradiation the sodiated neutral peptide molecule $[M-H+Na]^0$ is liberated into the gas-phase. By use of the corona discharge this minority species can undergo gas-phase protonation, resulting in an increased formation of the $[M+Na]^+$.
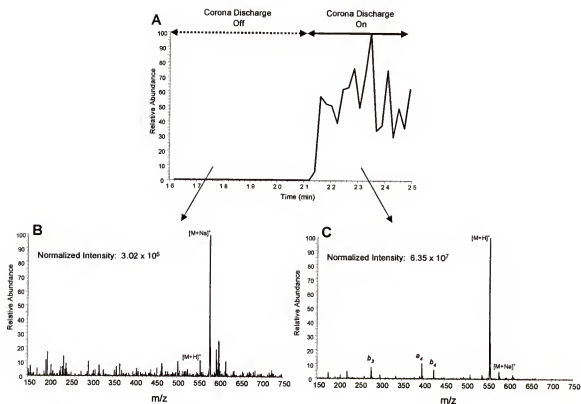
Figure 6-1. LD-APCI-MS and AP-IR-MALDI-MS analysis of leu-enkephalin in
50% aqueous glycerol solution (100 pmol loaded). (A) Ion
chromatogram for [M+H]⁺ of leu-enkephalin (m/z 556) during
constant scanning with corona discharge toggled off and on. (B)
Mass spectrum with corona discharge off (100 single-shot spectra
averaged) (C) Mass spectrum with corona discharge on (5 single-
shot spectra averaged).

Finally, the b_4, b_3, and a_4 series fragment ions of leu-enkephalin are easily observed in Figure 6-1C, but can also be seen (with larger amounts loaded, data not shown) without the use of the corona discharge. Because the fragmentation can be observed under both ionization conditions, the likely cause can be attributed to collisional-induced dissociation (CID) in the region between the heated capillary exit and skimmer cone. With our home-built source, a high offset potential of ~ + 250 V must be applied to a tube lens (between heated capillary exit and skimmer cone) to assist declustering and to provide for a more efficient transmission of higher mass ions. For leu-enkephalin the fragmentation could be somewhat relieved by lowering this offset, but the signal of the molecular ion was also reduced. Further supporting this theory, the fragmentation was most pronounced with the lower mass peptides studied (e.g., leu-enkephalin), those that would be accelerated the most by the offset voltage.

An Evaluation of the Acid Modifier TFA

Acid modifiers, like TFA, are often used during MALDI matrix solution preparation[247] and have been reported to be advantageous in some cases.[248] In prior AP-IR-MALDI experiments, conducted by Laiko et al., 0.1 % TFA was added to the matrix solutions, but no comments were made regarding the role or effect of the acid.[109]

Figure 6-2 displays a series of mass spectra obtained from a 50% aqueous glycerol solution containing the peptide neurotensin 8-13 both without (Figure 6-2A and C) and with (Figure 6-2B and D) 0.1% TFA. The effect of TFA on the AP-IR-MALDI generated spectra can be seen by comparing Figure 6-2A
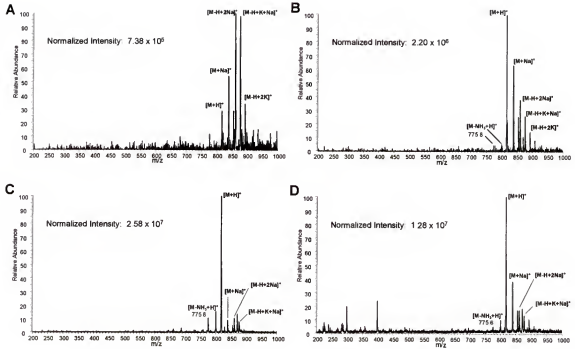
Figure 6-2. LD-APCI-MS and AP-IR-MALDI-MS studies of the acid additive TFA.
(A-B) represent AP-IR-MALDI generated spectra: (A) without 0.1%
TFA (B) with 0.1% TFA, (C-D) represent LD-APCI generated spectra:
(C) without 0.1% TFA (D) with 0.1% TFA. Sample consisted of 100
pmol neurotensin fragment 8-13 in a solution of 50% aqueous
glycerol, with each spectra representing the average of 25 single-
shot spectra.

and B. Here the production of the protonated molecule (m/z 817) is enhanced by a factor of ~ 10, through the use of the TFA additive. In this case, the TFA, like the corona discharge, is providing an alternate ionization route, that of protonation as opposed to cationization. Figure 6-2C and D display the effect of the corona discharge where the solution sampled in Figure 6-2C does not contain TFA and Figure 6-2D does. Using the corona discharge to enhance the AP-IR-MALDI generated signal provides ~ 100 fold increase in protonated molecule production without the TFA additive, a ~ 10 fold enhancement over the TFA additive.

Figure 6-2D displays the LD-APCI spectrum of the TFA containing matrix. Here the signal of the protonated molecule is somewhat suppressed as compared to the signal generated with no TFA present, but perhaps more distinguishing is the elevated background. Specifically, a number of low mass species can now be observed that were not previously present. These ions were also detected in a blank and we propose that their formation is due to an excess of reagent ions formed by the initiation of the corona discharge. When TFA is present, a larger number of the analyte molecules are ionized, as evidenced by comparing Figure 6-2A and B. Consequently, the population of gas-phase neutral analyte species is lowered, so when the corona discharge is initiated the excess reagent ions will participate in ionization of the lower proton affinity matrix and background molecules.

To summarize, these data show that for AP-IR-MALDI at 10.6 μm, TFA enhances generation of the protonated molecule. However, also demonstrated

is that the use of a corona discharge can further enhance that signal by an order of magnitude. Because TFA is corrosive and its simultaneous use with the corona discharge was found to elevate background, the remaining work presented here was conducted without its use.

LD-APCI of Various Peptides

Figure 6-3 displays the LD-APCI generated spectra of several other peptides. The peptides sampled include des-Pro^2 bradykinin (Figure 6-3A), bradykinin (Figure 6-3B), arg-vasopressin (Figure 6-3C), and angiotensin I (Figure 6-3D). In each case the spectrum presented represents the average of 25 single-shot spectra with 100 pmol of each peptide loaded. The enhancements observed with the corona discharge were similar to those previously described in Figure 6-1. In fact, the equivalent AP-IR-MALDI spectra for angiotensin I failed to produce observable protonated molecules above the noise and cationized adducts were present at low signal to noise (~ 2). Therefore, despite the relatively high background that can be observed in Figure 6-3D, the LD-APCI method produced a marked improvement as compared to AP-IR-MALDI.

Sensitivity Considerations

For an analytical technique a measure of potential usefulness can be made by an evaluation of sensitivity. To assist this evaluation, a ten-fold dilution of the neurotensin 8-13 containing aqueous glycerol solution was performed and analyzed. Figure 6-4 displays the spectrum generated after the deposition of this solution onto the target (10 pmol loaded, average of 50 single-shot spectra).
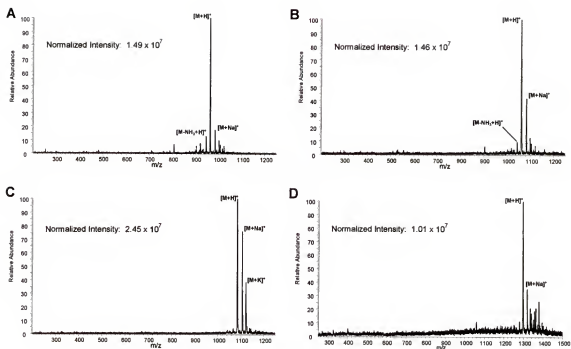
Figure 6-3. LD-APCI-MS mass spectra of varous peptides. (A) des-Pro^2 bradykinin, (B) bradykinin, (C) arg-vasopressin, and (D) angiotensin I. Each spectrum represents the average of 25 single-shot mass spectra with 100 pmol of analyte loaded.
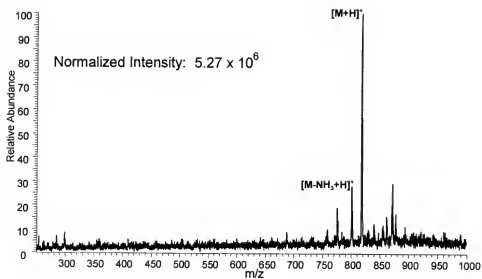
Figure 6-4. LD-APCI mass spectrum of neurotensin 8-13 (spectrum represents the average of 50 single-shot mass spectra, 10 pmol loaded).

Again, an intense protonated molecule was observed, but the background is elevated as a result of the dilution. At this level the corona discharge still induced an enhancement similar to those outlined above (data not shown). Next the sample was diluted by another factor of 10 and analyzed, but no analyte ions could be observed.

Several parameters could enhance the sensitivity of the current LD-APCI methodology. To date most AP-MALDI experiments have used multiple laser pulses per an extended ion accumulation period (200 – 400 ms)[103-108] to increase sensitivity -- a method that is in sharp contrast to the single laser pulse followed by an ion accumulation period of ~ 20 ms used in this study. The incorporation of multiple laser pulses could potentially be advantageous for LD-APCI to increase sensitivity. Other important considerations are the position of the corona needle and target and magnitude of the potential supplied to each. Parameters that upon further optimization are expected to improve ionization efficiency and transport. An alteration of reagent gas makeup (presently ambient air) should also show an effect upon the ionization efficiency. Pulsing the corona discharge, time-delayed appropriately after each laser pulse, could add advantageous temporal resolution and preferential discrimination among ion signals.[219] And not to be underestimated, the interfacing of this source to a modern, commercial instrument could provide significant improvements as well.

Conclusions

This chapter demonstrates that a corona discharge enhances the production of protonated molecules of numerous peptides following laser desorption at AP. In addition, the acid modifier TFA was found to increase the

production of the protonated molecule by a factor of ~ 10, under AP-IR-MALDI conditions. The corona discharge enhances the protonated molecule signal by a factor of ~ 100. From these data, it is clear that the ionization efficiency of the AP-IR-MALDI process can be significantly improved through the use of a supplemental ionization method, like the corona discharge.

Because the LD-APCI process does not require the matrix to play a role in ionization, numerous new analyte containing matrices can potentially be compatible with this method. Some examples might include the direct analysis and/or imaging of biological tissues or solutions (e.g., blood plasma or urine) at atmospheric pressure. While matrix extension is an important advantage that is possible with LD-APCI, the corona discharge can also be used as a valuable tool to examine the MALDI process. In short, it can be used as a probe to explore the gas-phase neutral population produced in the MALDI plume.

Finally, we have examined the LD-APCI sensitivity, which even in its present prototype form is reasonably good, but further improvements should result from thorough parametric optimization studies including the use of multiple laser pulses per ion accumulation period, target and corona needle positioning and voltages, and reagent gas composition alterations.

LASER DESORPTION-ATMOSPHERIC PRESSURE CHEMICAL IONIZATION:
A NOVEL ION SOURCE FOR DIRECT COUPLING OF POLYACRYLAMIDE
GEL ELECTROPHORESIS TO MASS SPECTROMETRY

Background

Over the past decade proteomics has become an important and popular

application of mass spectrometry. This popularity continues to be driven by the

development of novel technology for coupling protein characterization methods to

mass spectrometric analysis.[142,249-251] Due to the high complexity of most

biological samples, protein identification and characterization usually requires a

first dimension of separation. Two-dimensional polyacrylamide gel

electrophoresis (2-D PAGE) is the most widely employed protein separation

technique because of its ability to separate thousands of proteins in a single

analysis.[252,253] Accordingly, a great deal of effort has been spent to couple

PAGE to mass spectrometric (MS) analysis.

The most widely employed method involves staining the gel (after

electrophoresis), excision of spots, in-gel enzymatic digestion, extraction from the

gel, cleanup,[254] and mixing with a matrix-assisted laser desorption/ionization

(MALDI) matrix for time-of-flight mass spectrometric (MALDI-TOF-MS)

analysis.[255] In fact, this methodology has inspired the construction of robotic

workstations designed to automate peptide desalting, clean-up, and

concentration for MALDI-TOF-MS analysis.[256] Unfortunately, this approach relies

on chemical staining to determine protein location and then calls for removal of

the visualized spots with subsequent MS analysis. A potential limitation the method imposes is that regardless of MS sensitivity, only those spots stained will be processed for MS analysis.

Over the past decade numerous researchers have been working to develop methodology that would allow the direct MS analysis of PAGE. In this arrangement the entire gel can be imaged by MS, and thus eliminate the need for staining. Briefly, two main strategies have emerged with the first involving electroblotting from the PAGE to a membrane. Once on the membrane, the proteins or digested peptides were then coated with a MALDI matrix, placed inside the vacuum chamber and directly examined via UV-MALDI-MS[257-259] or IR-MALDI-TOF-MS.[260,261,141] In the second strategy, a MALDI matrix was applied directly to ultrathin gels (< 10 μm when dried) followed by UV-MALDI-TOF-MS analysis of both enzymatically produced peptides and the intact proteins.[135-137] In those studies, the use of thin gels served to concentrate the proteins into a smaller volume, allowing sub-picomole detection limits to be achieved.

Recently a third strategy has been suggested, in which a tunable, mid-infrared free-electron laser (FEL) tuned at 5.9 μm was used to desorb/ionize peptides placed on top of a frozen polyacrylamide gel.[262] The concept is that by tuning the laser to a strong absorption band of the gel, the gel material itself can be used as a MALDI matrix. Even so, the gel must be frozen and inserted into the vacuum system for analysis. The widespread application of this approach will likely be hindered by the complexity and cost of the FEL.

A commonality all the above described methods share is that the desorption/ionization step occurs inside the vacuum chamber. Gel sampling and/or imaging at atmospheric pressure (AP) would represent a significant advance in the coupling of proteomics to mass spectrometry. AP sampling would require less time via elimination of vacuum interlocks and would not require that the gel be frozen or dried prior to analysis. Additionally, gel analysis could be performed on mass spectrometers having AP inlets and could create a single instrument capable of a variety of ionization techniques (e.g., electrospray (ESI), APCI, AP-MALDI, LD-APCI).

A second universal feature shared by all of these methods is that desorption and ionization are accomplished in a single step, an approach that imposes restrictions regarding the development of direct MS sampling/imaging of PAGE. Either an exogenous matrix must be added or the desorption wavelength must be specifically tuned to match the maximum absorption of the gel.

Taking a different approach, our laboratory has been active in the development of a novel laser desorption-atmospheric pressure chemical ionization (LD-APCI) source.[220-222] In this technique an IR laser pulse at 10.6 μm is used to effect the desorption of neutral molecules at AP, followed by ionization in the gas-phase with a corona discharge.[220] The method draws on the fact that a substantially larger number of gas-phase neutral molecules, as opposed to ions, are produced during a laser desorption event. With this arrangement, desorption is decoupled from ionization, allowing for the individual optimization of each step with increased efficiency and selectivity. This benefit has been

recently highlighted for the analysis of aqueous peptide solutions where the use of the corona discharge enhanced the AP-IR-MALDI generated signal of the analyte protonated molecule by factors up to 1400.[221,243]

In contrast, for MALDI, matrixes must not only assist with the transport of the analyte into the gas-phase, but must also provide a means for ionization. However, in LD-APCI the matrix containing the analyte need not assist with the ionization, thereby opening the door to many new possible analyte containing matrixes, including polyacrylamide gels. Using the LD-APCI source, we present here the first, to our knowledge, mass spectrometric analysis of tryptic peptides directly from intact polyacrylamide gels at AP.

Experimental

Laser Desorption and Mass Spectrometer Interface

A detailed description of the LD-APCI source interface and mass spectrometer can be found in Chapter 4. Briefly, this source utilizes a heated capillary, AP inlet (ThermoFinnigan, San Jose, CA, USA) to transport the AP generated ions into vacuum for mass analysis. The gel slices were applied directly to a 4 mm diameter stainless steel removable target located ~ 3 mm axially from the heated capillary inlet and ~ 2 mm offset from center. The target was held at an offset potential of +2 kV (model 205A, Bertan Associates, Hicksville, NY, USA). The corona needle was positioned ~ 3 cm from the inlet of the heated capillary with the tip axially aligned. A potential of +8.1 kV, from a standard ESI power supply (Analytica, Branford, MA, USA) was used to generate the corona discharge.

Laser desorption was achieved by irradiation of the target with a pulsed CO_2 laser, operating at 10.6 μm (μ-TEA, Laser Science Inc., Franklin, MA, USA). The beam was focused to a spot diameter of ~ 0.5 mm (~ 10,000 J/m^2, assuming homogenous distribution) using a 10 cm focal length zinc selenide lens (Laser Research Optics, Providence, RI, USA). The laser pulsing was synchronized to coincide with the prescan period of the scan function, which was 1 ms before the ion injection period of each microscan.

The mass spectrometer used in these studies, a modified quadrupole ion trap system (Finnigan GCQ, ThermoFinnigan, Austin, TX, USA), was adapted to accept a two-stage differentially pumped vacuum chamber and fitted with an Analytica ESI source manifold (Branford, MA, USA).[220] This manifold was further modified to accept a metal heated capillary AP inlet. To prevent solvation of the ions, the heated capillary was maintained at 200 °C; an offset potential of +130 V was applied to assist de-clustering.

In certain cases, MALDI-TOF-MS analysis of tryptic peptides – extracted from in-gel digests – was performed. The MALDI-TOF mass spectrometer used in those cases was an Applied Biosystems Voyager-DE Pro (Framingham, MA) system, that was operated in the reflectron mode.

Sample preparation

The peptides and proteins used in this study were purchased from Sigma (St. Louis, MO, USA), except for the mutant human carbonic anhydrase protein (HCA II), whose synthesis has been described elsewhere.[264] For the initial desorption studies the peptide neurotensin 8-13 was dissolved at 1 mg/mL in

water and 2 μL of that solution was placed directly on top of a polyacrylamide gel slice. For that work, a small square (~ 4 mm x 4 mm) was cut from a gel and placed on the target, followed by the deposition of the neurotensin 8-13 peptide.

The polyacrylamide gels were purchased from BioRad (15% Tris-HCl Ready Gels, Hercules, CA, USA) and in cases where electrophoresis was performed the gels were stained (unless otherwise noted) with Coomassie brilliant blue after electrophoresis. Following staining, the spots were excised and washed twice with 200 mM NH_4HCO_3, pH 8 washing buffer. Next, the gel slices were brought to dryness in a SpeedVac (SVC100, Savant, Holbrook, NY, USA). Using the difference in gel mass (before and after drying), the gel slice was rehydrated in a trypsin (Promega, Madison, Wisconsin, USA) containing 50 mM NH_4HCO_3 solution (usually 6 – 15 μL depending on gel slice size). An effort was made to eliminate adding any additional liquid to prevent migration of tryptic peptides out of the gel. Once rehydrated the gel slices were incubated at 37 °C for 20 hours, after which the slices were placed on the LD-APCI target and directly analyzed.

For MALDI-TOF-MS analysis, the tryptic peptides were extracted during the in-gel enzymatic digestion by increasing the volume of the digestion solution (~ 35 μL). Cleanup of the digestion extract was accomplished by use of a C18 stationary phase-containing pipette tip (ZipTip, Millipore, Bedford, MA), followed by elution onto a MALDI target with a 15 mg/mL 4-hydroxy-α-cyanocinnamic acid matrix solution.

Results and Discussion

Preliminary experiments were aimed to determine whether the polyacrylamide gel could be used as a matrix to support the desorption of neutral biomolecules. To determine this, a 15% Tris-HCl polyacrylamide gel (BioRad, Ready Gels) was obtained, a small section (~ 4 mm x 4 mm) was cut and placed on the stainless steel target, and immediately thereafter 2 µl of an aqueous neurotensin 8-13 solution was deposited on top. The target was then mounted on the LD-APCI source and immediately sampled. The LD-APCI-MS analysis is presented in Figure 7-1. The effect of the corona discharge can be observed in Figure 7-1A, which displays the ion chromatogram of the [M+H]$^+$ ion of neurotensin 8-13 at m/z 817, with the corona discharge turned on and off during continuous scanning. Figure 7-1B and C exhibit mass spectra (the average of 5 single-shot spectra) that were obtained with and without the corona discharge, respectively.

As shown in Figure 7-1C, no detectable ions could be produced when the corona discharge was off. This result is not surprising since we have neither added exogenous MALDI matrix nor tuned our laser wavelength to coincide with the maximum absorbance of the gel to provide an ionization mechanism. However, by initiating the corona discharge the protonated molecule of neurotensin 8-13 is produced as the base peak (Figure 7-1B). These data provide evidence that ablation of the gel with 10.6 µm laser radiation at AP does produce a substantial number of intact gas-phase peptide molecules. By use of the corona discharge these gas-phase molecules can be ionized by proton
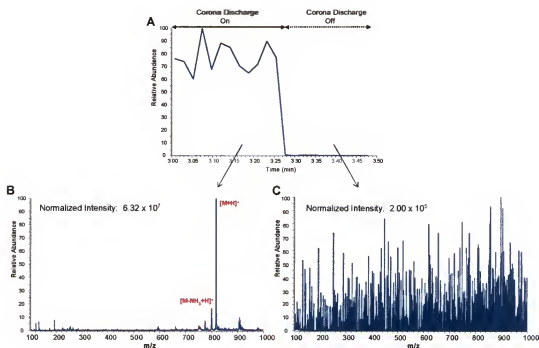
Figure 7-1. LD-APCI-MS analysis of the peptide neurotensin 8-13 directly from a polyacrylamide gel. (A) Ion chromatogram for [M+H]+ of neurotensin 8-13 (m/z 817) during constant scanning with corona discharge toggled on and off. (B) Mass spectrum with corona discharge on. (C) Mass spectrum with corona discharge off.

transfer, a gentle process since there is extensive collisional cooling at ambient pressure.

Direct Detection of Tryptic Peptides

Standard protein analysis

While the above described experiment demonstrates the benefit that can be obtained through the use of a two-step desorption/ionization process like LD-APCI, sampling neat peptides from the surface of a gel does not represent a realistic proteomics application. A more practical test of the method would be the detection of tryptic peptides arising from an in-gel enzymatic digestion, a process where peptides will be distributed throughout the gel, as opposed to being deposited on the surface. Therefore, the protein horse cytochrome c was obtained and loaded on another 15% Tris-HCl Ready Gel and electrophoresed. The gel was loaded with 1000, 500, 100, 50, and 10 pmol of the protein (in lanes 1-5, respectively) and was photographed following electrophoresis and staining (Figure 7-2A). For analysis the spots were excised, washed, dried, and rehydrated in a trypsin-containing solution. The gel slices were then incubated at 37 °C for 20 hours, after which the pieces were placed on the LD-APCI-MS target and directly analyzed.

Figure 7-2B and C present the LD-APCI-MS mass spectra (each the average of 15 single-shot spectra) that were obtained from the direct sampling of spots 1 and 2, respectively. Table 7-1 displays the expected peptides following a trypsin digest of equine cytochrome c. As labeled, 9 tryptic peptides of cytochrome c were observed in Figure 7-2B, and 6 in Figure 7-2C. No
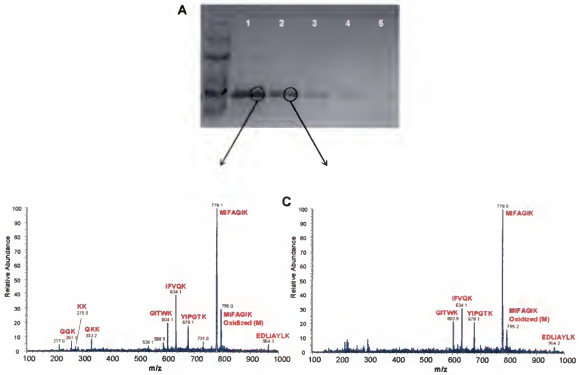
Figure 7-2. Direct LD-APCI-MS analysis of tryptic peptides from a
            polyacrylamide gel. (A) Photograph of Coomassie blue stained
            polyacrylamide gel following electrophoresis. (B) LD-APCI-MS
            analysis of stained spot from lane 1. (C) LD-APCI-MS analysis of
            stained spot from lane 2.

Table 7-1. Peptides resulting from a tryptic digest of horse cytochrome c.

Theortical m/z	Position	Peptide Sequence
1495.69	61 – 72	EELMEYLENPK
1470.68	40 – 53	TGQAPGFTYDANK
1168.62	28 – 38	TGPNLHGLFGR
1018.44	14 – 22	CAQCHTVEK
964.53	*92 – 99*	*EDLIAYLK*
779.44	*80 – 86*	*MIFAGIK*
678.38	*74 – 79*	*YIPGTK*
634.39	*9 – 13*	*IFVQK*
604.34	*56 – 60*	*GITWK*
547.27	1 – 5	GDVEK
434.18	101 – 104	ATNE
405.20	89 – 91	TER
332.23	*6 – 8*	*GKK***
284.17	26 – 27	HK
275.21	*87 – 88*	*KK***
261.15	*54 – 55, 23 – 25*	*NK, GGK*
204.13	6 – 7	GK
147.11	8, 39, 73, 87, 88, 100	K

*Bold entries represent peptides detected during PAGE-LD-APCI-MS analysis, ** denotes detected missed cleavages.

identifiable tryptic peptides were observed from the other spots. An interesting aspect observed in Figure 7-2B and C is that nearly every m/z detected results from a tryptic peptide of cytochrome c. This likely results because of the gas-phase neutral molecule population that is produced after a laser desorption event; only those with the highest proton affinities will be ionized by the corona discharge, peptides in this case. Protein identification was accomplished by entering the observed masses into an online database (Mascot), which correctly recognized the protein as cytochrome c. Further, because of the low background, the LD-APCI-MS technique has the potential to identify lower mass peptides that would normally be obscured by the matrix background produced during MALDI-TOF-MS analysis.

Figure 7-3 displays the LD-APCI-MS mass spectra of another protein (horse myoglobin, 1000 pmol) obtained directly from the gel following an in-gel enzymatic digestion. Again, nearly every tryptic peptide within the mass range of the instrument was detected (Table 7-2). And, once again, almost every detected mass can be attributed to the protein, rather than matrix background.

Detection of single amino-acid point mutations

The biological function of proteins can be altered by modifications carried out in the cell following synthesis (post-translational modification). These modifications include proteolytic cleavage and covalent modifications such as acetylation, glycosylation, hydroxylation, methylation, phosphorylation, etc. Additionally, up or down-regulation of post-translationally modified proteins can be associated with diseased or non-diseased cellular states. Amino acid
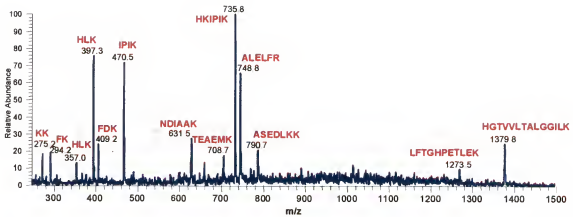
Figure 7-3. Direct LD-APCl-MS analysis of a polyacrylamide gel containing tryptic peptides of myoglobin. Mass spectrum represents the average of ~ 100 single-shot mass spectra, 1000 pmol protein loaded.

Table 7-2. Peptides resulting from a tryptic digest of horse myoglobin.

Theortical m/z	Position	Peptide Sequence
1885	103-118	YLEFISDAIIHVLHSK
1854	80-96	GHHEAELKPLAQSHATK
1816	1-16	GLSDGEWQQVLNVWGK
1607	17-31	VEADIAGHGQEVLIR
1503	119-133	HPGDFGADAQGAMTK
1379	*64-77*	*HGTVVLTALGGILK*
1272	*32-42*	*LFTGHPETLEK*
791	*57-63*	*ASEDLKK***
749	*134-139*	*ALELFR*
736	*97-102*	*HKIPIK***
709	*51-56*	*TEAEMK*
662	*57-62*	*ASEDLK*
650	148-153	ELGFQG
631	*140-145*	*NDIAAK*
470	*99-102*	*IPIK*
409	*43-45*	*FDK*
397	*48-50*	*HLK*
310	146-147	YK
294	*46-47*	*FK*
284	97-98	HK
275	*78-79*	*KK***
147	63, 78,79	K

*Bold entries represent peptides detected during PAGE-LD-APCI-MS analysis, ** denotes detected missed cleavages. Dashed lines mark scanned mass range.

changes are also observed, where a single amino acid is replaced by another in the protein's sequence. These amino acid polymorphisms may or may not affect biological function – i.e., mutagenic or silent, respectively.

Therefore, a method capable of rapidly monitoring protein modifications has potential value as an important tool for the early diagnosis of disease. In this section we report on the ability of the LD-APCI-MS methodology to detect single-amino acid polymorphisms in the protein human carbonic anhydrase II (HCA II). For this study mutant HCA II, with three single-point mutations, was prepared using methodology reported elsewhere.[264] The amino acid sequence of the HCA II was modified in the following manner: (1) residue 23, alanine (A) to cysteine (C), (2) residue 203, leucine (L) to cysteine (C), and (3) residue 205, cysteine (C) to serine (S).

1000 pmol of both mutant HCA II and wildtype (unmodified) HCA II were loaded (separately) onto a polyacrylamide gel and electrophoresed. As described above, the protein bands were excised, enzymatically digested, and mass analyzed directly by LD-APCI-MS and indirectly by MALDI-TOF-MS. The results are presented in Figure 7-4. Unfortunately, two of the mutations were contained in a single tryptic peptide whose molecular weight (~ 3500 daltons) was well beyond the mass range of our LD-APCI-MS instrument. However, the third mutation, located in the DFPIAK tryptic peptide (where A is replaced with C in the mutant), was observed in the LD-APCI-MS analysis of the wildtype HCA II (Figure 7-4A, m/z 690). Direct gel analysis of the mutant protein band did not produce signal at m/z 690, but a new mass was observed at m/z 722 (Figure 7-
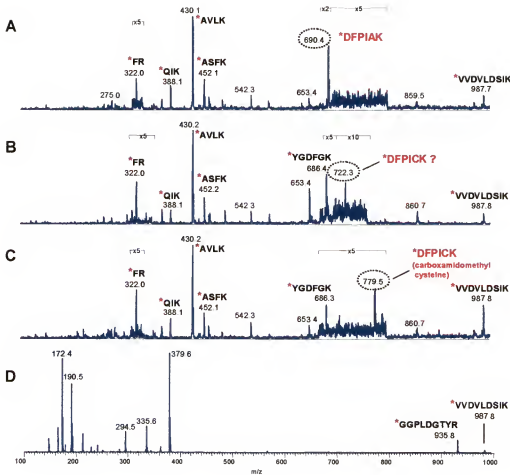
Figure 7-4. LD-APCI and MALDI mass spectra of in-gel protein digests. (A) Direct in-gel LD-APCI sampling of human carbonic anhydrase II (HCA II) wildtype protein digest, (B) HCA II mutant, (C) HCA II mutant treated with iodoacetamide prior to digestion, and (D). MALDI-TOF analysis of HCA II mutant (iodoacetamide treated) in-gel digest extract. The LD-APCI-MS data represents the average of ~ 100 single-shot mass spectra, while the MALDI-TOF-MS mass spectrum results from the accumulation of 100 single-shot mass spectra.

4B), albeit with poor S/B. A shift of +32 daltons corresponds to the replacement of A with C.

Nonetheless, that identification could be considered tentative; therefore, to confirm the mutation, another protein band containing the mutant HCA II was treated with iodoacetamide prior to enzymatic digestion. This reagent selectively reacts with cysteine residues to produce carboxamidomethyl cysteine, which should add 57 daltons to the tryptic peptide residue of interest. LD-APCI-MS analysis of that band is shown in Figure 7-4C. Indeed, a new peak can be observed at m/z 779, a shift of +57 daltons. Note, 6 other tryptic peptides were observed in the LD-APCI-MS analysis of both the mutant and the wildtype HCA II protein bands.

For a comparison, the tryptic peptides from one of the mutant HCA II protein bands was extracted, following in-gel enzymatic digestion, and prepared for MALDI-TOF-MS analysis. Cleanup of the digestion extract was accomplished by use of a C18 stationary phase-containing pipette tip (ZipTip), followed by elution onto a MALDI target with a 15 mg/ml 4-hydroxy-α-cyanocinnamic acid matrix solution. The MALDI-TOF-MS analysis of the digest extract is presented in Figure 7-4D. Only two tryptic peptides were observed in the 100 – 1000 dalton mass range in the MALDI-TOF-MS analysis, neither of which correspond to the mutant peptide. Moreover, a significant number of matrix background peaks can be observed in the low mass range. To be fair, a number of other tryptic peptides were detected by MALDI-TOF-MS analysis in the mass range of 1000 –

2500; however, the tryptic peptide carrying the other two mutations was not observed.

From these data, there is little question that the LD-APCI direct approach outperforms MALDI-TOF-MS analysis in the 100 – 1000 dalton mass range. And in this case, LD-APCI detected one of the three mutations, while MALDI-TOF-MS analysis detected none. Moreover, the technique offers a more rapid and convenient method, compared to MALDI, and has potential to become a valuable tool for both proteomics and the diagnosis of disease.

Parameter Studies

That said, much work remains before the method can be sucessfully implemented for these proposed applications. Sensitivity and mass range are two Figures of Merit that will require further evaluation and improvement. The remaining sections of this chapter discuss important parameters such as the effect of digestion volume and gel staining on sensitivity. Finally, the last section presents other strategies for enhancing sensitivity and mass range.

Digestion volume

Most protocols written for in-gel enzymatic digestion of proteins are designed to cover the entire gel slice with a large volume of enzyme-containing solution. In that procedure the peptides, once produced by enzymatic cleavage of the protein, are free to migrate out of the gel and accumulate within the digestion solution. Following digestion the remaining peptides are extracted from the gel with a series of solvents. Those solutions are then combined, desalted, and concentrated for further analysis MS analysis.

However, in a direct gel analysis approach extraction of the peptides from the gel will result in a degradation of sensitivity. Therefore, for the LD-APCI-MS analyses presented above, the standard in-gel digestion protocol was modified such that small volumes of digestion solution were added to the gel slices to minimize peptide extraction. But this method raised other concerns about the efficiency of the digestion process. For example, is an excess of solution necessary for proper enzyme function?

To answer this question, we performed a series of in-gel enzymatic digestions on a mixture of two unresolved proteins (bovine hemoglobin and horse cytochrome c) with varying digestion volumes. The volumes of enzyme solution were 15 μL, 25 μL, and 35 μL; note the enzyme concentration was adjusted such that each volume delivered the same magnitude of enzyme.

Figure 7-5A presents a diagram of the digestion process for the differing volumes. Because the gel slices were rehydrated (following dehydration with a vacuum centrifuge) with the digestion solution, there was no excess digestion solution for the lowest volume, 15 μL. Figure 7-5B displays the number of detected tryptic peptides (S/B > 3) of the two proteins for each digestion volume. From these data increased digestion volumes result in reduced peptide detection efficiency, a trend explained by peptide extraction.

Gel staining

For all analyses presented above, the stain Coomassie brilliant blue (G-250) was utilized to locate the protein bands before excision and digestion. Consequently, upon LD-APCI-MS analysis the gel bands still accommodated the

A

Digestion Tube →

Gel Slice →

Digestion Solution

15 μL   25 μL   35 μL

B

Identified Peptides

Digestion Volume (μl)
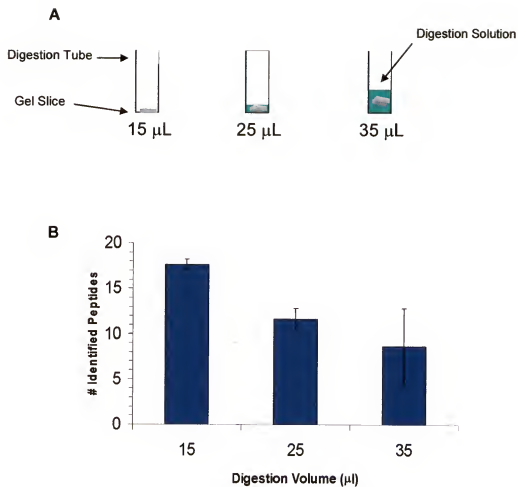
Figure 7-5. Digestion solution volume studies. (A) Diagram depicting various volumes of digestion solution. (B) Number of LD-APCI-MS detected peptides resulting from varying digestion volumes.

stain and its effect on the process was unknown. Initially, we surmised the presence of stain during the analysis was probably not beneficial. To examine this hypothesis, we compared LD-APCI-MS mass spectra of enzymatically-digested protein-containing gels stained with a variety of chemicals (Coomassie brilliant blues G-250, R-250, biosafe G-250 and silver stain with two types of destaining) to those exposed to no stain.

The results of this analysis are shown in Figure 7-6A-F. Surprisingly sampling of the Coomassie stained gels generated the greatest number of detected tryptic peptides, producing higher-quality spectra than even the unstained gels. The silver stained gel showed some detectable peptides, albeit with poor S/B, when the stain was left in the gel (Figure 7-6E); however, when the silver stain was removed, prior to digestion using the MS sensitive protocol from the manufacturer, no detectable tryptic peptides were produced. The gels stained with Coomassie brilliant blues were bright blue in color, the silver stain bands (not destained) were gray, while the non-stained and the silver destained bands were clear.

Based on the visual difference and mass spectra, we propose the stain molecules could be playing a role in the analyte desorption process. Specifically, absorbance by the matrix at the wavelength of the incident photons is critical for molecular desorption. Figure 7-7A displays an FTIR transmission spectra of a polyacrylamide gel (solid line), while Figure 7-7B,C display those for Coomassies brilliant blue G-250 and R-250, respectively. From these spectra it is clear these
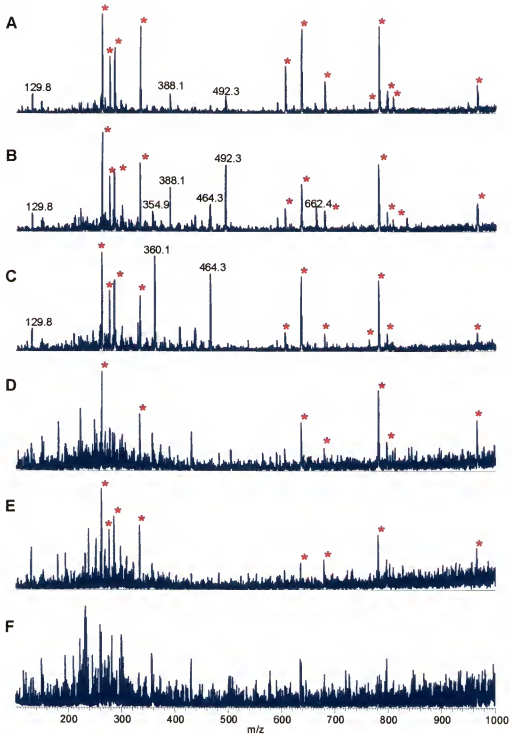
Figure 7-6. LD-APCI-MS mass spectra of gel slices following in-gel protein digests, following various chemical staining methods. Coomassie brilliant blues G-250 (A), Biosafe G-250 (B), and R-250 (C), no stain (D), silver without destain (E), silver destained (F). * denotes detected cytochrome c tryptic peptides.
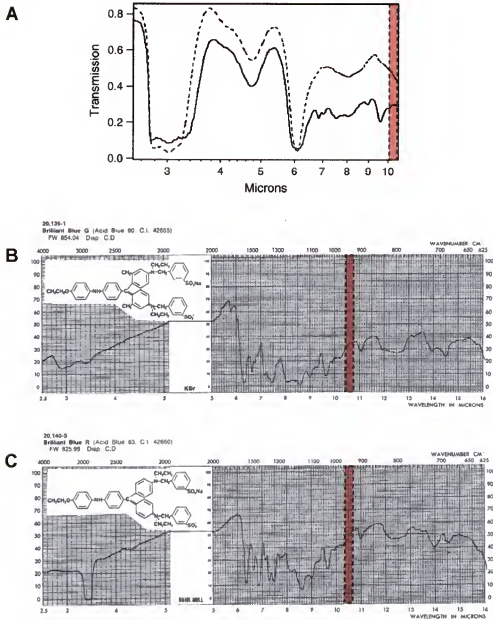
Figure 7-7. FTIR transmission spectra. (A) Transmission spectra of 7.5% native polyacrylamide gel (solid line) and water (dashed line).[262] Transmission spectra of Coomassie brilliant blues G-250 (B) and R-250 (C).[269] Dashed lines indicate wavelength region used in these studies.

stain molecules exhibit a strong absorbance at 10.6 microns, possibly explaining the enhanced peptide signals obtained in their presence.

We attempted to characterize any absorbance differences between Coomassie stained gels and their non-stained counterparts by use of attenuated total reflectance spectroscopy (ATR). Using this device, the sample was placed on a crystal surface and absorbance spectra were recorded for both stained and non-stained gel slices. However, because the gels were moist and the ATR provides minimal sample penetration, the resultant absorbance spectra were identical to the gel storage buffer and no useful comparison could be made. A transmission attachment was designed to allow collection of absorbance spectra in the tranmission mode, but in this arrangement no photons were transmitted.

Considering the difficulties in obtaining a direct absorbance comparison, we prepared glycerol solutions of both Coomassie stains and evaluated their LD-APCI mass spectra. Figure 7-8 displays the LD-APCI mass spectrum of Coomassie G-250 in a solution of glycerol. The major peaks (m/z's 464, 492, 662) in the spectrum result from fragmentation of the molecule and were observed in the direct gel analysis data. It is interesting that Coomassie R-250, (differing from G-250 by only two methyl groups) produced only a single peak at m/z 517 (data not shown), whose identity we cannot assign. And yet direct gel analysis of R-250 stained protein yields a prominent m/z at 464, but lacks m/z 517.

In any case, difficulties in acquiring comparable absorbance data prevent the positive comfirmation of our hypothesis – that staining elevates the
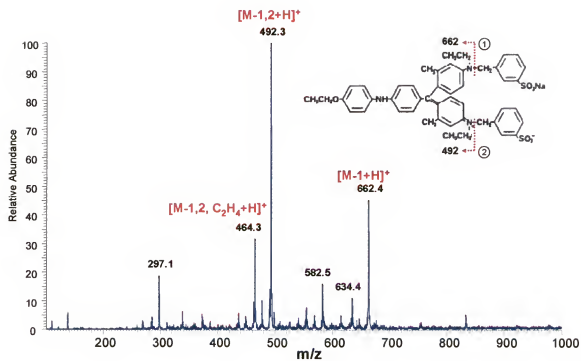
Figure 7-8. LD-APCI-MS mass spectrum of Coomassie G-250 contained in a solution of glycerol.

absorbance of the gel at 10.6 microns and thereby increases the peptide detection sensitivity. Alternatively, one could effect desorption at a wavelength of ~ 3.0 microns, where the gel has a significantly higher absorbance, to further evaluate this theory. Unfortunately, this experiment was not performed since a photon source at this wavelength was not available for use.

Sensitivity

Based on these results, the LD-APCI-MS approach to direct gel sampling has promise to become a valuable tool for proteomics research, but several issues must be further evaluated and/or improved. Because no analyte signals were observed from spots where less than 500 pmol had been loaded, sensitivity is one of these concerns. There are several parameters that could have an impact on sensitivity including staining, digestion procedure, and numerous source conditions that upon further optimization will likely lead to improvements in detectable amount.

Though those parameters are expected to produce sensitivity enhancements, the most straightforward route to improved sensitivity is calculated to arise from the use of thinner gels. This is proposed because despite the deeper penetration depth of IR vs. UV irradiation,[263] inspection of the gel slices after sampling revealed the removal of very little material from the surface of the gel. Since the gels employed in this study were 1 mm thick, the majority of the loaded sample was not subjected to LD-APCI-MS analysis, assuming a homogenous protein distribution within the gel. A particularly well-suited approach may be that of ultrathin layer gel electrophoresis,[265-267] where gels as thin as 25 μm have been used.[268] Through the use of thinner gels, the

volume containing the protein will be significantly lowered, thereby allowing for the loading of less protein, which should translate into increased sensitivity.

Other questions regarding the mass range of the technique must also be addressed. The home-built ion trap mass spectrometer used in these studies has a limited mass range (< 1500). However, the instrument cannot optimally inject and mass analyze ions across its entire mass range (100-1500). Therefore, future experiments on modern commercial instrumentation will be necessary to determine the upper mass range limit of the technique.

Conclusions

The data presented here demonstrate LD-APCI-MS as a viable new approach for the direct AP coupling of PAGE to MS. Additionally, with a more thorough evaluation of the preparation and analysis steps, significant improvements in sensitivity and time efficiency are likely. Future studies will evaluate the use of isoelectric focusing as a second dimension (2D PAGE) and incorporate the use of thinner gels, which is expected to concentrate proteins and further improve sensitivity. Presently the technique offers numerous advantages regarding the coupling of PAGE and MS. The required steps involving in-gel digestion, extraction, and sample cleanup prior to either MALDI-TOF or LC-ESI-MS analysis are both labor-intensive and time-consuming. In contrast, PAGE-LD-APCI-MS eliminates extraction, cleanup, and sample preparation, an approach that potentially translates into a more convenient, robust methodology for the rapid identification of proteins. To summarize, the work presented here represents the first successful direct-AP coupling of PAGE to MS for tryptic

peptide analysis and provides evidence supporting the further development of the LD-APCI source.

CHAPTER 8
CONCLUSIONS

The continued development of mass spectrometry is of high importance to numerous fields of science. Evidence of this importance can be seen in the recent awarding of the 2002 Nobel Prize in Chemistry, awarded for "the development of methods for the identification and structure analyses of biological macromolecules". Two of this year's award winners were mass spectrometrists who played critical roles in the development of electrospray ionization (ESI, John B. Fenn) and matrix-assisted laser-desorption/ionization (MALDI, Koichi Tanaka).

This dissertation has focused on laser desorption methods for mass spectrometry and presents alternatives to MALDI for applications such as mass spectrometric imaging. For imaging, the matrix deposition process is time-consuming and can perturb the analyte's spatial distribution. Laser desorption/chemical ionization (LD/CI) is an approach that decouples desorption from ionization and eliminates the need for an exogenous matrix. This approach was used to desorb/ionize the environmental contaminant 3,3',4,4'-tetrachlorobiphenyl (TCB) from the intestinal tissue of catfish; however, imaging under the confines of the vacuum system presented numerous problems including tissue shrinkage, limited spatial resolution, and difficult sample manipulation.

To eliminate these concerns a novel laser desorption-atmospheric pressure chemical ionization source (LD-APCI) was designed, constructed, and

175

evaluated. The goal of this design was to circumvent the problems of sampling under vacuum conditions while still utilizing the benefits from decoupling of the desorption and ionization events. Preliminary experiments with the new source utilized the anti-psychotic drug spiperone in a solution of glycerol. There the two-step approach produced protonated spiperone molecule signals ~ 150 times larger than that of the one-step AP-MALDI method. These results confirmed that during a laser desorption event a substantially larger number of neutral molecules, as opposed to ions, are desorbed. Therefore, an analytical method, like LD-APCI, that can put to use both the desorbed neutral molecules and the desorbed ions can generate greater sensitivity compared to those that only employ the desorbed ions (AP-MALDI).

Fundamental studies of laser desorption at atmospheric pressure (AP-LD) were performed and demonstrated several unique characteristics of the method. The first determined ion temporal pulse width following both LD-APCI and AP-MALDI to be approximately 10 ms. Because of the relatively short ion pulse, we have proposed new methodology to optimize coupling of both methods to quadrupole ion trap mass spectrometers. Another aspect examined was laser fluence, which demonstrated the two-step approach of LD-APCI able to produce ion signal at a fluence about 40 times lower than AP-MALDI. Finally the quantitative potential of LD-APCI was evaluated and shown promising. We argue that all AP-LD methods should show improved quantitative potential compared to their vacuum-counterparts since they have a greater compatibility with liquid matrixes.

Biological molecule analysis is an area of great interest for mass spectrometry in general, and Chapter 6 explored the LD-APCI source for its ability to desorb/ionize numerous peptides. This study demonstrated that for peptides, like pharmaceuticals, the two-step approach produced significant increases in sensitivity as compared to AP-MALDI. We also assert that observation of the desorbed neutral molecule population following a laser desorbtion event could provide a unique window for fundamental studies of the ionization processes in MALDI.

Numerous advantages are gained through the decoupling of the desorption and ionization processes, and Chapter 7 of this dissertation quite possibly presents the most promising of them all. That advantage is the ability to sample natural analyte-containing matrixes directly without the need for prior extraction, cleanup, or special matrix addition. Here we present the first direct mass spectrometric analysis of tryptic peptides from a polyacrylamide gel following electrophoresis. Other potential applications for the technique include the direct sampling of biological molecules, pharmaceuticals, or environmental contaminants from biological tissues or solutions.

Overall, we have found the LD-APCI method to be surprisingly robust and are convinced that upon further optimization and development it could play an important role in the field of mass spectrometry. In its present form we have demonstrated it to enhance AP-MALDI generated ion signal, give insight into the MALDI ionization process, and provide a unique means to directly sample polyacrylamide gels for tryptic peptides.

LIST OF REFERENCES

1. Watson JT, Biemann K. *ibid.* **1965**, 37, 844.

2. Van Lear GE, McLafferty FW. *Annual Reviews in Biochemistry.* **1969**, 38, 298.

3. Gray WR, Wojcik LH, Futtrell JH. *Biochemical and Biophysical Research Communications.* **1970**, 41, 1111.

4. Torgerson DF, Skowronski RP, Macfarlane RD. *Biochemical and Biophysical Research Communications.* **1974**, 60, 616.

5. Macfarlane RD, Torgerson DF. *Science.* **1976**, 191, 920.

6. Benninghoven A, Sichtermann W. *Organic Mass Spectrometry.* **1977**, 12, 595.

7. Grade H, Winograd N, Cooks RG. *Journal of the American Chemical Society.* **1977**, 99, 7725.

8. Posthumus MA, Kistemaker PG, Meuzelaar HLC, Ten Noever de Brauw MC. *Analytical Chemistry.* **1978**, 50, 985-991.

9. Barber M, Bordoli RS, Sedgwick RD, Tyler AN. *Journal of the Chemical Society-Chemical Communications.* **1981**, 325-327.

10. Barber M, Bordoli RS, Sedgwick RD, Tyler AN. *Nature.* **1981**, 293, 270-275.

11. Karas M, Bachmann D, Bahr U, Hillenkamp F. *International Journal of Mass Spectrometry.* **1987**, 78, 53-68.

12. Karas M, Hillenkamp F. *Analytical Chemistry.* **1988**, 60, 2299-2301.

13. Williams P. *Science.* **1991**, 252: 1865-1865.

14. Buehler RJ, Flanigan E, Greene LJ, Friedman L. *Journal of the American Chemical Society.* **1974**, 96, 3990-3999.

15.   Zhigilei LV, Kodali PBS, Garrison BJ. *Chemical Physics Letters*. **1997**, 276, 269-273.

16.   Zhigilei LV, Kodali PBS, Garrison BJ. *Journal of Physical Chemistry B*. **1997**, 101, 2028-2037. (1997)

17.   Zeifman MI, Garrison BJ, Zhigilei LV. *Applied Surface Science*. **2002**, 7971, 1-8.

18.   Ziefman MI, Garrison BJ, Zhigilei LV. *Journal of Applied Physics*. **2002**, 92, 2181-2193.

19.   Yingling YG, Zhigilei LV, Garrison BJ, Koubenakis A, Labrakis J, Georgiou S. *Applied Physics Letters*. **2001,** 78, 1631-1633.

20.   Metta D, Diamond H, Barnes RF, Milsted J, Gray J, Henderson PJ, Stevens CM. *Journal of Inorganic Nuclear Chemistry*. **1965**, 27, 33.

21.   Benninghoven A, Sichtermann W. *Organic Mass Spectrometry*. **1977**, 12, 595-597.

22.   Grade H, Winograd N, Cooks RG. *Journal of the American Chemical Society*. **1977**, 99, 7726-7727.

23.   Benninghoven A. *Surface Science*. **1973**, 35, 427-457.

24.   Busch KL, Cooks RG. *Science*. **1982**, 218, 247-254.

25.   Rinehart KL. *Science*. **1982**, 218, 254-260.

26.   Kerr RA. *Science*. **1982**, 216, 163-164.

27.   Vastola FJ, Pirone AJ, Knox BE. *Proceedings of the ASTM Committee E-14, 14th Annual Conference on Mass Spectrometry and Allied Topics*. **1966**, Dallas, TX, 78.

28.   Vastola FJ. *Applied Spectroscopy*. **1968**, 22, 374.

29.   Vastola FJ. *Organic Mass Spectrometry*. **1968**, 1, 499.

30.   Vastola FJ, Mumma RO, Pirone AJ. *Organic Mass Spectrometry*. **1970,** 3, 101-104.

31.   Mumma RO, Vastola FJ. *Organic Mass Spectrometry*. **1972,** 6, 1373-1376.

32. Van Breemen, RB, Snow M, Cotter RJ. *International Journal of Mass Spectrometry and Ion Processes*. **1983**, 49, 35-50.

33. Cotter RJ. *Analytical Chemistry*. **1980**, 52, 1767-1770.

34. Perchalski RJ, Yost RA, Wilder BJ. *Analytical Chemistry*. **1983**, 55, 2002-2005.

35. Speir JP, Gorman GS, Cornett DS, Amster IJ. *Analytical Chemistry,* **1991**. 63, 65-69.

36. Tembreull R, Lubman DM. *Analytical Chemistry*. **1986**, 58, 1299-1303.

37. Tembreull R, Lubman DM. *Analytical Chemistry*. **1987**, 59, 1082-1088.

38. Li L, Lubman DM. *Applied Spectroscopy*. **1989**, 43, 543-549.

39. Li L, Lubman DM. *Analytical Chemistry*. **1988**, 60, 1409-1415.

40. Hillenkamp F, Karas, M, Beavis RC, Chait BT. Analytical Chemistry. **1991**, 63, 1193A-1203A.

41. Yamashita M, Fenn JB. *Journal of Physical Chemistry*. **1984**, 88: 4451.

42. Vertes A, Gijbels R, Levine RD. *Rapid Communications in Mass Spectrometry*. **1990**, 4, 228-233.

43. Karas M, Bahr U, Ingendoh A, Nordhoff E, Stahl B, Strupat K, Hillenkamp F. *Analytica Chimica Acta*. **1990**, 241, 175-185.

44. Busch KL. *Journal of Mass Spectrometry*. **1995**, 30, 233-240.

45. Kampmeier J, Dreisewerd K, Schurenberg M, Strupat K. *International Journal of Mass Spectrometry and Ion Processes*. **1997**, 169/170, 31-41.

46. Strupat K, Kampmeier J, Horneffer V. *International Journal of Mass Spectrometry and Ion Processes*. **1997**, 169/170, 43-50.

47. Papantonakis MR, Kim J, Hess WP, Haglund RF. *Journal of Mass Spectrometry*. **2002**, 37, 639-647.

48. Zenobi R, Knochenmuss R. *Mass Spectrometry Reviews*. **1998**, 7, 337-366.

49. Karas M, Gluckmann M, Schafer J. *Journal of Mass Spectrometry*. **2000**, 35, 1-12.

50.   Chiarelli MP, Gross ML. *Analytical Chemistry.* **1989**, 61, 1895-1900.

51.   Li Yunzhi Y, McIver RT. *Rapid Communications in Mass Spectrometry.* **1994**, 8, 743-749.

52.   Loboda AV, Krutchinsky AN, Bromirski M, Ens W, Standing KG. *Rapid Communications in Mass Spectrometry.* **2000**, 14, 1047-1057.

53.   Baldwin MA, Medzihradszky KF, Lock CM, Settineri TA, Burlingame AL. *Analytical Chemistry.* **2001**, 73, 1707-1720.

54.   Strobel FH, SoloukiT, White MA, Russell DH. *Journal of the American Society for Mass Spectrometry.* **1991**, 2, 91-94.

55.   Chien BM, Michael SM, Lubman DM. *Rapid Communications in Mass Spectrometry.* **1993**, 7, 837-843.

56.   Fountain ST, Lee H, Lubman DM. *Rapid Communications in Mass Spectrometry.* **1994**, 8, 487-494.

57.   Whittal RM, Li L. *Analytical Chemistry.* **1995**, 67, 1950-1954.

58.   Brown RS, Lennon JJ. *Analytical Chemistry.* **1995**, 67, 1998-2003.

59.   Bestal ML, Juhasz P, Martin SA. *Rapid Communications in Mass Spectrometry.* **1995**, 9, 1044-1050.

60.   Paul W, Steinwedel H. *German Patent.* **1956**, 944,900.

61.   Paul W, Steinwedel H. *U.S. Patent.* **1960**, 2,939,952.

62.   Jonscher KR, Yates JR. *Analytical Biochemistry.* **1997**, 244, 1-15.

63.   Stafford GC, Kelley PE, Syka JEP, Reynolds WE, Todd JFJ. *International Journal of Mass Spectrometry and Ion Processes.* **1984**, 60, 85-98.

64.   Louris JN, Cooks RG, Syka JEP, Kelley PE, Stafford GC, Todd JFJ. *Analytical Chemistry.* **1987**, 59, 1677-1685.

65.   March RE. *Rapid Communications in Mass Spectrometry.* **1988**, 12, 1543-1554.

66.   Louris JN, Brodbelt-Lustig JS, Cooks RG, Glish GL, Van Berkel GJ, McLuckey SA. *International Journal of Mass Spectrometry and Ion Processes.* **1990**, 96, 117-137.

67. Tucker DB, Hameister CH, Bradshaw DJ, Hoekman DJ, Weber-Grabau M. *Proceedings of the 36th ASMS Conference on Mass Spectrometry and Allied Topics.* **1988**, San Francisco, CA. 628.

68. Heller DN, Lys I, Cotter RJ, Manuel Uy O. *Analytical Chemistry.* **1989**, 61, 1083-1086.

69. Louris JN, Amy JW, Ridley TY, Cooks RG. *International Journal of Mass Spectrometry and Ion Processes.* **1989**, 88, 97.

70. Doroshenko VM, Cotter RJ. *Rapid Communications in Mass Spectrometry.* **1993**, 7, 822-827.

71. Doroshenko VM, Cornish TJ, Cotter RJ. *Rapid Communications in Mass Spectrometry.* **1992**, 6, 753-757.

72. Doroshenko VM, Cotter RJ. *Analytical Chemistry.* **1995**, 67, 2180-2187.

73. Doroshenko VM, Cotter RJ. *Rapid Communciations in Mass Spectrometry.* **1996**, 10, 65-73.

74. Doroshenko VM, Cotter RJ. *Analytical Chemistry.* **1996**, 68, 463-472.

75. Glish GL, Goeringer DE, Asono KG, McLuckey SA. *International Journal of Mass Spectrometry and Ion Processes.* **1989**, 94, 15-24.

76. Chambers DM, Goeringer DE, McLuckey SA, Glish GL. *Analytical Chemistry.* **1993**, 65, 14-20.

77. Alexander ML, Hemberger PH, Cisper ME, Nogar. *Analytical Chemistry.* **1993**, 65, 1609-1614.

78. Garrett AW, Cisper ME, Nogar NS, Hemberger PH. *Rapid Communications in Mass Spectrometry.* **1994**, 8, 174-178.

79. Gill CG, Garrett AW, Nogar NS, Hemberger PH. *Rapid Communications in Mass Spectrometry.* **1997**, 11, 551-556.

80. Robb DB, Blades MW. *International Journal of Mass Spectrometry.* **1999**, 190/191, 69-80.

81. Schlunegger UP, Stoeckli M, Caprioli RM. *Rapid Communications in Mass Spectrometry.* **1999**, 13, 1792-1796.

82.   Dale JM, Yang M, Whitten WB, Ramsey JM. *Analytical Chemistry*. **1994**, 66, 3431-3435.

83.   Hong K, Song K, Cha H, Yang M, Lee J, Lee G. *Microchemical Journal*. **1999**, 63, 9-17.

84.   Beavis RC, Chait BT. *Chemical Physics Letters*. **1991**, 181, 479-484.

85.   McIntosh A, Donovan T, Brodbelt J. *Analytical Chemistry*. **1992**, 64, 2079-2083.

86.   Schwartz JC, Bier ME. *Rapid Communications in Mass Spectrometry*. **1993**, 7, 27-32.

87.   Jonscher K, Currie G, McCormack AL, Yates JR. *Rapid Communications in Mass Spectrometry*. **1993**, 7, 20-26.

88.   Jonscher K, Yates JR. *Journal of Biological Chemistry*. **1997**, 272, 1735-1741.

89.   Bristow AWT, Creaser CS. *Rapid Communications in Mass Spectrometry*. **1995**, 9, 1465-1469.

90.   Bristow AWT, Creaser CS, Nelieu S, Sinhorn J. *Analyst*. **1996**, 121, 1425-1428.

91.   Creaser CS, Stygall JW. *Trends in Analytical Chemistry*. **1998**, 17, 583-593.

92.   Qin J, Steenvoorden RJJM, Chait BT. *Analytical Chemistry*. **1996**, 68, 1784-1791.

93.   Qin J, Chait BT. *Analytical Chemistry*. **1996**, 68, 2102-2107.

94.   Qin J, Chait BT. *Analytical Chemistry*. **1996**, 68, 2108-2112.

95.   Qin J, Chait BT. *Analytical Chemistry*. **1997**, 69, 4002-4009.

96.   Hall BJ, Goolsby B, Brodbelt JS. *Applied Spectroscopy*. **1999**, 53, 1361-1366.

97.   Troendle FJ, Reddick CD, Yost RA. Journal *of the American Society for Mass Spectrometry*. **1999**, 10, 1315-1321.

98.   Krutchinsky AN, Chait BT. *Analytical Chemistry*. **2001**, 73, 5066-5077.

99. Krutchinsky AN, Chait BT. *Journal of the American Society for Mass Spectrometry*. **2002**, 13, 129-134.

100. Lennon JD, Glish GL. *Analytical Chemistry*. **1997**, 69, 2525-2529.

101. Lippa T, Taranenko NI, Prasad CR, Doroshenko VM. *European Journal of Mass Spectrometry*. **2002**, 8, 263-271.

102. Laiko VV, Baldwin MA, Burlingame AL. *Analytical Chemistry*. **2000**, 72, 652-657.

103. Laiko VV, Moyer SC, Cotter RJ. *Analytical Chemistry*. **2000**, 72, 5239-5243.

104. Keough T, Lacey MP, Strife RJ. *Rapid Communications in Mass Spectrometry*. **2001**, 15, 2227-2239.

105. Moyer SC, Cotter RJ, Woods AS. *Journal of the American Society for Mass Spectrometry*. **2002**, 13, 274-283.

106. Galicia MC, Vertes A, Callahan JH. *Analytical Chemistry*. **2002**, 74, 1891-1895.

107. Creaser CS, Reynolds JC, Harvey DJ. *Rapid Communications in Mass Spectrometry*. **2002**, 16, 176-184.

108. Moyer SC, Cotter RJ. *Analytical Chemistry*. **2002**, 74, 469A-476A.

109. Laiko VV, Taranenko NI, Berkout VD, Yakshin MA, Prasad CR, Lee SH, Doroshenko, VM. *Journal of the American Society for Mass Spectrometry*. **2002**, 13, 354-361.

110. Laiko VV, Taranenko NI, Berkout VD, Musselman, Doroshenko VM. *Rapid Communications in Mass Spectrometry*. **2002**, 16, 1737-1742.

111. Hercules DM. *Microchemical Journal*. **1988**, 38, 3-23.

112. Vaeck LV, Struyf H, Roy WV, Adams F. *Mass Spectrometry Reviews*. **1994**, 13, 189-208.

113. Vaeck LV, Struyf H, Roy WV, Adams F. *Mass Spectrometry Reviews*. **1994**, 12, 209.

114. Vaeck LV, Poels K, De Nollin S, Hachimi A, Gijbels R. *Cell Biology International*. **1997**, 21, 635-648.

115. Todd PJ, Schaaff TG, Chaurand P, Caprioli RM. *Journal of Mass Spectrometry.* **2001**, 36, 355-369.

116. Pacholski ML, Winograd N. *Chemical Reviews.* **1999**, 99, 2977-3005.

117. McMahon JM, Short RT, McCandlish CA, Brenna JT, Todd PJ. *Rapid Communications in Mass Spectrometry.* **1996**, 10, 335-340.

118. Colliver TL, Brummel CL, Pacholski ML, Swanek FD, Ewing AG, Winograd N. *Analytical Chemistry.* **1997**, 69, 2225-2231.

119. Todd PJ, McMahon JM, Short RT, McCandlish CA. *Analytical Chemistry.* **1997**, 69, 529A-535A.

120. Pacholski ML, Cannon DM, Ewing AG, Winograd N. *Journal of the American Chemical Society.* **1999**, 121, 4716-5717.

121. Braun RM, Beyder A, Xu J, Wood MC, Ewing AG, Winograd, N. *Analytical Chemistry.* **1999**, 71, 3318-3324.

122. Cannon DM, Pacholski ML, Winograd N, Ewing AG. *Journal of the American Chemical Society.* **2000**, 122, 603-610.

123. Caprioli RM, Farmer TB, Gile J. *Analytical Chemistry.* **1997**, 69, 4751-4760.

124. Garden RW, Sweedler JV. *Analytical Chemistry.* **2000**, 72, 30-36.

125. Li L, Garden RW, Romanova EV, Sweedler JV. *Analytical Chemistry.* **1999**, 71, 5451-5458.

126. Chaurand P, Stoeckli M, Caprioli RM. *Analytical Chemistry.* **1999**, 71, 5263-5270.

127. Stoeckli M, Farmer TB, Caprioli RM. *Journal of the American Society for Mass Spectrometry.* **1999**, 10, 67-71.

128. Spengler V, Hubert M. *Journal of the American Society for Mass Spectrometry.* **2002**, 13, 735-748.

129. Koomen JM, Stoeckli M, Caprioli RM. *Journal of Mass Spectrometry.* **2000**, 35, 258-264.

130. Gusev AI, Vasseur OJ, Proctor A, Sharkey AG, Hercules DM. *Analytical Chemistry.* **1995**, 67, 4565-4570.

131. Guittard J, Hronowski XL, Costello CE. *Rapid Communications in Mass*

132. Mehl JT, Hercules DM. *Analytical Chemistry*. **2000**, 72, 68-73.

133. Chen YC, Shiea J, Sunner J. *Journal of Chromatography A*. **1998**, 826, 77-86.

134. Wu JY, Chen YC. *Journal of Mass Spectrometry*. **2002**, 37, 85-90.

135. Loo RRO, Stevenson TI, Mitchell C, Loo JA, Andrews PC. *Analytical Chemistry*. **1996**, 68, 1910-1917.

136. Loo RRO, Mitchell C, Stevenson TI, Martin SA, Hines WM, Juhasz P, Patterson DH, Peltier JM, Loo JA, Andrews PC. *Electrophoresis*. **1997**, 18, 382-390.

137. Loo RRO, Cavalcoli JD, Van Bogelen RA, Mitchell C, Loo JA, Moledover B, Andrews PC. *Analytical Chemistry*. **2001**, 73, 4063-4070.

138. Walker AK, Rymar G, Andrews PC. *Electrophoresis*. **2001**, 22, 933-945.

139. Eckerskorn C, Strupat K, Scheluder D, Hochstrasser D, Sanchez JC, Lottspeich F, Hillenkamp F. *Analytical Chemistry*. **1997**, 69, 2888-2892.

140. Binz PA, Muller M, Walther D, Bienvenut WV, Gras R, Hoogland C, Bouchet G, Gasteiger E, Fabbretti R, Gay S, Palagi P, Wilkins MR, Rouge V, Tonella L, Paesano S, Rossellat G, Karmime A, Bairoch A, Sanchez JC, Appel RD, Hochstrasser DF. *Analytical Chemistry*. **1999**, 71, 4981-4988.

141. Schleuder D, Hillenkamp F, Strupat K. *Analytical Chemistry*. **1999**, 71, 3238-3247.

142. Lahm HW, Langen H. *Electrophoresis*. **2000**, 21, 2105-2114.

143. Hille JM, Freed AL, Watzig H. *Electrophoresis*. **2001**, 22, 4035-4052.

144. Muller M, Gras R, Appel RD, Bienvenut WV, Hochstrasser DF. *Journal of the American Society for Mass Spectrometry*. **2002**, 13, 221-231.

145. Troendle FJ. Ph.D. Dissertation. **2000**, University of Florida.

146. Coon JJ, Troendle FJ, Yost RA. *Proceedings of the 48th ASMS Conference on Mass Spectrometry and Allied Topics*. Long Beach, CA, **2000**.

147. Troendle FJ, Yost RA. *Proceedings of the 47th ASMS Conference on Mass Spectrometry and Allied Topics*. Dallas, TX, **1999**.

148. Reyzer ML, Korfmacher WA, Ng K, Hsieh Y, Caprioli RM. *Proceedings of the 50th ASMS Conference on Mass Spectrometry and Allied Topics*. Orlando, FL, **2002**.

149. Coon JJ, James MO, Yost RA. *Proceedings of the 49th ASMS Conference on Mass Spectrometry and Allied Topics*. Chicago, IL, **2001**.

150. Kruse RA, Romanova EV, Rubakhin SS, Page JS, Sweedler JV. *Proceedings of the 50th ASMS Conference on Mass Spectrometry and Allied Topics*. Orlando, FL, **2002**.

151. Reddick CD. Ph.D. Dissertation. **1997**, University of Florida.

152. Griffin TP. Ph.D. Dissertation. **1995**, University of Florida.

153. Zhang H, Caprioli RM. *Journal of Mass Spectrometry*. **1996**, 31, 690-692.

154. Gusev AI, Wilkinson WR, Proctor A, Hercules DM. *Analytical Chemistry*. **1995**, 67, 1034-1041.

155. Nicola AJ, Gusev AI, Proctor A, Jackson EK, Hercules DM. *Rapid Communications in Mass Spectrometry*. **1995**, 9, 11-64-1171.

156. Onnerfjord P, Ekstrom S, Bergquiest J, Nilsson J, Laurell T, Marko-Varga G. *Rapid Communications in Mass Spectrometry*. **1999**, 12, 315-322.

157. Gobom J, Kraeuter KO, Persson R, Steen H, Reopsorff P, Ekman R. *Analytical Chemistry*. **2000**, 72, 3320-3326.

158. Hensel RR, King RC, Owens KG. *Rapid Communications in Mass Spectrometry*. **1997**, 11, 1785-1793.

159. De Voogt P, Brinkman UA. *Halogenated Biphenyls, Terphenyls, Naphthalenes, Dibenzodioxins and Related Products*, Elsevier-North Holland, Amsterdam, **1989**, 3.

160. Safe SH. *Critical Reviews in Toxicology*. **1994**, 24, 2, 87-149.

161. Schmidt LJ, Hesselberg RJ. *Archives of Environmental Contamination and Toxicology*. **1992**, 23, 37-44.

162. Lausevic M, Jiang X, Metcalfe CD, March RE. *Rapid Communications in Mass Spectrometry*. **1995**, 9, 10, 927-936

163. Lausevic M, Plomley JB, Jiang X, March RE, Metcalfe CD. *European Mass Spectrometry.* **1995**, 1, 2, 149-159.

164. Kierkegaard A, Balk L, Tjarnlund U, De Wit CA, Jansson B. *Environmental Science and Technology.* **1999**, 33, 1612-1617.

165. Madenjian CP, Schmidt LJ, Chernyak SM, Elliott RF, Desorcie TJ, Quintal RT, Begnoche LJ, Hesselberg RJ. *Environmental Science and Technology.* **1999**, 33, 3768-3773.

166. Madenjian CP, Schmidt LJ, Elliott RF, Desorcie TJ, Quintal RT, Begnoche LJ, Hesselberg RJ, Holey ME. *Environmental Science and Technology.* **1998**, 32, 3063-3067.

167. Burreau S, Axelman J, Broman D, Jakobsson E. *Environmental Toxicology and Chemistry.* **1997**, 16, 2508-2513.

168. James MO, Kleinow KM, *Aquatic Toxicology: Molecular, Biochemical and Cellular perspectives.* Lewis Publishers, CRC Press, Boca Raton, **1994**, 1-35.

169. Kleinow KM, James MO, Tong Z, Venugopalan CS. *Environmental Health Perspectives.* **1998**,106, 155-166.

170. James MO, Altman AH, Morris K, Kleinow KM, Tong Z. *Drug Metabolism and Disposition.* **1997**,25, 346-354.

171. Gadagbui BKM, James MO. *Journal of Biochemical and Molecular Toxicology.* **2000**,14, 148-154.

172. James MO. *Superfund Grant Proposal.* **1999**, 355-389.

173. Van Asperen J, Van Tellingen O, Tijssen F, Schinkel AH, Beijnen JH. *British Journal of Cancer.* **1999**, 79(1), 108-113.

174. Wandel C, Kim RB, Guengerich FP, Wood AJ. *Drug metabolism and Disposition.* **2000**, 28(8) 895-898.

175. Westphal K, Weinbrenner A, Giessmann T, Stuhr M, Franke G, Zschiesche M, Oertel R, Terhaag B, Kroemer HK, Siegmund W. *Clinical Pharmacology & Therapeutics.* **2000**, 68(1), 6-12.

176. Saitoh H, Aungst BJ. *Pharmaceutical Research.* **1995**,12(9), 1304-1310.

177. Jai-nhuknan J, Cassady CJ. *Analytical Chemistry.* **1998**, 70, 5122-5128.

178. Goheen SC, Wahl KL, Campbell JA, Hess WP. *Journal of Mass Spectrometry*. **1997**, 32, 820-828.

179. Knochenmuss R, Karbach V, Wiesli Y, Breuker K, Zenobi R. *Rapid Communications in Mass Spectrometry*. **1998**, 12, 529-534.

180. Eskinju M, Zollner P, Schmid ER. *European Mass Spectrometry*. **1998**, 4, 157-162.

181. Oehme M, Stockl D, Knoppel H. *Analytical Chemistry*. **1986**, 58, 554-558.

182. Cairns T, Siegmund EG. *Analytical Chemistry*. **1981**, 53, 1599-1603.

183. Stemmler EA, Hites RA. *Analytical Chemistry*. **1985**, 57, 684-692.

184. Swackhamer DL, Charles MJ, Hites RA. *Analytical Chemistry*. **1987**, 59, 913-917.

185. Stemmler EA, Hites RA, Arbogast B, Budde WL, Deinzer ML, Dougherty RC, Eichelberger JW, Foltz RL, Grimm C, Grimsrud EP, Sakashita C, Sears LJ. *Analytical Chemistry*. **1988**, 60, 781-787.

186. Crow FW, Bjorseth A, Knapp KT, Bennett R. *Analytical Chemistry*. **1981**, 53, 619-625.

187. Doughtery, R.C. *Analytical Chemistry*. **1981**, 53, 625A-636A.

188. Oehme M, Stockl D, Knoppel H. *Analytical Chemistry*. **1986**, 58, 554-558.

189. Stockl D, Budzikiewicz H. *Organic Mass Spectrometry*. **1982**, 17, 470-474.

190. Chapman JR. *Practical Organic Mass Spectrometry,* 2nd ed., John Wiley and Sons, New York, USA, **1993**.

191. Harrison AG. *Chemical Ionization Mass Spectrometry,* 2nd ed., CRC Press, Boca Raton, FL, USA, **1992**.

192. Vasiljevic TM, Lausevic MD, March RE. *Journal of the Serbian Chemical Society*. **2000**, 65, 431-438.

193. Baldwin MA, Medzihradszky KF, Lock CM, Fisher B, Settineri TA, Burlingame AL. *Analytical Chemistry*. **2001**, 73, 1707-1720.

194. Laboda AV, Krutchinsky AN, Bromirski M, Ens W, Standing KG. *Rapid Communications in Mass Spectrometry.* **2000**, 14, 1047-1057.

195. O'Connor PB, Costello CE. *Rapid Communications in Mass Spectrometry.* **2001**, 15, 1862-1868.

196. Stockle R, Setz P, Deckert V, Lippert T, Wokaun A, Zenobi R. *Analytical Chemistry.* **2001**, 73, 1399-1402.

197. Kolaitis L, Lubman DM. *Analytical Chemistry.* **1986**, 58, 2137-2142.

198. Rees, JA. *Electrical Breakdown in Gases.* **1973**.

199. Sigmond RS. *Journal of Applied Physics.* **1982**, 891-898.

200. Shahin MM. *Journal of Chemical Physics.* **1966**, 45, 2600-2605.

201. Horning EC, Horning MG, Carroll DI, Dzidic I, Stillwell RN. *Analytical Chemistry.* **1973**, 936-943.

202. Carroll DI, Dzidic I, Stillwell RN, Horning EC, Horning MG. *Analytical Chemistry.* **1974**, 706-710.

203. Dzidic I, Carroll DI, Stillwell RN, Horning EC. *Analytical Chemistry.* **1975**, 1308-1312.

204. Carroll DI, Dzidic I, Stillwell RN, Horning EC. *Analytical Chemistry.* **1975**, 1956-1959.

205. Dzidic I, Carroll DI, Stillwell RN, Horning EC. *Analytical Chemistry.* **1976**, 1763-1768.

206. Dzidic I, Carroll DI, Stillwell RN, Horning EC. *Journal of the American Chemical Society.* **1974**, 5258-5259.

207. Horning EC, Carroll DI, Dzidic KD, Haegele KD, Horning MG, Stillwell RN. *Journal of Chromatographic Science.* **1974**, 725-729.

208. Horning EC, Carroll DI, Dzidic KD, Haegele KD, Horning MG, Stillwell RN. *Journal of Chromatography.* **1974**, 13-21.

209. Carroll DI, Dzidic I, Stillwell RN, Haegele DK, Horning EC. *Analytical Chemistry.* **1975**, 2369-2373.

210. Carroll DI, Dzidic I, Horning EC, Stillwell RN. *Applied Spectroscopy Reviews.* **1981**, 337-406.

211. Bruins AP. *Trends in Analytical Chemistry.* **1994**, 13, 37-43.

212. Pavlik M, Skalny JD. *Rapid Communications in Mass Spectrometry.* **1997**, 11, 1757-1766.

213. Coon JJ, Yost RA, James MO, Harrison WW. *17th Asilomar Conference on Mass Spectrometry.* Pacific Grove, CA, **2001**.

214. McHale KJ, Yost RA. *Proceedings of the 48th ASMS Conference on Mass Spectrometry and Allied Topics.* Long Beach, CA, **2000**.

215. Bruins AP. *Mass Spectrometry Reviews.* **1991**, 10: 53-77.

216. Sunner J, Nicol G, Kebarle P. *Analytical Chemistry.* **1988**, 60, 1300-1307.

217. Sunner J, Ikonomou MG, Kebarle P. *Analytical Chemistry.* **1988**, 60, 1308-1313.

218. Escandon NA, Zimmerman DC, McCall RB. *Journal of Pharmacology and Experimental Therapeutics.* **1994**, 268, 441-447.

219. Harrison WW, Yang C, Oxley E *Analytical Chemistry.* **2001**, 73, 480A-487A.

220. Coon JJ, McHale KJ, Harrison WW. *Rapid Communications in Mass Spectrometry.* **2002**, 16, 681-685.

221. Coon JJ, Harrison WW. *Analytical Chemistry.* **2002**, 74, 5600-5605.

222. Coon JJ, Steele HA, Laipis PJ, Harrison WW. *Journal of Mass Spectrometry.* **2002**, 37, 1163-1167.

223. Ens W, Mao Y, Mayer F, Standing KG. *Rapid Communications in Mass Spectrometry.* **1991**, 5, 117-123.

224. Karas M. *Fundamental Processes in Sputtering of Atoms and Molecules.* **1993**, 43, 623-641.

225. Braun R, Hess PI. *Journal of Chemical Physics.* **1993**, 99, 8330-8340.

226. Feldhaus, Dreisewerd K, Menzel C, Berkenkamp S, Hillenkamp F. *Proceedings of the 48th ASMS Conference on Mass Spectrometry and Allied Topics*. Long Beach, CA, **2000**.

227. Dreisewerd K, Schurenberg M, Karas M, Hillenkamp F. *International Journal of Mass Spectrometry and Ion Processes*. **1995**, 141, 127-148.

228. Nelson RW, McLean MA, Hutchens TW. *Analytical Chemistry*. **1994**, 66, 1408.

229. Muddiman DC, Gusev AI, Proctor A, Hercules DM. *Analytical Chemistry*. **1994**, 66, 2362-2368.

230. Whittal RM, Paicic MM, Hindsgaul O, Li L. *Analytical Chemistry*. **1995**, 67, 3509-3515.

231. Muddiman DC, Gusev AI, Proctor A, Hercules DM. *Journal of Mass Spectrometry*. **1995**, 30, 1469-1479.

232. Tang X, Sadeghi M, Olumee Z, Vertes A. *Analytical Chemistry*. **1996**, 68, 3740-3745.

233. Bruenner BA, Yip T, Hutchens TW. *Rapid Communications in Mass Spectrometry*. **1996**, 10, 1797-1801.

234. Hensel RR, King RC, Owens KG. *Rapid Communications in Mass Spectrometry*. **1997**, 11, 1785-1793.

235. Wu J, Chatman K, Harris K, Siuzdak G. *Analytical Chemistry*. **1997**, 69, 3767-3771.

236. Ling YC, Lin L, Chen YT. *Rapid Communications in Mass Spectrometry*. **1998**, 12, 317-327.

237. Desiderio DM, Wirth U, Lovelace JL, Fridland G, Umstot ES, Nguyen T, Schiller PW, Szeto HS, Clapp JF. *Journal of Mass Spectrometry*. **2000**, 35, 725-733.

238. Kang MJ, Tholey A, Heinzle E. *Rapid Communications in Mass Spectrometry*. **2000**, 14, 1972-1978.

239. Gobom J, Kraeuter KO, Persson R, Steen H, Roepstorff, Ekman R. *Analytical Chemistry*. **2000**, 72, 3320-3326.

240. Hunter EP, Lias SG. *Journal of Physical and Chemical Reference Data*. **1998**, 27, 413-656.

241. Speir JP, Amster IJ. *Analytical Chemistry.* **1992**, 64, 1041-1045.

242. Belov ME, Myatt CP, Derrick PJ. *Chemical Physics Letters.* **1998**, 284, 412-418.

243. Coon JJ, Harrison WW. *Proceedings of the 50th ASMS Conference on Mass Spectrometry and Allied Topics.* Orlando, FL, **2002**.

244. Berkenkamp S, Menzel C, Karas M, Hillenkamp F. *Rapid Communications in Mass Spectrometry.* **1997**, 11, 1399-1406.

245. Caldwell KL, Murray KK. *Applied Surface Science.* **1998**, 127-129, 242-247.

246. Menzel C, Berkenkamp S, Hillenkamp F. *Rapid Communications in Mass Spectrometry.* **1999**, 13, 26-32.

247. Beavis RC, Chait BT. *Rapid Communications in Mass Spectrometry.* **1989**, 3, 432-435.

248. Karas M, Bahr U, Ingendoh E, Nordhoff B, Stahl K, Strupat K, Hillenkamp F. *Analytica Chimica Acta.* **1990**, 241, 175-185.

249. Gygi SP, Aebersold R. *Current Opinion in Chemical Biology.* **2000**, 4, 489-494.

250. Gevaert K, Vandekerckhove J. *Electrophoresis.* **2000**, 21, 1145-1154.

251. Griffin TJ, Aebersold R. *The Journal of Biological Chemistry.* **2001**, 276, 45497-45500.

252. Hamdan M, Galvani M, Righetti PG. *Mass Spectrometry Reviews.* **2001**, 20, 121-141.

253. Hille JM, Freed AL, Watzig H. *Electrophoresis.* **2001**, 22, 4035-4052.

254. Courchesne PL, Patterson SD. *BioTechniques.* **1997**, 22, 244.

255. Williams K, LoPresti M, Stone K. *Optimization of In-Gel Digest Protocol in Techniques in Protein Chemistry VIII*, Marshak D. (ed). Academic Press, **1997**.

256. Lopez MF. *Electrophoresis.* **2000**, 21, 1082-1093.

257. Zaluzec EJ, Gage DA, Allison J, Watson JT. *Journal of the American Society for Mass Spectrometry.* **1994**, 5, 230-237.

258. Vestling MM, Fenselau C. *Mass Spectrometry Reviews.* **1995**, 14, 169-178.

259. Ogorzalek Loo RR, Mitchell C, Stevenson TI, Loo JA, Andrews PC. *International Journal of Mass Spectrometry.* **1997**, 169, 273-290.

260. Strupat K, Karas M, Hillenkamp F, Eckerskorn C, Lottspeich. *Analytical Chemistry.* **1994**, 66, 464-470.

261. Eckerskorn C, Strupat K, Schleuder D, Hochstrasser D, Sanchez JC, Lottspeich F, Hillenkamp F. *Analytical Chemistry.* **1997**, 69, 2888-2892.

262. Baltz-Knorr M, Ermer DR, Schriver KE, Haglund RF. *Journal of Mass Spectrometry.* **2002**, 37, 254-258.

263. Kampmeier J, Dreisewerd K, Schurenberg M, Strupat K. *International Journal of Mass Spectrometry and Ion Processes.* **1997**, 169-170, 31-41.

264. Steele HA. M.S. Thesis. **2001**, University of Florida.

265. Gerstner A, Csapo Z, Sasvari-Szekely M, Guttman A. *Electrophoresis.* **2000**, 21, 834-840.

266. Guttman A, Ronai Z. *Electrophoresis.* **2000**, 21, 3952-3964.

267. Guttman A, Csapo Z, Robbins D. *Proteomics.* **2002**, 2, 469-474.

268. Brumley RL, Smith LM. *Nucleic Acids Research.* **1991**, 19, 4121-4126.

269. Pouchert CJ, ed. *The Aldrich Library of Infrared Spectra*, Aldrich Chemical Company. Milwaukee, USA, **1975**.

BIOGRAPHICAL SKETCH

Joshua J. Coon was born on August 29, 1976, in Alma, Michigan, but during his childhood resided in the rural outskirts of a small-town in the north-central lower peninsula named Lake, Michigan. The town was so small it did not have a public school; therefore his elementary education was taken at the Weidman Elementary School, an institute of the consolidated Chippewa Hills School District. Following elementary school, he attended the Chippewa Hills High School located in Remus, Michigan.

His parents, Jacques and Sandra, enjoyed raising cattle and farming as a hobby. Consequently, Josh was often recruited to assist with daily farm chores. This experience taught him several important lessons; the most important lesson was that farming was probably not for him.

In 1994 Josh graduated from high school and enrolled at Central Michigan University in Mt. Pleasant, MI. He enjoyed chemistry and pursued it as his major course of study. It was there that he met his future wife, Heather Steele. At CMU Josh was first exposed to mass spectrometry as an operator of the departmental service instruments. He enjoyed living in Michigan.

Growing up in northern Michigan offered many unique opportunities. For example, during high school Josh discovered that Michigan possessed many unspoiled rivers and that these rivers were home to the finest of all the fishes, the trout. He became fixated on the art of fly fishing and his vehicle accumulated

countless miles beating down two-track dirt roads in pursuit of the fish. As an example of his obsession, during college and with the help of his father, he became interested in boat building to gain better access to the fish he had not yet caught. His first boat was a 24 foot long AuSable riverboat that was completed in the winter of 1995. He constructed two other driftboats during the next two years.

After completion of his undergraduate degree, Josh began graduate school in the Department of Chemistry at the University of Florida during the fall of 1998. His fiancée, Heather, moved with him to Gainesville and also pursued a graduate degree at UF. He will graduate in December, 2002, and has accepted a post-doctoral position with Donald F. Hunt at the University of Virginia. There he hopes to gain further experience in the field of biological mass spectrometry.
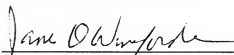
Josh hopes to put his education to use in an academic position at a major research institution, preferably in a land where the streams run cold and the trout are abundant.

I certify that I have read this study and that in my opinion it conforms to acceptable standards of scholarly presentation and is fully adequate, in scope and quality, as a dissertation for the degree of Doctor of Philosophy.

Willard W. Harrison, Chairman
Professor of Chemistry

I certify that I have read this study and that in my opinion it conforms to acceptable standards of scholarly presentation and is fully adequate, in scope and quality, as a dissertation for the degree of Doctor of Philosophy.
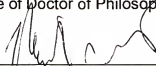
James D. Winefordner
Graduate Research Professor of Chemistry

I certify that I have read this study and that in my opinion it conforms to acceptable standards of scholarly presentation and is fully adequate, in scope and quality, as a dissertation for the degree of Doctor of Philosophy.
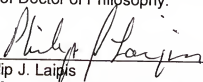
Kathryn R. Williams
Scholar in Chemistry

I certify that I have read this study and that in my opinion it conforms to acceptable standards of scholarly presentation and is fully adequate, in scope and quality, as a dissertation for the degree of Doctor of Philosophy.

Michael J. Scott
Associate Professor of Chemistry

I certify that I have read this study and that in my opinion it conforms to acceptable standards of scholarly presentation and is fully adequate, in scope and quality, as a dissertation for the degree of Doctor of Philosophy.

Philip J. Laipis
Professor of Biochemistry and
Molecular Biology

This dissertation was submitted to the Graduate Faculty of the Department of Chemistry in the College of Liberal Arts and Sciences and to the Graduate School and was accepted as partial fulfillment of the requirements for the degree of Doctor of Philosophy.

December, 2002

Dean, Graduate School